

UC Davis

UC Davis Electronic Theses and Dissertations

Title

Simulation of Different PCM Integrated Wall Designs for Residential Buildings in California Climate Zone-12

Permalink

<https://escholarship.org/uc/item/71n334d0>

Author

Raykar, Shubhankar Suhas

Publication Date

2022

Peer reviewed|Thesis/dissertation

Simulation of Different PCM Integrated Wall Designs for Residential Buildings in California
Climate Zone-12

By

SHUBHANKAR SUHAS RAYKAR
THESIS

Submitted in partial satisfaction of the requirements for the degree of

MASTER OF SCIENCE

in

Mechanical and Aerospace Engineering

in the

OFFICE OF GRADUATE STUDIES

of the

UNIVERSITY OF CALIFORNIA

DAVIS

Approved:

Vinod Narayanan, Chair

John Kissock

Benjamin Shaw

Committee in Charge

2022

ACKNOWLEDGEMENTS

I would like to take a moment to thank all the people who were instrumental throughout the process of my graduate studies.

First and foremost, I'd like to thank my supervisor and mentor, Prof. Vinod Narayanan for giving me the opportunity to work on this project while providing me the guidance and support necessary to successfully complete it.

I would like to express my gratitude to Theresa Pistochni, Co-Director of Engineering and Derrick Ross, Research and Development Engineer at the Western Cooling Efficiency Center both of whom played an instrumental role in this project. Their guidance helped me throughout this journey. Also, they shared important EnergyPlus generated data that played a crucial role in this project.

I would also like to express my gratitude to the members of my committee, Prof. Kissock and Prof. Shaw, for taking the time to review my work amidst their busy schedules.

My friends and family for providing me their undying support and always motivating me when I definitely needed it.

Lastly, I'd like to acknowledge my lab mates: Ramuel Safarkoolan, Antash Najib, Ines-Noelly Tano, and Emily Fricke. They always provided me a great conversation or good laugh when the going was tough.

Abstract

Phase Change Materials (PCMs) have the potential to reduce the cooling and heating energy consumption of buildings. The high latent heat of PCMs helps them to absorb and release large amounts of energy when the PCM changes phase from solid to liquid and from liquid to solid respectively. The climatic conditions and the thermophysical properties of the PCMs play a crucial role and thus, understanding the impact using a particular PCM in a particular climatic condition needs to be understood thoroughly before adding PCM to the building envelope. Previous research has shown that addition of PCM to building envelopes does not always reduce energy consumption.

In this research project, the performance and heat transfer characteristics of two PCMs integrated in a typical residential wall in California was characterized using simulations. PCM 1 is a spackle type product that can be applied to the inner wall and consists of 53% PCM. PCM 1 is a blend of different PCMs and has a melting range from 280K (6.85°C) to 300K (26.85°C). PCM 2 is a salt based PCM and is encapsulated inside panels of plastic material. PCM 2 has melting 294.15K (21°C) to 294.95K (21.8°C). The typical residential wall with no PCM integrated was used as a baseline and a total of 8 PCM-integrated wall designs were studied using simulations, and their impact on reducing cooling and heating energy consumption in comparison to the baseline case was analyzed. The Sacramento weather was used in these studies and representative days of Winter, Summer, and Shoulder were tested. Addition of PCM 1 to the inner wall surface did not produce any significant energy savings for the Winter day and Shoulder day. But adding PCM 1 to the inner wall surface produced 6.7% drop in the cumulative heat leaving the inner wall surface and entering the house for the Summer day and thus, has the potential to reduce cooling energy consumption. Addition of PCM 2 to the inner wall surface does not reduce the energy consumption of the Winter day and the Summer day to have any significant

impact. PCM Next to Stud was a design tested where the PCM was placed between the stud and the insulation. PCM inside Insulation+Stud Layer was another design tested where cubes of PCM were uniformly distributed inside the Insulated+Stud blended layer. For the PCM Next to Studs and PCM inside Insulation+Stud layer the behaviors of PCM 1 and PCM 2 are significantly different but results in reduced heating energy consumption for the two Winter representative days simulated. The results indicated that for all the different wall designs tested in the Sacramento weather no significant energy savings are generated by use of the two specific PCMs characterized in this study.

Table of Contents

| | |
|----------------------------------|-----|
| Background | 1 |
| Literature Review | 3 |
| Objectives | 10 |
| Baseline (No PCM) Cases | 15 |
| PCM 1 Cases | 37 |
| PCM 2 Cases | 66 |
| PCM at Different Locations Cases | 99 |
| Conclusions | 123 |

Table of Figures

| | |
|---|----|
| Figure 1. Global energy savings due to PCM passive systems in building envelope [8] | 4 |
| Figure 2. Typical wall construction in California | 16 |
| Figure 3. Boundary conditions imposed on different wall surfaces | 18 |
| Figure 4. Temperature profiles imposed on inner and outer wall surfaces | 18 |
| Figure 5. Mesh generated for full wall..... | 20 |
| Figure 6. Heat flux 24-hour profile at inner wall surface for Winter day on full wall with no PCM | 22 |
| Figure 7. Heat flux 24-hour profile at outer wall surface for Winter day on full wall with no PCM..... | 23 |
| Figure 8. Blended wall model..... | 25 |
| Figure 9. Comparison of heat flux 24-hour profiles at inner wall surface of full wall and blended wall for Winter day | 26 |
| Figure 10. Comparison of heat flux 24-hour profiles at outer wall surface of full wall and blended wall for Winter day | 26 |
| Figure 11. Comparison of heat flux 24-hour profiles at inner wall surface of full wall and blended wall for Summer day | 27 |
| Figure 12. Comparison of heat flux 24-hour profiles at outer wall surface of full wall and blended wall for Summer day | 28 |
| Figure 13. Comparison of heat flux 24-hour profiles at inner wall surface of full wall and blended wall for Shoulder day | 29 |
| Figure 14. Comparison of heat flux 24-hour profiles at outer wall surface of full wall and blended wall for Shoulder day | 29 |
| Figure 15. 24-hour temperature profile at inner wall surface on a typical Winter day with inner wall convective boundary condition | 33 |
| Figure 16. 24-hour heat flux profile at inner wall surface on a typical Winter day with inner wall convective boundary condition | 33 |
| Figure 17. 24-hour temperature profile at inner wall surface on a typical Summer day with inner wall convective boundary condition | 35 |
| Figure 18. 24-hour heat flux profile at inner wall surface on a typical Summer day with inner wall convective boundary condition | 35 |
| Figure 19. Specific heat versus temperature curve for PCM 1 | 38 |
| Figure 20. Blended wall model with PCM 1 layer next to Gypsum layer..... | 41 |
| Figure 21. Comparison of inner wall surface temperature profiles for No PCM, 3mm PCM 1 layer, 6mm PCM 1 layer, and 9mm PCM 1 layer for a Winter day | 43 |
| Figure 22. Comparison of outer wall surface temperature profiles for No PCM, 3mm PCM 1 layer, 6mm PCM 1 layer, and 9mm PCM 1 layer for a Winter day | 44 |
| Figure 23. Comparison of inner wall surface heat flux profiles for No PCM, 3mm PCM 1 layer, 6mm PCM 1 layer, and 9mm PCM 1 layer for a Winter day..... | 46 |
| Figure 24. Comparison of outer wall surface heat flux profiles for No PCM, 3mm PCM 1 layer, 6mm PCM 1 layer, and 9mm PCM 1 layer for a Winter day..... | 47 |
| Figure 25. Comparison of inner wall surface temperature profiles for No PCM, 3mm PCM 1 layer, 6mm PCM 1 layer, and 9mm PCM 1 layer for a Summer day..... | 48 |

| | |
|---|----|
| Figure 26. Comparison of outer wall surface temperature profiles for No PCM, 3mm PCM 1 layer, 6mm PCM 1 layer, and 9mm PCM 1 layer for a Summer day..... | 49 |
| Figure 27. Comparison of inner wall surface heat flux profiles for No PCM, 3mm PCM 1 layer, 6mm PCM 1 layer, and 9mm PCM 1 layer for a Summer day | 51 |
| Figure 28. Comparison of outer wall surface heat flux profiles for No PCM, 3mm PCM 1 layer, 6mm PCM 1 layer, and 9mm PCM 1 layer for a Summer day | 52 |
| Figure 29. Comparison of inner wall surface temperature profiles for No PCM, 3mm PCM 1 layer, 6mm PCM 1 layer, and 9mm PCM 1 layer for a Shoulder day | 53 |
| Figure 30. Comparison of outer wall surface temperature profiles for No PCM, 3mm PCM 1 layer, 6mm PCM 1 layer, and 9mm PCM 1 layer for a Shoulder day | 54 |
| Figure 31. Comparison of inner wall surface heat flux profiles for No PCM, 3mm PCM 1 layer, 6mm PCM 1 layer, and 9mm PCM 1 layer for a Shoulder day | 55 |
| Figure 32. Comparison of outer wall surface heat flux profiles for No PCM, 3mm PCM 1 layer, 6mm PCM 1 layer, and 9mm PCM 1 layer for a Shoulder day | 56 |
| Figure 33. Comparison of inner wall surface heat flux profiles obtained from EnergyPlus (E+) for No PCM, 3mm PCM 1 layer, 6mm PCM 1 layer, and 9mm PCM 1 layer for a Winter day | 59 |
| Figure 34. Comparison of inner wall surface heat flux profiles obtained from EnergyPlus (E+) for No PCM, 3mm PCM 1 layer, 6mm PCM 1 layer, and 9mm PCM 1 layer for a Summer day | 60 |
| Figure 35. Comparison of inner wall surface heat flux profiles obtained from EnergyPlus (E+) for No PCM, 3mm PCM 1 layer, 6mm PCM 1 layer, and 9mm PCM 1 layer for a Shoulder day | 61 |
| Figure 36. Comparison of inner wall surface heat flux profiles obtained from EnergyPlus (E+) for No PCM, 6mm PCM 1 layer, and 6 x 1mm PCM 1 layers for a Winter day..... | 63 |
| Figure 37. Comparison of inner wall surface heat flux profiles obtained from EnergyPlus (E+) for No PCM, 6mm PCM 1 layer, and 6 x 1mm PCM 1 layers for a Summer day | 64 |
| Figure 38. Comparison of inner wall surface heat flux profiles obtained from EnergyPlus (E+) for No PCM, 6mm PCM 1 layer, and 6 x 1mm PCM 1 layers for a Shoulder day | 65 |
| Figure 39. Solid-liquid (ice-water) interface location as a function of time from analytical solution | 70 |
| Figure 40. Mesh generated for water freezing simulation | 73 |
| Figure 41. Boundary conditions for water freezing simulation | 74 |
| Figure 42. Comparison of mushy zone location from simulation and solid-liquid interface from analytical solution | 75 |
| Figure 43. Comparison of ice layer height from simulation and solid-liquid interface from analytical solution | 76 |
| Figure 44. Constructed curve of specific heat (C_p) as a function of temperature for PCM 2 | 77 |
| Figure 45. Boundary conditions for comparison of PCM 2 melting using enthalpy porosity approach and solid C_p curve approach..... | 79 |
| Figure 46. Comparison of temperature as a function of time at 2mm from isothermal boundary between the enthalpy porosity approach and solid C_p approach..... | 81 |
| Figure 47. Comparison of temperature as a function of time at 4mm from isothermal boundary between the enthalpy porosity approach and solid C_p approach..... | 82 |
| Figure 48. Comparison of temperature as a function of time at 6.3mm from isothermal boundary between the enthalpy porosity approach and solid C_p approach..... | 83 |
| Figure 49. Comparison of heat flux as a function of time at the isothermal boundary between the enthalpy porosity approach and solid C_p approach | 84 |

| | |
|---|-----|
| Figure 50. Blended wall model with PCM 2 layer next to Gypsum layer..... | 86 |
| Figure 51. Comparison of inner wall surface temperature profiles between Winter 1 No PCM, Winter 1 PCM 2, Winter 2 No PCM, and Winter 2 PCM 2 | 90 |
| Figure 52. Comparison of inner wall surface heat flux profiles between Winter 1 No PCM, Winter 1 PCM 2, Winter 2 No PCM, and Winter 2 PCM 2..... | 92 |
| Figure 53. Comparison of outer wall surface heat flux profiles between Winter 1 No PCM, Winter 1 PCM 2, Winter 2 No PCM, and Winter 2 PCM 2..... | 93 |
| Figure 54. Comparison of inner wall surface temperature profiles between Summer 1 No PCM, Summer 1 PCM 2, Summer 2 No PCM, and Summer 2 PCM 2..... | 94 |
| Figure 55. Comparison of inner wall surface heat flux profiles between Summer 1 No PCM, Summer 1 PCM 2, Summer 2 No PCM, and Summer 2 PCM 2 | 96 |
| Figure 56. Comparison of outer wall surface heat flux profiles between Summer 1 No PCM, Summer 1 PCM 2, Summer 2 No PCM, and Summer 2 PCM 2 | 97 |
| Figure 57. Wall model with PCM inside Insulation + Stud layer | 100 |
| Figure 58. Comparison of outer wall surface temperature profiles between Winter 1 No PCM, Winter 1 PCM 1, Winter 1 PCM 2, Winter 2 No PCM, Winter 2 PCM 1, and Winter 2 PCM 2 with PCM inside Insulation + Stud layer wall model..... | 103 |
| Figure 59. Comparison of inner wall surface temperature profiles between Winter 1 No PCM, Winter 1 PCM 1, and Winter 1 PCM 2 with PCM inside Insulation + Stud layer | 104 |
| Figure 60. Comparison of inner wall surface temperature profiles between Winter 2 No PCM, Winter 2 PCM 1, and Winter 2 PCM 2 with PCM inside the Insulation + Stud layer | 105 |
| Figure 61. Comparison of PCM mass-averaged temperature profiles between Winter 1 PCM 1, Winter 1 PCM 2, Winter 2 PCM 1, and Winter 2 PCM 2 with PCM inside Insulation + Stud layer wall model | 106 |
| Figure 62. Comparison of inner wall surface heat flux profiles between Winter 1 No PCM, Winter 1 PCM 1, and Winter 1 PCM 2 with PCM inside Insulation + Stud layer wall model | 108 |
| Figure 63. Comparison of inner wall surface heat flux profiles between Winter 2 No PCM, Winter 2 PCM 1, and Winter 2 PCM 2 with PCM inside Insulation + Stud layer wall model | 109 |
| Figure 64. Comparison of outer wall surface heat flux profiles between Winter 1 No PCM, Winter 1 PCM 1, Winter 1 PCM 2, Winter 2 No PCM, Winter 2 PCM 1, and Winter 2 PCM 2 with PCM inside Insulation + Stud layer wall model..... | 110 |
| Figure 65. Full wall model with PCM Next to the Stud | 111 |
| Figure 66. Comparison of outer wall surface temperature profiles between Winter 1 No PCM, Winter 1 PCM 1, Winter 1 PCM 2, Winter 2 No PCM, Winter 2 PCM 1, and Winter 2 PCM 2 with PCM Next to the Stud wall model | 114 |
| Figure 67. Comparison of inner wall surface temperature profiles between Winter 1 No PCM, Winter 1 PCM 1, and Winter 1 PCM 2 with PCM Next to the Stud wall model..... | 115 |
| Figure 68. Comparison of inner wall surface temperature profiles between Winter 2 No PCM, Winter 2 PCM 1, and Winter 2 PCM 2 with PCM Next to the Stud wall model..... | 116 |
| Figure 69. Comparison of PCM mass-averaged temperature profiles between Winter 1 PCM 1, Winter 1 PCM 2, Winter 2 PCM 1, and Winter 2 PCM 2 with PCM Next to the Stud wall model | 117 |
| Figure 70. Comparison of inner wall surface heat flux profiles between Winter 1 No PCM, Winter 1 PCM 1, and Winter 1 PCM 2 with PCM Next to the Stud wall model | 119 |
| Figure 71. Comparison of inner wall surface heat flux profiles between Winter 2 No PCM, Winter 2 PCM 1, and Winter 2 PCM 2 with PCM Next to the Stud wall model | 120 |

Figure 72. Comparison of outer wall surface heat flux profiles between Winter 1 No PCM, Winter 1 PCM 1, Winter 1 PCM 2, Winter 2 No PCM, Winter 2 PCM 1, and Winter 2 PCM 2 with PCM Next to the Stud wall model..... 121

Table of Tables

Table 1. Complete list of simulations cases performed in this study 11

Table 2. Thermophysical properties of material used in typical construction wall 17

Table 3. Thermophysical properties of mass-averaged blended layer 24

Table 4. Thermophysical properties of PCM 1 37

Table 5. Specific heat equation for different temperature ranges for PCM 1 39

Table 6. Thermophysical Properties of PCM 2 66

Table 7. Thermophysical properties of water and ice 72

Table 8. Thermal conductivity of PCM 2 in melting temperature range as a function of temperature..... 78

Table 9. Different cases run for PCM 2 and their inner wall surface boundary conditions..... 87

Table 10. Different cases run for PCM inside Insulation + Stud layer and their inner wall surface boundary conditions 101

Table 11. Different cases run for PCM Next to the Stud and their inner wall surface boundary conditions 112

Chapter 1: Background

Buildings contribute to 75% of the electricity consumption and 40% of the total energy consumption in the U.S [1]. About 40% of the greenhouse gases emissions in the US can be attributed to building energy consumption [2]. The highest contributors to building energy consumption in the U.S. are space cooling and heating requirements [2]. The demands from the space cooling and heating requirements continue to rise with increased demand for thermal comfort. Thus, to meet these requirements an effective approach is to increase the building thermal mass. Typical U.S. home buildings have a low thermal mass and thus, one method to improve the thermal performance of buildings is to incorporate phase change materials (PCMs) to increase the thermal mass of buildings [3][4].

Previous research has shown that incorporation of PCMs in buildings that act as Latent Heat Thermal Energy Storage (LHTES) systems significantly reduces the heating and cooling requirements [5]. PCMs can store and release a significant amount of energy during the melting and solidification processes compared to the energy storage offered by sensible heat. PCMs have a large thermal storage capacity over a limited range of temperatures and can act as an isothermal reservoir in that range. This temperature selective behavior of PCMs renders them an actively researched solution for building efficiency. Soares et al. [6] carried out a detailed review of the different PCM LHTES systems to improve building energy efficiency. From their work, it was concluded that PCM LHTES systems improve the indoor thermal comfort, increase the building envelope performance, decrease the space conditioning requirements, reduce space conditioning loads, reduce the cost associated with the operation of active space conditioning equipment, and utilize solar energy to enhance building performance. Although PCM LHTES systems have a huge potential in saving energy spent on thermal comfort there many parameters which need to be accounted for and thus, for saving energy, the optimal PCM solutions for each climate have yet to be identified.

PCM LHTES systems offer a wide variety of benefits and their impact can be studied by considering various output variables such as decrease in heat transfer through the walls, heat transfer delay, indoor air temperature rise or drop, increase in indoor thermal comfort time, natural gas savings, electricity savings, and energy associated cost savings. The effectiveness of a particular PCM solution is highly dependent on the geographic location, local climatic conditions, and the desired impact on the building envelope. Thus, a wide range of PCM LHTES studies have been carried out across the globe to find the optimal PCM LHTES solution for that region with different objectives.

Chapter 2: Literature Review

Although PCMs have been well researched, there is still a large potential around the globe to leverage the thermal capacity offered by PCMs. Saffari et al. [7] studied the impact of shows how different parts of the world have leveraged passive PCM systems to reduce building energy consumption as shown in Figure 1. But it can be seen that the majority of the world can still benefit from the development of climatic condition-specific PCM solutions. This study concluded that the optimal PCM peak melting temperature for San Francisco is 20.06°C and this can lead to annual heating energy savings of 760 kWh or 3.8%. Similar, cooling and heating annual energy savings and optimal PCM peak melting temperature for different cities have been provided in this study. This study also concluded, that for cooling dominant climates PCM melting of 26°C with a melting range of 24-28°C leads to higher energy savings, and for heat dominant climates PCM melting with 20°C with a melting range of 18-22°C leads to higher energy savings.

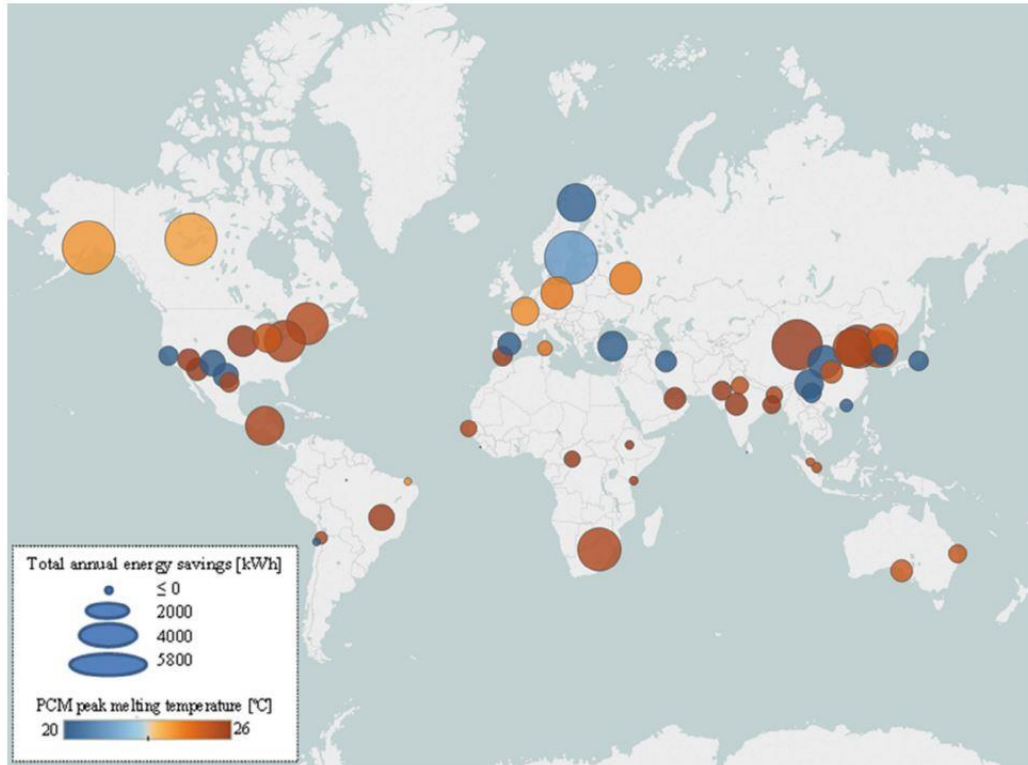


Figure 1. Global energy savings due to PCM passive systems in building envelope [8]

PCMs can be used to passively cool buildings which reduce the cooling energy demand and improve the indoor comfort conditions. The benefits offered by PCMs can only be extracted if the PCMs melting properties and the temperature conditions in that geographical location are aligned to effectively leverage the high thermal storage offered by the PCM. Thus, there is a need to numerically analyze the performance of the passive PCM solutions before physically implementing them. Simulation tools such as ANSYS Fluent can help to understand the detailed 3D behavior of the PCM integrated walls, but to estimate the energy and cost savings, whole building energy simulations are needed and can be carried using software such as EnergyPlus. Typically, whole-building energy simulations assume 1D heat transfer, and thus, these models need to be validated against experimental results and 3D models built using software such as ANSYS Fluent.

EnergyPlus is a whole building energy simulation software and this has been widely used to estimate the annual building energy consumption for buildings with and without PCMs. Tabares-Velasco et al. [8] verified and validated the PCM model in EnergyPlus by conducting analytical verification, comparative testing, and empirical validation. From this exercise of verification and validation, they identified limitations and developed guidelines for using the EnergyPlus PCM model as follows: time steps equal to or shorter than three minutes should be used, accuracy issues can arise when modeling PCMs with strong hysteresis, and default CondFD (which stands for one-dimensional Conduction Finite Difference) can be used with acceptable monthly and annual results. But for accurate hourly performance and analysis, smaller node spacing of 1/3 the default value in EnergyPlus should be used. This study helped in understanding the limitations of whole building energy simulation software and how to overcome them using a systematic approach.

Numerical and experimental studies were carried out by Kosny et al. [9] to analyze the thermal performance of blown fiberglass insulation that was modified with spray-applied microencapsulated PCM. Whole building energy simulations were carried out for different US climates using EnergyPlus. Kosny et al. [10] also studied bio-based PCM that was encapsulated between 2 plastic films and estimated a 10% reduction in wall-generated annual heating and cooling loads due to the addition of the bio-based PCM. Evola et al. [11] simulated lightweight buildings using EnergyPlus to improve thermal comfort by using PCMs. Through their results defined new indicators that help in better using PCMs to improve thermal comfort inside buildings. Tardieu et al. found good agreement between the thermal performance results predicted by EnergyPlus and the long-term measurements conducted in an office size test room in Auckland, New Zealand [12]. Significant thermal energy storage benefits were observed by using PCM-gypsum wallboards and they reduced the daily indoor temperature fluctuations on a typical summer day by 4°C. Tetlow et al. parametrically evaluated the benefits and limitations of incorporating PCMs in the internal wall insulation for retrofitting “hard to treat” houses in the UK using

EnergyPlus [13]. Other building energy simulation tools that have been widely used for estimating the thermal performance of PCM solutions are ESP-r and TRNSYS. Schossig et al. [14] simulated a lightweight office using ESP-r and showed that application of microencapsulated PCMs in interior walls reduced the reduced cooling load in summer. Kuznik et al. [15] used TRNSYS Type 60 to model the thermal behavior of an external wall PCM integrated into it. They validated the TRNSYS model through the experiments they conducted.

Integration of PCM in the building envelope is not always beneficial in reducing energy consumption but instead is strongly affected by climatic conditions, PCM melting temperature, and occupant behavior [16]. Wijesuriya et al. [17] concluded that in heating dominant climates the melting point of PCMs needs to be optimized to increase the annual energy savings. In this study, annual building energy simulations were conducted using EnergyPlus and BEopt for a home in Phoenix to optimize PCM properties and location [17]. Wijesuriya et al. [17] found that in addition to PCM properties and location, the mode of convection is also important to achieve optimal PCM performance. They concluded that forced convection improved heat transfer between the walls and indoor air and thus, kept the living zones cooler and reduced temperature fluctuations. Using optimal PCM locations and high-efficiency fans they observed maximum cost savings of 29.4%. From these studies, it can be understood that for PCM latent heat to be leveraged appropriate conditions need to exist both outside and inside the building.

Jamil et al. [18] carried out an experimental and numerical study using EnergyPlus to investigate the effect of integrating Macro-encapsulated BioPCM™ Q25 in a typical duplex house in Melbourne, Australia during the summer months from January 2015 to March 2015. This study compared the maximum zone air temperature reduction and reduction in thermal discomfort hours for two bedrooms, one of which had PCM integrated into the ceiling and the other one had no PCM integration. The results show that maximum zone air temperature reduction is achieved when the preceding night temperatures are low enough to completely solidify the PCM. The complete solidification of the PCM is more strongly

affected by the zone air temperature than the outdoor air temperature. To fully utilize the PCM, the low zone air temperature needed to exist for a significant amount of time because of the low conductivity of the PCM. To maximize the reduction in thermal discomfort hours the windows needed to be kept open at night and the internal doors need to be shut to avoid air mixing. This change in occupant behavior was shown to increase the reduction in thermal discomfort hours from 34% to 52%. Additionally, spreading the same amount of PCM to the ceilings and walls improves the effectiveness as the heat transfer surface area increases. This study points out the importance of occupant behavior and material properties of the PCM used.

Lee et al. [19] carried out an experimental study on two test houses in Lawrence, KS for the cooling season. These houses were constructed like a typical North American residential construction with dimensions 1.83m x 1.83m x 1.22m and the air-conditioning was scaled down to meet the heating and cooling requirements. This study focused on evaluating the effect of PCM on heat flux reduction and heat transfer time delay. The PCM was incorporated in thin layers placed longitudinally within the walls at different depths and the impact of location was studied. Location 1 corresponded to the PCM placed between the wallboard and the insulation board and the following locations were placed 1.27cm, 2.54cm, 3.81cm, and 5.08 cm from the wallboard. The goal of this study was to find out the effect of the PCM location within the wall cavity on the heat transfer reduction and management for the South and West walls. Based on heat flux reduction alone PCM location 3 was the best location for PCM in the South wall. Also, all the performance parameters improved the most for location 3 in the South wall except for peak delay. At locations 1 and 2 in the West wall, the PCM melting and heat flux reductions were similar to the corresponding South wall location but an increase in the daily heat transfer was observed, and this was opposite to what was seen in the South wall. At location 3 in the West wall, the PCM completely melts before the peak heat flux occurs and thus, the PCM at location 3 in the West wall does not absorb a huge amount of heat during peak time. This study concluded that adding PCM to the

West wall helped in heat transfer management but did not help with energy savings. This shows that the location of the PCM can have no impacts on energy savings or can increase the energy consumption. Thus, the combination of climatic conditions, PCM properties, and PCM location needs to be tested using numerical studies.

Modeling of Phase Change Materials

A Stefan problem is a moving boundary problem and it describes the phase change processes of melting and solidification. The moving boundary is the interface between the solid and liquid phases and the location of the moving boundary is calculated based on the energy balance condition called the Stefan condition. The Stefan problem can be simplified by neglecting the convective term from the energy equation and considering conduction as the dominant mode of heat transfer. Since the convective term is neglected there is no need to solve the Navier-Stokes equation and this is the simplest form of the Stefan problem. There are very few analytical solutions available and they mainly apply to one-dimensional cases with infinite or semi-infinite regions. Additionally, these analytical solutions exist only for cases with very simple initial and boundary conditions and constant thermal properties [20]. One such analytical solution describing the freezing of a semi-infinite slab of water that uses similarity solutions has been provided by Slattery [21]. The different similarity solutions to the Stefan problem can be found in [22][23].

Due to lack analytical solutions to complicated solidification and melting problems numerical solutions have been developed and applied to study the phase change behavior of different materials and to develop practical applications of PCMs. The displacement rate of the phase change boundary is controlled by the latent heat lost or absorbed at the boundary and this is an additional equation that needs to be solved to obtain numerical solution of solidification and melting problems. The energy

transfer at the boundary and the corresponding location of the boundary is presented in the following equation:

$$L\rho \left(\frac{ds(t)}{dt} \right) = k_s \left(\frac{\delta T_s}{\delta x} \right) - k_l \left(\frac{\delta T_l}{\delta x} \right)$$

Where L is the latent heat of fusion, ρ is the density, $s(t)$ is the boundary location as a function of time, t is the time, x is the location, k_s is the conductivity of the solid, and k_l is the conductivity of the liquid.

The enthalpy porosity developed by Voller et al. [24] is most commonly used for modeling solidification and melting. This method has been further popularized because of its implementation in the commercial software ANSYS Fluent. The enthalpy porosity method belongs to fixed-domain methods category. This method does not require the explicit tracking of the solid-liquid interface. The temperature inside a cell is used to estimate the liquid fraction and instead of sharp transition between solid and liquid there exists a mushy zone between them. This method is able to accurately capture physics in situations when the natural convection is strong and this method is fast to converge and has a high accuracy [25]. Assis et al. [26][27] conducted experiments on commercially available paraffin wax and performed melting of spherical shells with varying diameters. They conducted transient numerical simulations using the enthalpy porosity method. Kamkari et al. [28] conducted experiments using lauric acid in a rectangular enclosure. They imposed isothermal boundary conditions on one side and all other sides were insulated. They captured the solid-liquid interface position by taking photographs at different times. Additionally, they studied the impact of varying the inclination on melting time. They developed their own numerical model based on the enthalpy porosity approach and validated it using their experimental results. Another method that belongs to the fixed-domain category is the effective heat capacity method [25]. In this method, the latent heat of fusion is incorporated into the specific heat capacity of the PCM. Thus, the specific heat capacity when using this method is essentially a function of temperature with higher specific heat capacity values in the melting temperature range.

Chapter 3: Objectives

The goal of this project is to develop a better understanding of how passive PCM solutions can be used to reduce the energy consumption of residential buildings in the state of California. It is important to reduce the overall energy consumption, but it is equally important to reduce the energy consumption during peak hours. Such reduction not only has cost benefits for the residents but it also plays an important role in reducing the negative environmental impact due to use of peaker power plants.

Passive PCM solutions are sensitive to a wide range of parameters such as climatic conditions, seasonal variations, building construction type, building orientation, building layout, indoor set-point temperature, the quantity of PCM, location of PCM in building envelope, melting temperature, and range of PCM, latent heat of PCM, and other thermophysical properties of PCM. It is important to note that adding PCM to building envelope might help in one season, but based on the literature review it can be guessed that it can have negative impacts during other seasons and thus, it is crucial to analyze the impact of adding PCM throughout the year.

In this study, the impact of two PCM products was analyzed, namely PCM 1 and PCM 2. Based on the method of application of the PCM products and the recommendations from manufacturers PCM 1 was applied on the inner wall surface in layers of 3 mm, 6 mm, and 9 mm whereas PCM 2 was applied on the inner wall surface in a layer of 6.3 mm. These layers were added on top of the drywall gypsum layer which is the innermost layer of the typical wall construction employed in California. In addition to these locations two more PCM locations were tested- the first was with PCM distributed throughout the insulation, and second was with PCM located along the thickness of the studs in the insulation cavity.

Another parameter that was varied was the season and this was done by simulating the three representative days each of which represented a season. The three representative days simulated were Winter day, Summer day, and Shoulder day. The Winter day is representative from December 1st to February 28th, the Summer day is a representative day from June 1st to August 31st, and Shoulder day is

a representative from Spring in California between March 1st to May 31st. Table 1 represents the different simulations that were conducted as a part of this project.

Table 1. Complete list of simulations cases performed in this study

| Sr. No. | PCM Product | PCM Location (and Thickness, if applicable) | Seasonal Day | Case Description |
|---------|-------------|---|--------------|--|
| 1 | No PCM | Not Applicable | Winter | No PCM, Winter Day (Baseline Case) with Temperature Boundary Conditions and Full Wall Model |
| 2 | No PCM | Not Applicable | Summer | No PCM, Summer Day (Baseline Case) with Temperature Boundary Conditions and Full Wall Model |
| 3 | No PCM | Not Applicable | Shoulder | No PCM, Shoulder Day (Baseline Case) with Temperature Boundary Conditions and Full Wall Model |
| 4 | No PCM | Not Applicable | Winter | No PCM, Winter Day (Baseline Case) with Temperature Boundary Conditions and Blended Wall Model |
| 5 | No PCM | Not Applicable | Summer | No PCM, Summer Day (Baseline Case) with Temperature Boundary Conditions and Blended Wall Model |
| 6 | No PCM | Not Applicable | Shoulder | No PCM, Shoulder Day (Baseline Case) with Temperature Boundary Conditions and Blended Wall Model |
| 7 | No PCM | Not Applicable | Winter | No PCM, Winter Day (Baseline Case) with Inner Wall Convective Boundary Conditions and Blended Wall Model |
| 8 | No PCM | Not Applicable | Summer | No PCM, Summer Day (Baseline Case) with Inner Wall Convective Boundary Conditions and Blended Wall Model |
| 9 | PCM 1 | Inner Wall, 3mm | Winter | PCM 1, 3mm Layer at Inner Wall, Winter Day with Temperature Boundary Conditions and Blended Wall Model |
| 10 | PCM 1 | Inner Wall, 6mm | Winter | PCM 1, 6mm Layer at Inner Wall, Winter Day with Temperature Boundary Conditions and Blended Wall Model |
| 11 | PCM 1 | Inner Wall, 9mm | Winter | PCM 1, 9mm Layer at Inner Wall, Winter Day with Temperature Boundary Conditions and Blended Wall Model |
| 12 | PCM 1 | Inner Wall, 3mm | Summer | PCM 1, 3mm Layer at Inner Wall, Summer Day with Temperature Boundary Conditions and Blended Wall Model |

| | | | | |
|----|--------|--------------------------------------|--------------------------------------|---|
| 13 | PCM 1 | Inner Wall, 6mm | Summer | PCM 1, 6mm Layer at Inner Wall, Summer Day with Temperature Boundary Conditions and Blended Wall Model |
| 14 | PCM 1 | Inner Wall, 9mm | Summer | PCM 1, 9mm Layer at Inner Wall, Summer Day with Temperature Boundary Conditions and Blended Wall Model |
| 15 | PCM 1 | Inner Wall, 3mm | Shoulder | PCM 1, 3mm Layer at Inner Wall, Shoulder Day with Temperature Boundary Conditions and Blended Wall Model |
| 16 | PCM 1 | Inner Wall, 6mm | Shoulder | PCM 1, 6mm Layer at Inner Wall, Shoulder Day with Temperature Boundary Conditions and Blended Wall Model |
| 17 | PCM 1 | Inner Wall, 9mm | Shoulder | PCM 1, 9mm Layer at Inner Wall, Shoulder Day with Temperature Boundary Conditions and Blended Wall Model |
| 18 | No PCM | Not Applicable | Winter 1 ($T_{\infty}=292.65K$) | No PCM, Winter 1 Day with Inner Wall Convective Boundary Conditions and Blended Wall Model |
| 19 | PCM 2 | Inner Wall, 6.3mm | Winter 1 ($T_{\infty}=292.65K$) | PCM 2, 6.3mm Layer at Inner Wall, Winter 1 Day with Inner Wall Convective Boundary Conditions and Blended Wall Model |
| 20 | No PCM | Not Applicable | Winter 2 ($T_{\infty}=294.5K$) | No PCM, Winter 2 Day with Inner Wall Convective Boundary Conditions and Blended Wall Model |
| 21 | PCM 2 | Inner Wall, 6.3mm | Winter 2 ($T_{\infty}=294.5K$) | PCM 2, 6.3mm Layer at Inner Wall, Winter 2 Day with Inner Wall Convective Boundary Conditions and Blended Wall Model |
| 22 | No PCM | Not Applicable | Summer 1 ($T_{\infty}=298.65K$) | No PCM, Summer 1 Day with Inner Wall Convective Boundary Conditions and Blended Wall Model |
| 23 | PCM 2 | Inner Wall, 6.3mm | Summer 1 ($T_{\infty}=298.65K$) | PCM 2, 6.3mm Layer at Inner Wall, Summer 1 Day with Inner Wall Convective Boundary Conditions and Blended Wall Model |
| 24 | No PCM | Not Applicable | Summer 2 ($T_{\infty}=294.8K$) | No PCM, Summer 2 Day with Inner Wall Convective Boundary Conditions and Blended Wall Model |
| 25 | PCM 2 | Inner Wall, 6.3mm | Summer 2 ($T_{\infty}=294.8K$) | PCM 2, 6.3mm Layer at Inner Wall, Summer 2 Day with Inner Wall Convective Boundary Conditions and Blended Wall Model |
| 26 | PCM 1 | PCM 1 inside Insulation + Stud layer | Winter 1 ($T_{\infty}=292.65K$) | PCM 1, In cubes inside Insulation + Stud layer, Winter 1 Day with Inner Wall Convective Boundary Condition and Blended Wall Model |

| | | | | |
|----|--------|--------------------------------------|-----------------------------------|---|
| 27 | PCM 2 | PCM 2 inside Insulation + Stud layer | Winter 1 ($T_{\infty}=292.65K$) | PCM 2, In cubes inside Insulation + Stud layer, Winter 1 Day with Inner Wall Convective Boundary Condition and Blended Wall Model |
| 28 | PCM 1 | PCM 1 inside Insulation + Stud layer | Winter 2 ($T_{\infty}=294.5K$) | PCM 1, In cubes inside Insulation + Stud layer, Winter 2 Day with Inner Wall Convective Boundary Condition and Blended Wall Model |
| 29 | PCM 2 | PCM 2 inside Insulation + Stud layer | Winter 2 ($T_{\infty}=294.5K$) | PCM 2, In cubes inside Insulation + Stud layer, Winter 2 Day with Inner Wall Convective Boundary Condition and Blended Wall Model |
| 30 | No PCM | Not Applicable | Winter 1 ($T_{\infty}=292.65K$) | No PCM, Winter 1 Day with Inner Wall Convective Boundary Conditions and Full Wall Model |
| 31 | PCM 1 | PCM 1 Next to Stud | Winter 1 ($T_{\infty}=292.65K$) | PCM 1, PCM 1 Next to Stud, Winter 1 Day with Inner Wall Convective Boundary Condition and Full Wall Model |
| 32 | PCM 2 | PCM 2 Next to Stud | Winter 1 ($T_{\infty}=292.65K$) | PCM 2, PCM 2 Next to Stud, Winter 1 Day with Inner Wall Convective Boundary Condition and Full Wall Model |
| 33 | No PCM | Not Applicable | Winter 2 ($T_{\infty}=294.5K$) | No PCM, Winter 2 Day with Inner Wall Convective Boundary Conditions and Blended Wall Model |
| 34 | PCM 1 | PCM 1 Next to Stud | Winter 2 ($T_{\infty}=294.5K$) | PCM 1, PCM 1 Next to Stud, Winter 2 Day with Inner Wall Convective Boundary Condition and Full Wall Model |
| 35 | PCM 2 | PCM 2 Next to Stud | Winter 2 ($T_{\infty}=294.5K$) | PCM 2, PCM 2 Next to Stud, Winter 2 Day with Inner Wall Convective Boundary Condition and Full Wall Model |

All these simulations were conducted using ANSYS Fluent. The temperature boundary conditions were obtained from EnergyPlus and converted into MS Excel files that could be directly used as a boundary condition in ANSYS Fluent. The inner wall convective boundary condition was directly implemented in ANSYS Fluent by selecting the convective heat transfer coefficient and freestream temperature. The main objective of this project is to develop insight into the heat transfer characteristics of a wall embedded with PCM and make informed recommendations regarding the choice of PCM, optimal PCM location, and PCM quantity to maximize energy savings. Additionally, the objective is also to develop recommendations about what are the desirable and undesirable qualities the passive PCM solution must

exhibit to reduce energy consumption from heating and cooling in residential buildings in California
Climate Zone 9.

Chapter 4: No PCM (Baseline) Simulations

To better understand the impact PCMs have on the heat transfer characteristics of the wall, it is crucial to develop a baseline “ No PCM” model of a typical residential building wall in California (CA). The geometry of this wall replicated a typical residential building wall in CA and the material properties were chosen such that they accurately represent the thermal properties of the wall. The No PCM model was developed for 3 representative days: Winter, Summer, and Shoulder. Conducting these No PCM simulations of a wall provided a standard against which the PCM integrated wall designs were compared to understand the difference that addition of PCMs was making to the heat transfer characteristics.

Modeling Domain

The goal of this project was to find optimal retrofit PCM solutions to improve the energy savings in residential buildings in CA and thus, the domain for these simulations were typical walls in residential buildings in CA. Based on the climatic conditions and time of the day the outer side of the wall will experience different combinations of convective and radiative conditions that will yield an outer wall temperature. Similarly, based on the set-point temperature of the air-conditioning system inside the house and the time of day the convective and radiative conditions will yield an inner wall temperature. These inner wall and outer wall temperatures will fluctuate throughout the 24-hour cycle and these will act as boundary conditions to the walls of the residential building. These temperature profiles applied as boundary conditions were obtained from EnergyPlus. The output from these simulations was in the form of heat flux variations at the inner and outer wall and the temperatures of the different components of the wall throughout the 24-hour cycle.

A typical residential wall is constructed with 2x4 studs spaced 16 inches on center. Additionally, there is wood at the top and bottom of the wall as well as surrounding the window and door frames which yield a total of 20-25% wood in the wall [29]. There are numerous combinations of the wall models possible

with different numbers and locations of windows and doors and different wall heights. Thus, to simplify the modeling process the wall geometry was built with 4x4 studs spaced 16-inch on center and this yields 22% wood in the wall. It is important to note that the 4x4 studs are actually 3.5 inches thick and 3.5 inches wide. The innermost layer of the wall is made up of gypsum, next, there is a layer of insulation and stud, following which there is a layer of plywood and finally the outermost layer is stucco. The construction of the wall is shown in Figure 2. The modeling domain is a wall section that is 24 inches tall and 16 inches wide. The thicknesses of the different wall layers are:

- 12.7 mm (0.5 inch) gypsum drywall (inside surface)
- 88.9 mm (3.5 inches) wood (fir) studs and fiberglass insulation (if insulated)
- 12.7 mm (0.5 inch) plywood
- 22.2 mm (0.875 inch) stucco (outside surface)

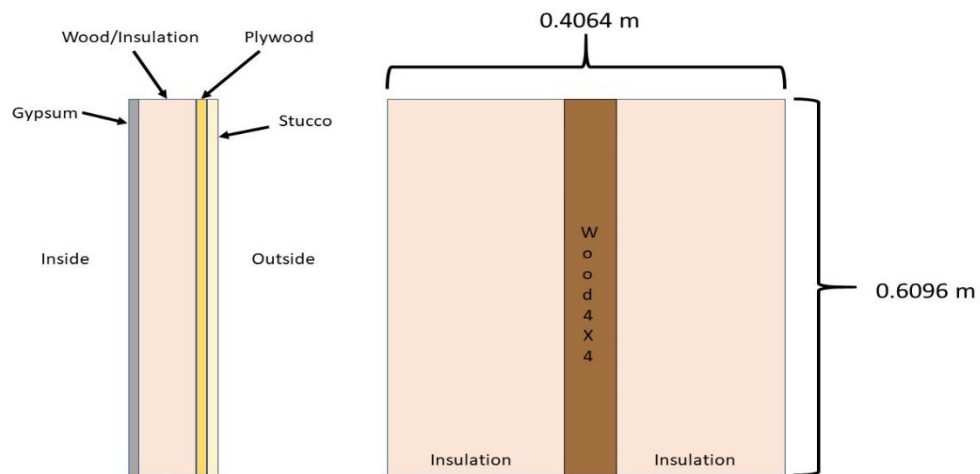


Figure 2. Typical wall construction in California

Wall Material Properties

To accurately calculate the heat flux at the inner and outer wall under different temperature boundary conditions it is necessary to obtain reliable material properties. The properties of stucco and gypsum drywall were obtained from a building reference model published by the Department of Energy [30].

The properties of plywood were obtained from Engineering Equation Solver (EES, F-Chart Inc.). The stud is typically made up of fir wood and thus, properties of fir wood used in wall framing are obtained from an Oak Ridge National Lab (ORNL) study on thermal properties of common woods used in construction [31].

The insulation used in the model is fiberglass insulation with an R-value of 15 ($^{\circ}\text{Fft}^2\text{hr}/\text{BTU}$) or 2.64 ($\text{m}^2\text{K}/\text{W}$) in the 88.9 mm deep insulation section was modeled at the minimum specified installation density [32]. The thermal conductivity was calculated from the R-value. The mass weighted approach was used for calculating the specific heat capacity for the fiberglass insulation and air combination. The material properties for all the wall materials are summarized in Table 2.

Table 2. Thermophysical properties of material used in typical construction wall

| Material Name | Density (kg/m^3) | Specific Heat Capacity ($\text{J}/\text{kg-K}$) | Thermal Conductivity ($\text{W}/\text{m-K}$) |
|-------------------|------------------------------------|---|--|
| Gypsum | 640 | 1130 | 0.16 |
| Fir Wood | 510 | 1700 | 0.14 |
| Insulation | 37 | 811 | 0.0337 |
| Plywood | 545 | 1215 | 0.12 |
| Stucco | 1866 | 879 | 0.72 |

Boundary Conditions

The complete wall section had 6 outer surfaces on which different boundary conditions were imposed as shown in Figure 3:

- Surfaces 1 and 2: Insulated boundary conditions imposed on them ensure no heat in the simulation was lost laterally, which reflects the insulated conditions from the laboratory test plan.
- Surfaces 3 and 4: Symmetry condition imposed which simulates the remainder of the wall since only the quarter wall was modeled.
- Surface 5: Inside wall surface with temperature versus time boundary condition.
- Surface 6: Outside wall surface with temperature versus time boundary condition.

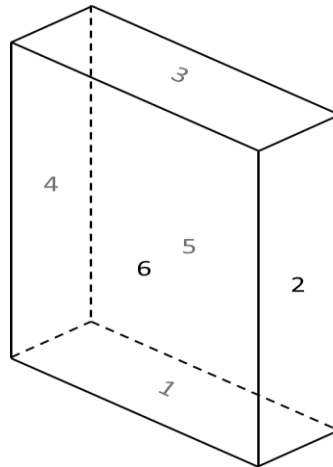


Figure 3. Boundary conditions imposed on different wall surfaces

An example of the typical inner wall and outer wall temperature profiles are provided in Figure 4.

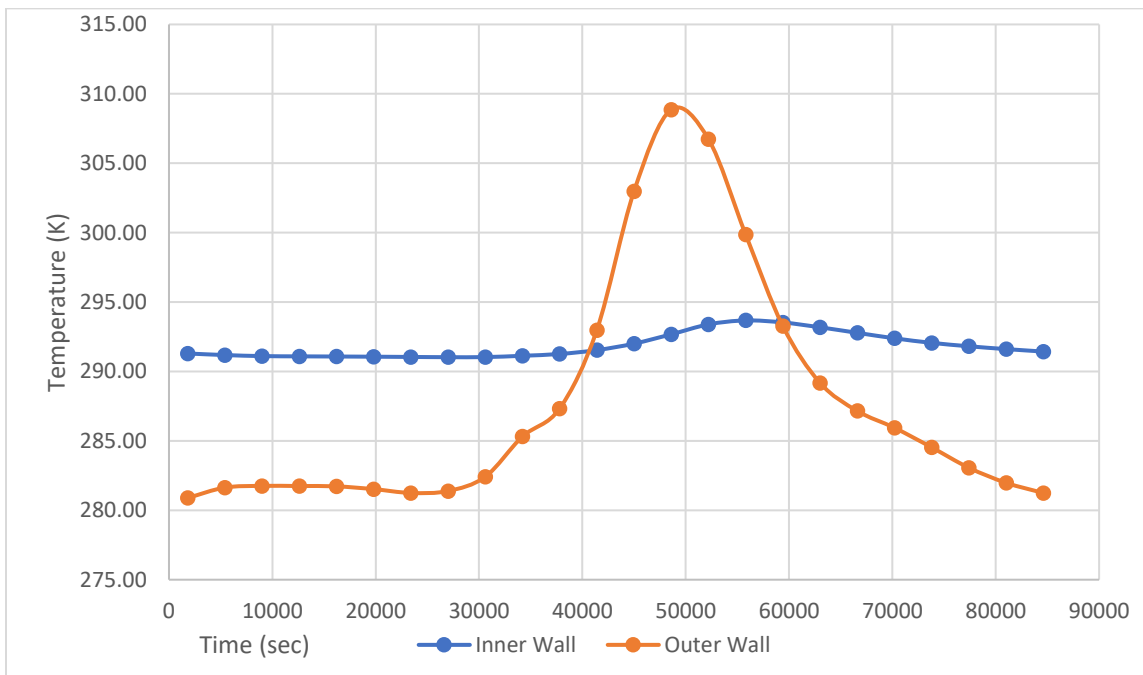


Figure 4. Temperature profiles imposed on inner and outer wall surfaces

At time 0 seconds it is midnight and the temperature profiles depicted in Figure 4 belong to a typical winter day.

Initial Conditions and Simulation Time

The transient simulation was significantly influenced by the initial condition. Therefore, it was important to choose an appropriate initial condition or to run the 24 h temperature profile multiple times until the heat flux profile between consecutive days was repeated. The identical heat flux profiles ensure that the simulation results were independent of the initial condition and depicted what happens when the wall was exposed to such conditions. The simulations were repeated for identical days to reduce the impact of initial conditions. The results showed that the heat flux profiles of days 2 and 3 were the same and thus, were independent of initial conditions.

Solver Settings and Mesh Quality

ANSYS Fluent is a finite-volume-based simulation software. The No PCM model wall materials were all solid and hence there was no need to solve the mass and momentum equations. Only a solution to the energy equation was required. In the case when the PCM was modeled using the Solidification/ Melting module in ANSYS Fluent the mass and momentum equations were solved. PCM 1 was modeled as a solid layer (since the PCM is inside the solid matrix) and the solution of the energy equation was sufficient in this case. For PCM 2 the Solidification/ Melting module in ANSYS Fluent was turned ON, the PCM was treated as a liquid or solid based on its temperature and hence the mass and momentum equations were solved as well. The Solidification/ Melting module uses the enthalpy formulation method to track the location of the melting front. This case involved significantly more amount of computational power and time because of the need to solve the mass and momentum equations as well. The SIMPLE scheme was used for pressure-velocity coupling.

A second-order implicit scheme was used for the transient formulation. The use of an implicit scheme ensures there was no possibility of the calculations becoming unstable and this also provided greater flexibility in selecting the time step size. The time step used in these simulations was 300 seconds and the solutions were recorded after every two -time steps.

The stud has a much higher thermal conductivity as compared to the insulation and thus, has a much higher heat flux passing through it. To account for this higher heat flux density the mesh had a higher number of elements around the stud as opposed to the insulation as shown in Figure 5 which had no PCM layer. For the No PCM case, there was no additional layer of PCM on the inside surface next to the gypsum drywall layer. The PCM cases had PCM layers of different thicknesses and the meshing of these PCM layer followed a similar trend with more elements close to the stud but had higher element density across the PCM thickness as compared to the other materials. The total number of elements in the mesh were 5832000, maximum skewness of the mesh was 0.214, and average skewness was 0.00214. The mesh used was structured and non-uniform.

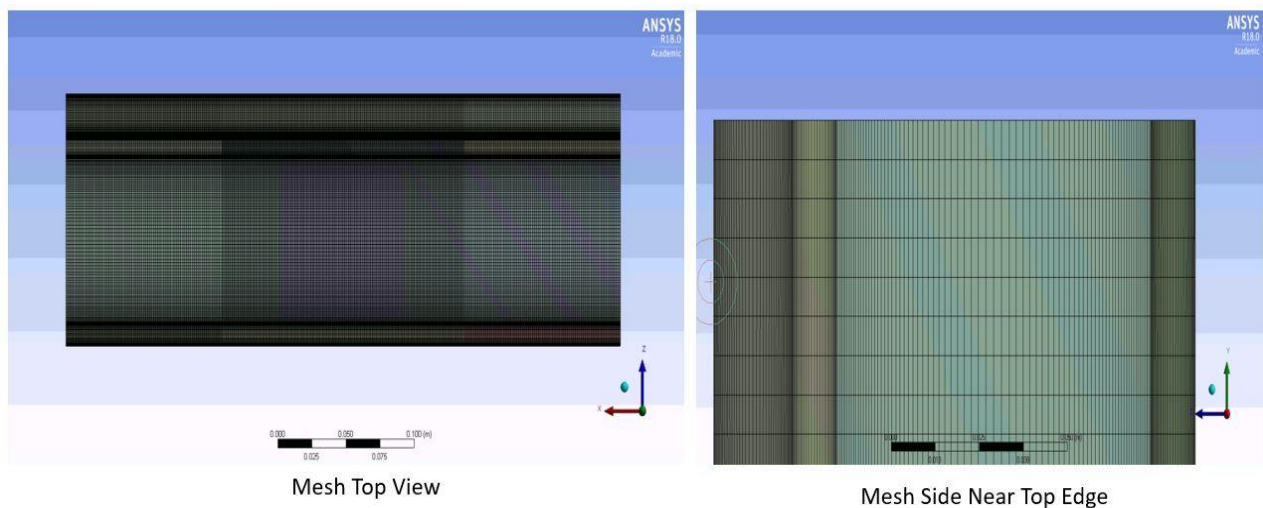


Figure 5. Mesh generated for full wall

No PCM Cases (Baseline Cases): Full Wall Results

The No PCM case represents the full wall with no PCM embedded in it at any location. This case was important to understand how the wall behaves without the PCM under the boundary conditions of different representative days. This case served as a baseline for comparison of the difference with PCM cases against the no PCM case. It helped assess the effectiveness of the proposed PCM solution in reducing energy consumption.

Figure 6 represents the heat flux at the inner wall surface in this case gypsum drywall throughout the 24-hour cycle under typical Winter conditions imposed by the Winter representative day. Similarly, Figure 7 represents the heat flux at the outer wall surface, in this case, stucco. At 0 hours in these graphs, the time is 12 midnight, and thus, during the first few hours, it is nighttime. The sign convention is such that positive heat flux indicates heat entering the wall surface and negative heat flux represents heat leaving the wall surface. Thus, positive heat flux on the inner wall surface represents heat traveling from inside the house to the inner wall surface, and negative heat flux represents heat traveling from the inner wall surface to inside the house. Similarly, positive heat flux on the outer wall surface represents heat traveling from the outside to the outer wall surface and negative heat flux represents heat traveling from the outer wall surface to outside the house. The heat flux values plotted in these graphs are area-weighted average heat flux values.

For the first 7.5 hours, the heat flux on the outer wall surface is negative indicating that the house is losing heat to the outside and this, is expected as the house is warmer than the outside. Similarly, for the first 10 hours, the heat flux on the inner wall surface is positive which indicates that heat is traveling from inside the house to the walls. As the radiation from the sun starts heating up the outer wall surface the heat reverses its direction and the heat from outside starts traveling into the house and this continues from 7.5 hours to 14.5 hours with the peak occurring at 12.5 hours. At the inner wall surface,

the heat flux is fairly constant positive value for the first 10 hours, indicating that heat flows into the inner wall from the house. The heat flux starts reducing in magnitude beyond 10 hours and changes direction 14.5 hours. The change in direction indicates that beyond 14.5 hours and until 20 hours the inner wall surface rejects heat into the house. This rejection of heat starts at 14.5 hours and this corresponds to when the heat flux on the outer wall surface changes direction. Beyond 20 hours the inner wall surface starts receiving heat from inside the house and this continues till the end of the 24-hour cycle.

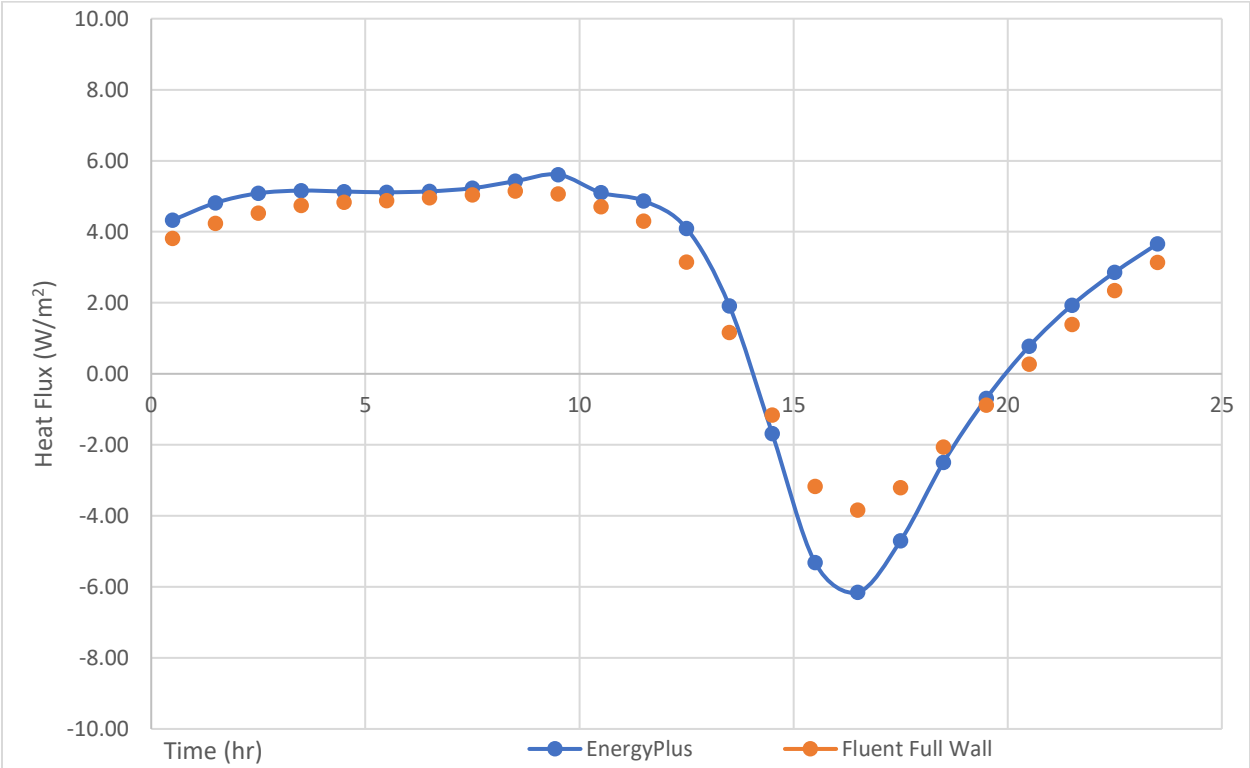


Figure 6. Heat flux 24-hour profile at inner wall surface for Winter day on full wall with no PCM

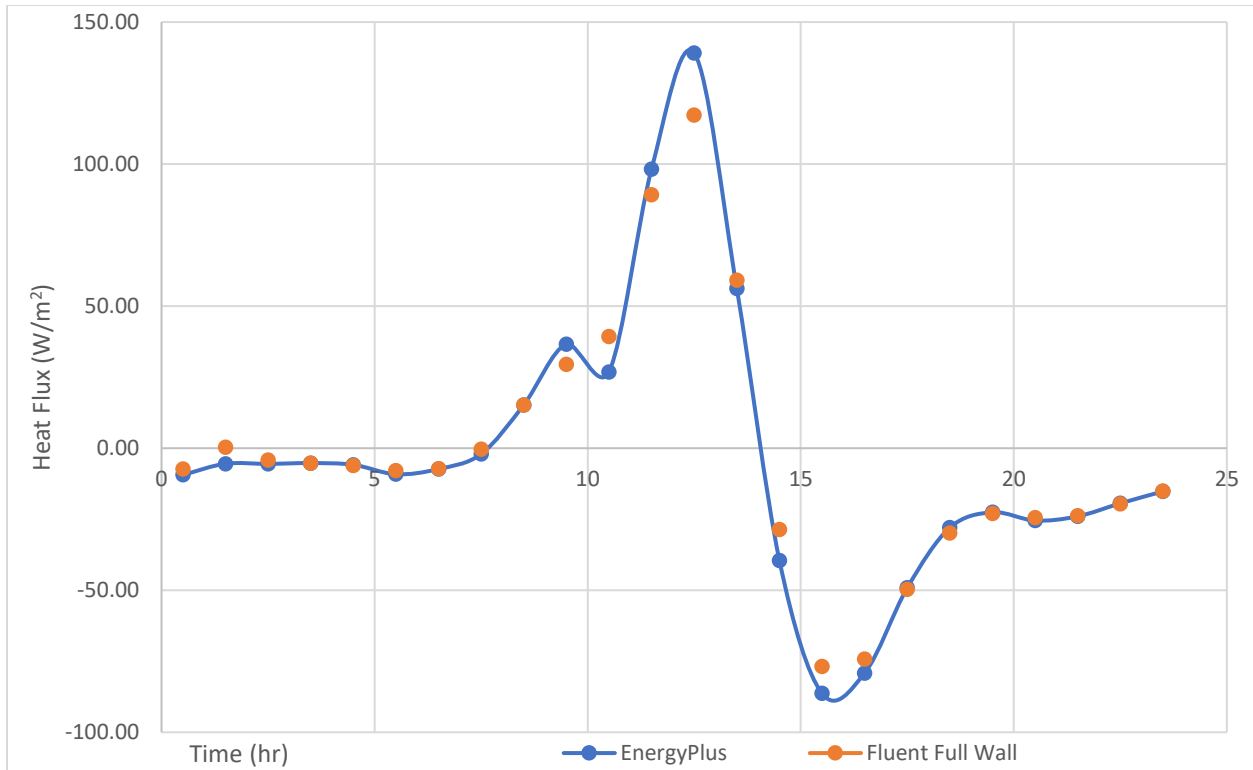


Figure 7. Heat flux 24-hour profile at outer wall surface for Winter day on full wall with no PCM

Comparing the heat flux values between the EnergyPlus model and the ANSYS Fluent model, it is evident that the agreement between the two is stronger for the outer wall as compared to the inner wall. This difference exists because of the way the EnergyPlus domain is setup. The layer that contains the stud and insulation has vertical sections of stud in between the insulation and this type of wall construction cannot be built in EnergyPlus. EnergyPlus can only build and simulate single material layers. Thus, the thermophysical properties of stud and insulation were mass-weighted to develop the properties of the single-layer which acted as a blend of the insulation and stud. This difference in the physical domain gives rise to the difference in the heat flux profile. In ANSYS Fluent the material layers can be broken into as many elements as the user decides but this flexibility is not available in EnergyPlus. In EnergyPlus each layer has only one interior node and this was another difference in the two modeling approaches.

It was estimated that adding the PCM layer to the models can affect their agreement and thus, the domain used in ANSYS Fluent was changed to match that of EnergyPlus.

ANSYS Fluent Blended Wall Model

For the cases, where PCM is applied on the inner wall surface and for the No PCM case the stud and insulation were merged into one single layer with mass-weighted thermophysical properties. The properties of the insulation + stud layer are given in Table 3. This modified wall domain will be referred to as the blended wall and the original wall domain will be referred to as the complete wall in the report hereafter. The blended wall domain exactly matches the simulation domain used in EnergyPlus and thus, it was expected that the ANSYS Fluent with blended wall and EnergyPlus will show a better agreement of the heat fluxes.

Table 3. Thermophysical properties of mass-averaged blended layer

| Density | Specific Heat Capacity | Thermal Conductivity |
|-------------------------|-------------------------------|-----------------------------|
| 140.5 kg/m ³ | 1517 J/kg-K | 0.056 W/m-K |

Figure 8 shows the Fluent Blended Wall. The total number of elements in this new mesh was 475000, maximum skewness of the mesh was 2.14×10^{-3} , and average skewness of the mesh was 2.14×10^{-4} . The mesh used was structured and non-uniform. The material properties of the other materials, boundary conditions, solver settings, initial conditions, and simulation time were all exactly same as the Full Wall model.

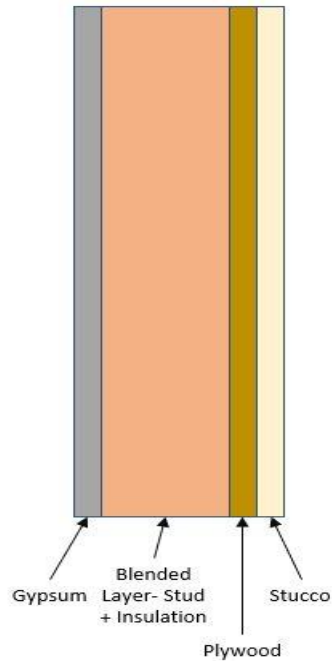


Figure 8. Blended wall model

Result Comparison: EnergyPlus, ANSYS Fluent Complete Wall and ANSYS Fluent Blended Wall

To better understand the impact of the blended wall domain the baseline cases for Summer day and Shoulder day were simulated using both the complete wall and blended wall. Figure 9, Figure 10, Figure 11, Figure 12, Figure 13, and Figure 14 show the comparison between heat flux profiles of the EnergyPlus model, the ANSYS Fluent complete wall model, and the ANSYS Fluent blended wall model under the three different representative day boundary conditions.

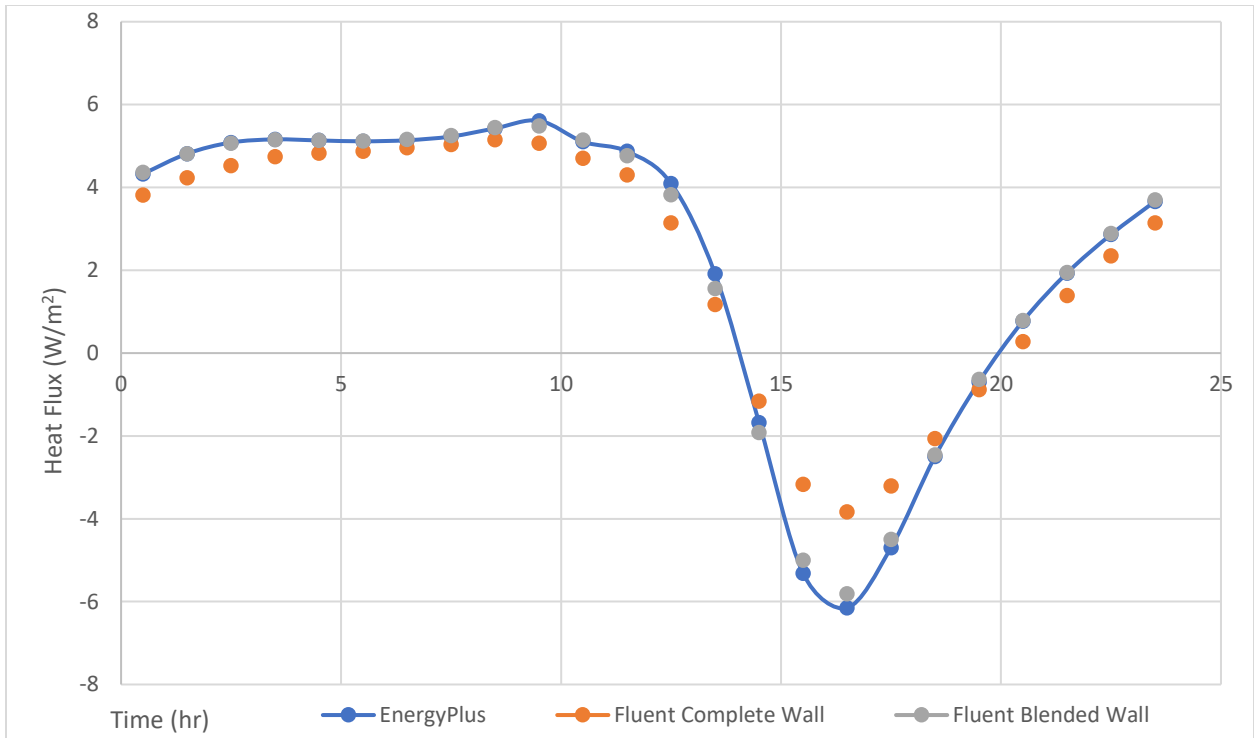


Figure 9. Comparison of heat flux 24-hour profiles at inner wall surface of full wall and blended wall for Winter day

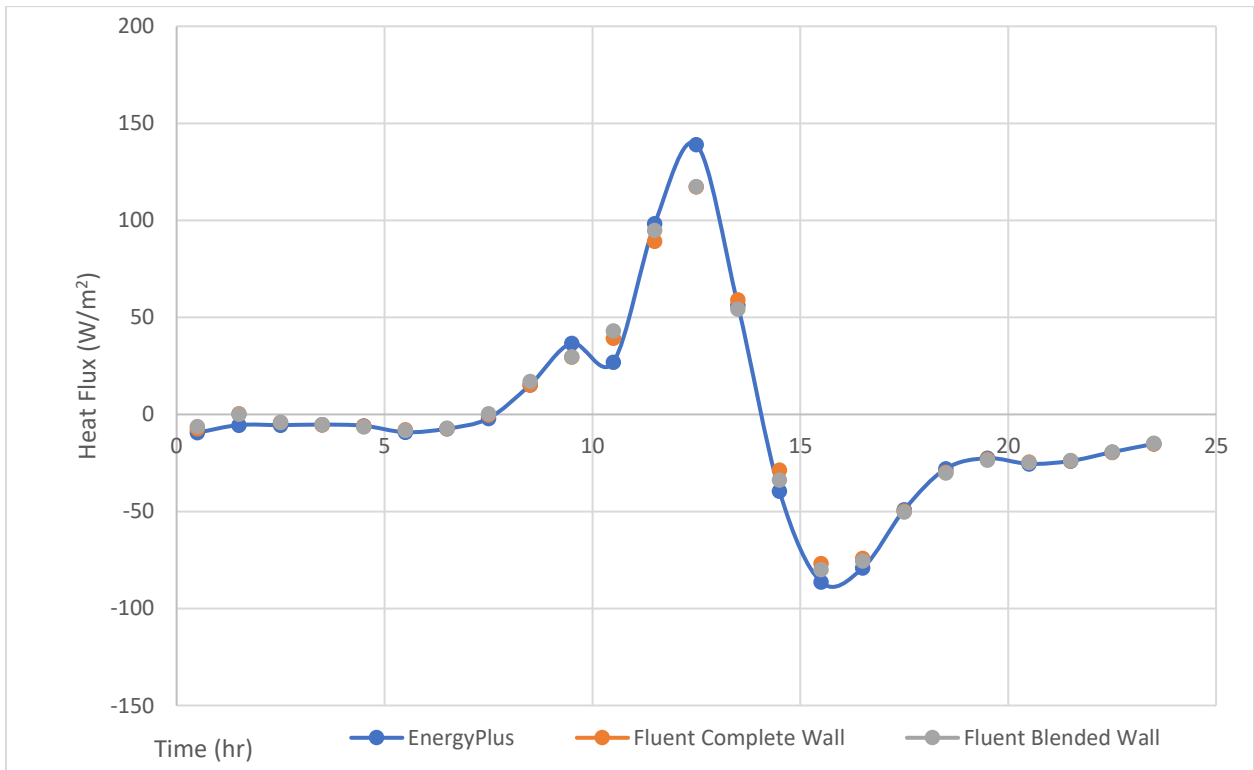


Figure 10. Comparison of heat flux 24-hour profiles at outer wall surface of full wall and blended wall for Winter day

Figure 12 shows that the heat flux on the outer wall surface on the Summer day is negative from 0 hours to 5 hours and this indicates that the heat is going outside the house as the outside is cooler than the house and its walls. Similarly, the heat flux on the inner wall surface is positive and is increasing at a steady rate from 0 hours to 5 hours as shown in Figure 11. At the the outer wall, the heat flux changes direction and the heat starts entering the outer wall surface as the solar radiations start picking up and it remains positive till 15 hours with the peak heat flux occurring at 10.5 hours. From 5 hours to 11.5 hours the inner wall surface continues to receive heat from inside the house but beyond 11.5 hours the heat flux at the inner wall changes directions and the house starts heating up from the radiation outside. This rejection of heat into the house continues until midnight.

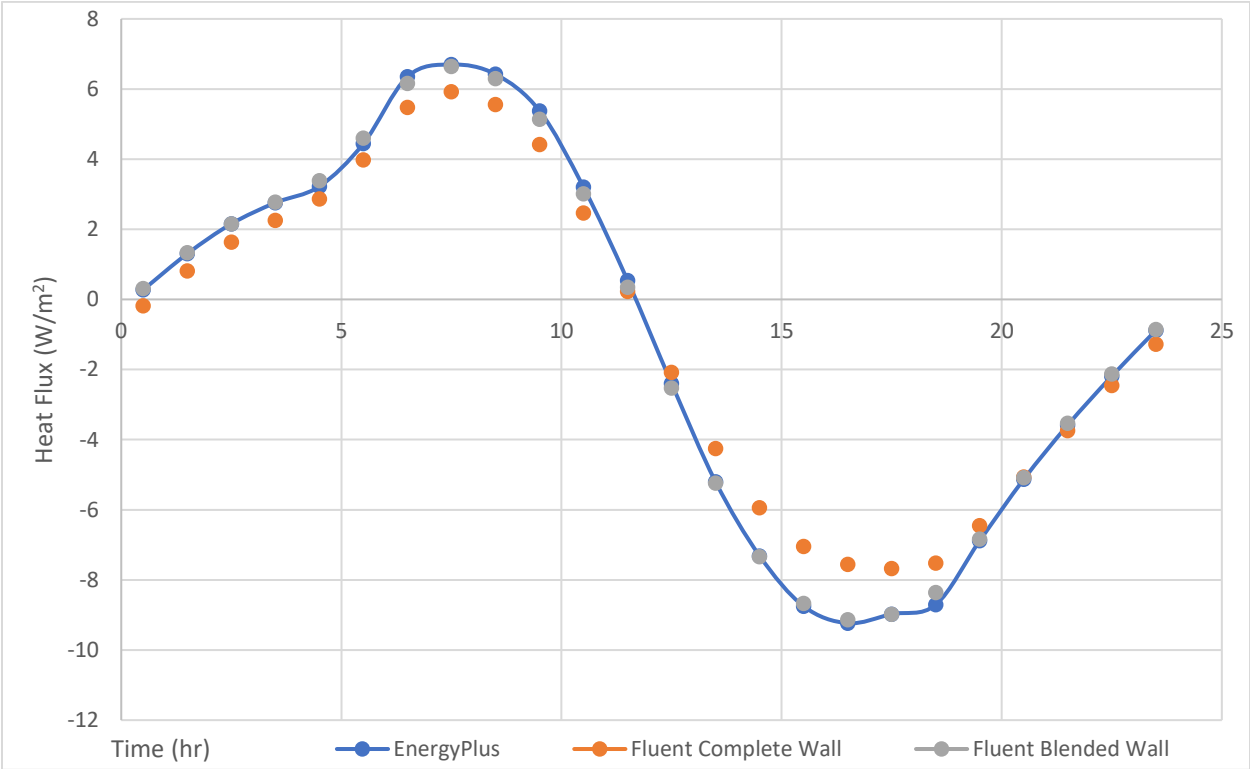


Figure 11. Comparison of heat flux 24-hour profiles at inner wall surface of full wall and blended wall for Summer day

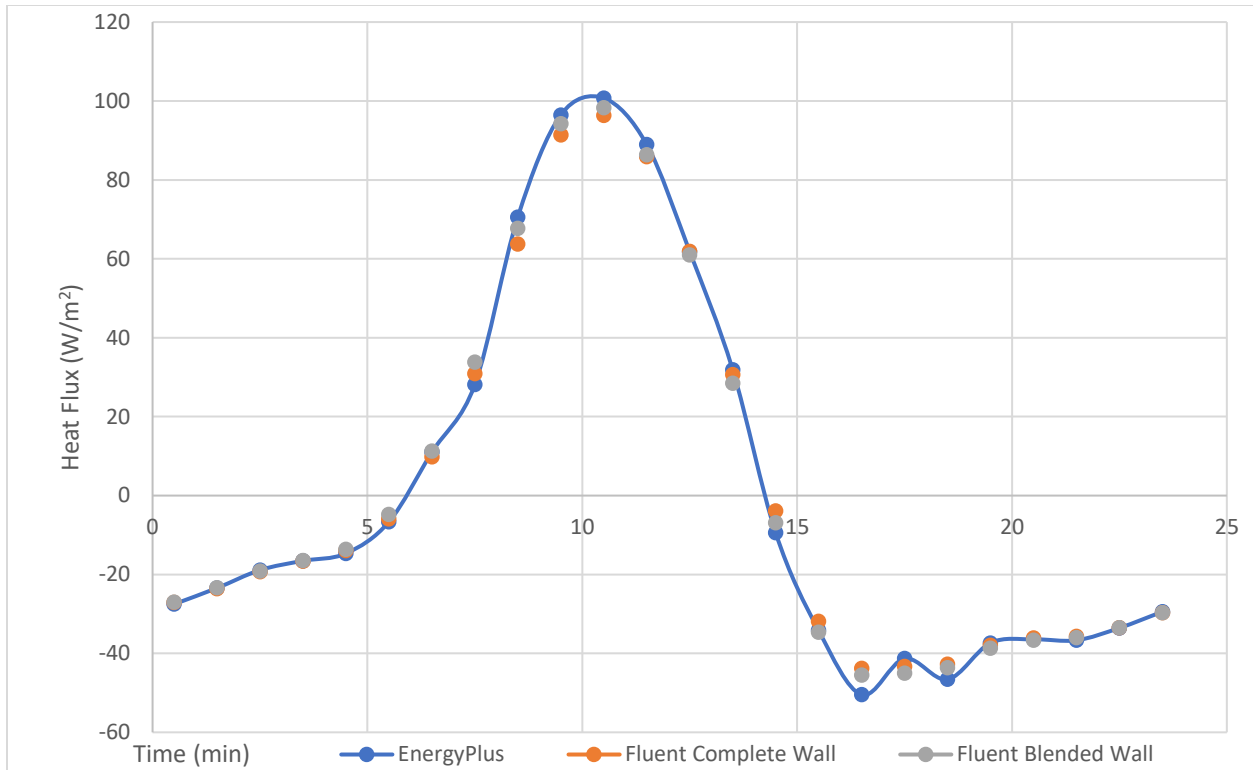


Figure 12. Comparison of heat flux 24-hour profiles at outer wall surface of full wall and blended wall for Summer day

Figure 14 shows that between 0 hours to 5 hours the outer wall surface is losing heat to the outside as the outside is cooler than the walls and the house on a Shoulder day. At the inner wall surface, heat flux is positive indicating that the heat is entering the surface from inside the house as shown in Figure 13. Solar radiation starts building up after sunrise and this is observed by the change in direction of the outer wall surface heat flux occurring at 6.5 hours and remains positive until 11.5 hours with the peak occurring at 9.5 hours. Between 5 hours and 10 hours the heat flux at the inner wall surface increases and then decreases until it changes direction at 12.5 hours. Between 12.5 hours and 17.5 hours, the inner wall surface heat flux is negative indicating that the heat is entering the house. Beyond 17.5 hours the heat flux changes direction again and this trend is similar to what is observed on the Winter day.

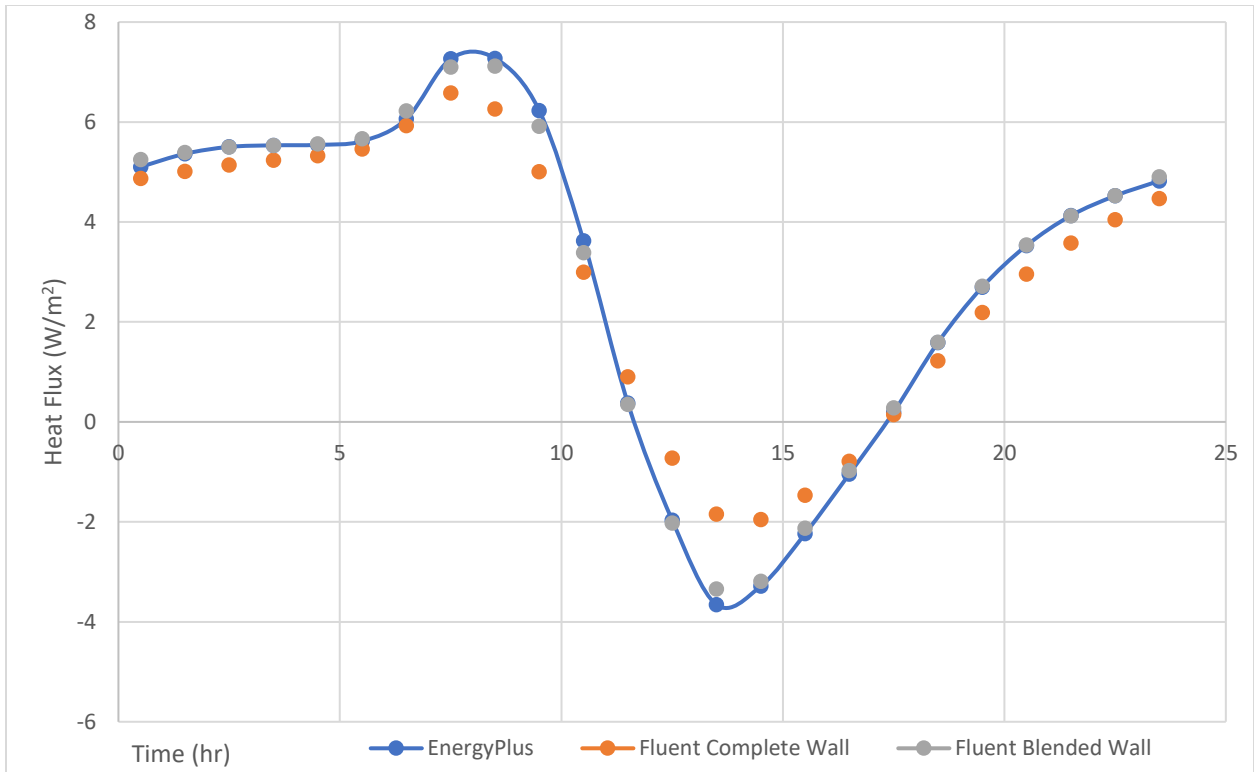


Figure 13. Comparison of heat flux 24-hour profiles at inner wall surface of full wall and blended wall for Shoulder day

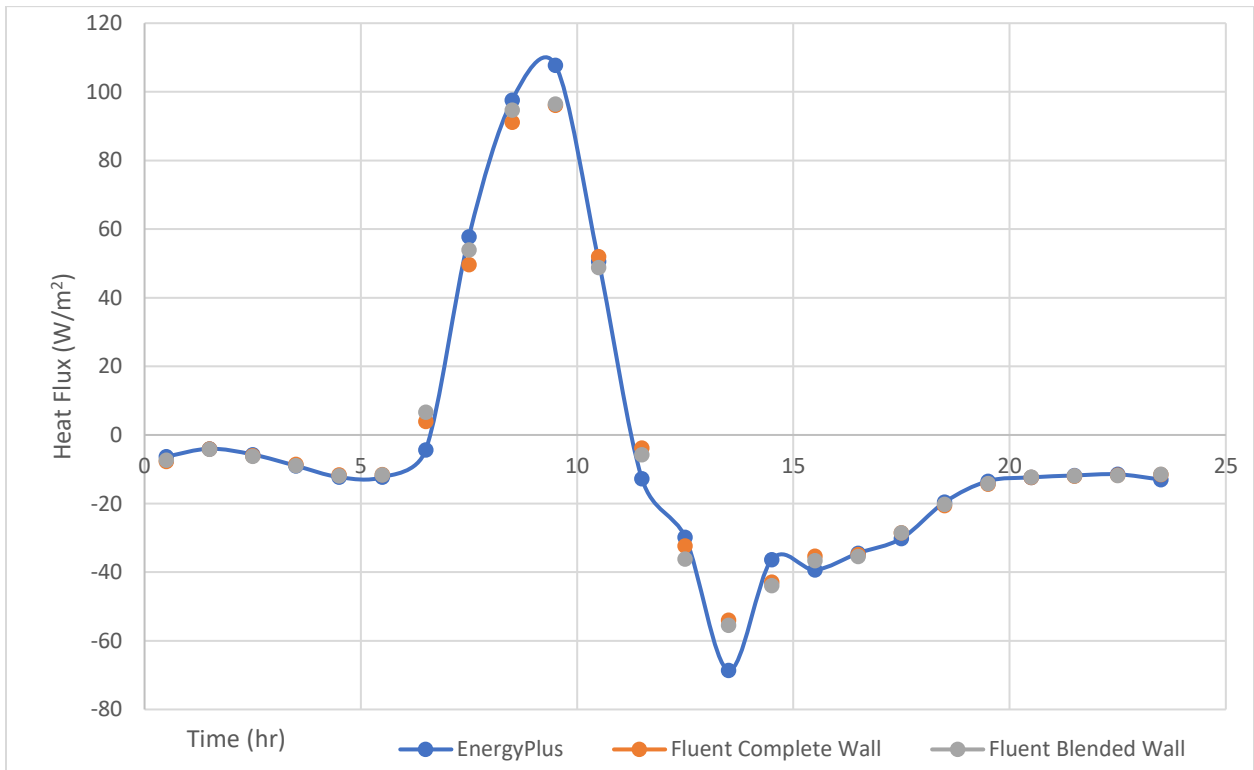


Figure 14. Comparison of heat flux 24-hour profiles at outer wall surface of full wall and blended wall for Shoulder day

Analyzing the figures it is evident that the Fluent Blended Wall model does indeed agree much better with the EnergyPlus model than the Fluent Complete Wall model. This is reflected in the mean average error which is 0.097 W/m^2 between the EnergyPlus model and the Fluent Blended Wall model and this is much lower than the average mean error between the EnergyPlus model and the Fluent Complete Wall model which is 0.65 W/m^2 for the Winter day at the inner wall surface. This trend is observed in the representative days of Summer and Shoulder as well at both the inner wall and outer wall. The difference between the behaviors of the Fluent Complete Wall model and the Fluent Blended Wall model is visible from 15 hours to 20 hours on the inner wall surface for the Winter day, 15 hours to 20 hours on the inner wall surface of the Summer day, and 11.5 hours to 16.5 hours on the inner wall surface of the Shoulder day. Even though there are differences in the magnitude of the heat flux between the three different models the times at which the peaks occur and the direction of the heat flux changes are well aligned.

Thus, the better agreement of the ANSYS Fluent Block Wall model with the EnergyPlus model meant that, henceforth, all the models with PCM attached to the inner wall were simulated with a block wall geometry with an appropriate PCM layer on the inner side.

Block Wall No PCM with Inner Wall Convective Boundary Condition

It was decided that moving forward the Fluent Block Wall will be used for PCM 1 and PCM 2 simulations where the PCM was applied to the inner wall. For PCM 1 cases, the temperature profile boundary conditions were applied at both the walls and these were generated using EnergyPlus. But for the cases with PCM 2 there were no EnergyPlus generated temperature profiles that could be used as a boundary condition. Thus, for modeling PCM 2 the outer walls used the temperature profile boundary condition obtained from the No PCM cases of the corresponding representative day. This was done because it was

observed that for the No PCM case and the different PCM 1 cases the temperature profiles for the outer wall were almost the same with no significant changes caused by the presence or absence of the PCM. The inner wall boundary condition used for PCM 2 cases was a convective boundary condition. This meant that additional Fluent Block Wall with No PCM models had to be developed using an inner wall convective boundary condition as well. These models helped in better comparing the performance of PCM 2 cases with the No PCM cases as they had the exact same boundary conditions as the PCM 2 cases.

The Fluent Block Wall with No PCM and inner wall convective boundary condition had the exact same modeling domain, mesh, solver settings, material properties, and outer wall boundary condition as the Fluent Block Wall with No PCM and temperature boundary conditions at both walls. The only change was the inner wall boundary condition was changed to a convective boundary condition.

Setting the inner wall boundary conditions to convective boundary condition required two inputs the convection heat transfer coefficient (h_c in W/m^2K) and the free stream temperature ($T_{\infty,indoor}$ in K). The convective heat transfer coefficient was determined using the mixed and forced convection model for ceiling diffuser configurations that gave different relations for the convective heat transfer coefficient at the ceilings, walls, and floor based on the empirical correlation developed by [33]. The correlation for used for the walls was:

$$h_c = 1.208 + 1.012 * ACH^{0.604}$$

where, ACH stands for air changes per hour. ASHRAE recommends that homes receive 0.35 ACH but not less than 15 cubic feet of air per minute per person as the minimum ventilation rate in residential buildings. Thus, the ACH was set equal to 0.35 and the corresponding convective heat transfer coefficient for the walls with ceiling diffuser configurations is 1.744 W/m^2K . The free stream temperature was the other input that was needed for the convective boundary condition. The free

stream temperature was set to 19.5°C for Winter representative days and 25.5°C for Summer representative days.

Results with Inner Wall Convective Boundary Condition during Winter and Summer

Figure 15 shows the temperature profile of the inner wall surface during the Winter representative day. Between 0 hours to 10 hours the temperature gradually drops from 291K to 290K at 7.5 hours and remains constant until it reaches 10 hours. The outer wall heat flux in this case follows the exact same trends as seen in Figure 10. Sunrise occurs at around 7.3 hours and the outer wall temperature starts increasing rapidly and the effect reaches the inner wall surface at 10 hours. Between 10 hours and 16.8 hours the temperature of the inner wall surface increases to 294.5K and then drops steadily to 291K at 24 hours as seen in Figure 15.

Figure 16 shows the inner wall surface heat flux profile during the Winter representative day. Between 0 hours and 10 hours the heat flux rises steadily from 3 W/m² to 4.6 W/m² which means that during the heat iflows from the inside the house into the walls. Both Figure 15 and Figure 16 show sudden changes occurring 10 hours and this is due the impact of the solar radiation reaching the inner wall surface. Between 10 hours and 14.5 hours the heat flux changes from 4.6 W/m² to -0.12 W/m² and this indicates that during this time the amount of heat leaving the inside of house reduces. At 14.5 hours the heat flux has changed direction and now the heat is traveling from the walls into the house. Between 14.5 hours and 20.5 hours the heat flux is entering the house and the goal is to maximize this period with the use of PCMs. Another goal of using the PCMs is increasing the amount of heat traveling from outside to inside so that the heaters do not need to be turned ON during these times. Beyond 20.5 hours the heat flux becomes positive again and the heat travels from inside the house into the walls.

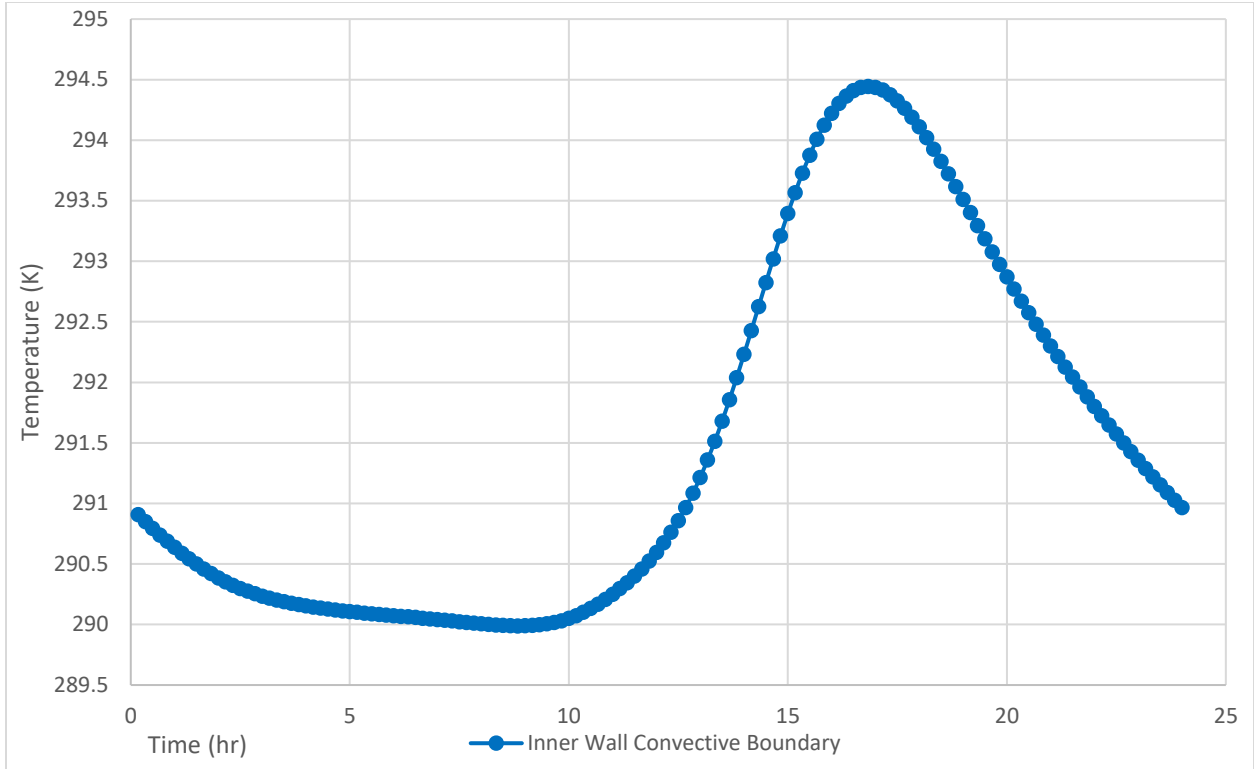


Figure 15. 24-hour temperature profile at inner wall surface on a typical Winter day with inner wall convective boundary condition

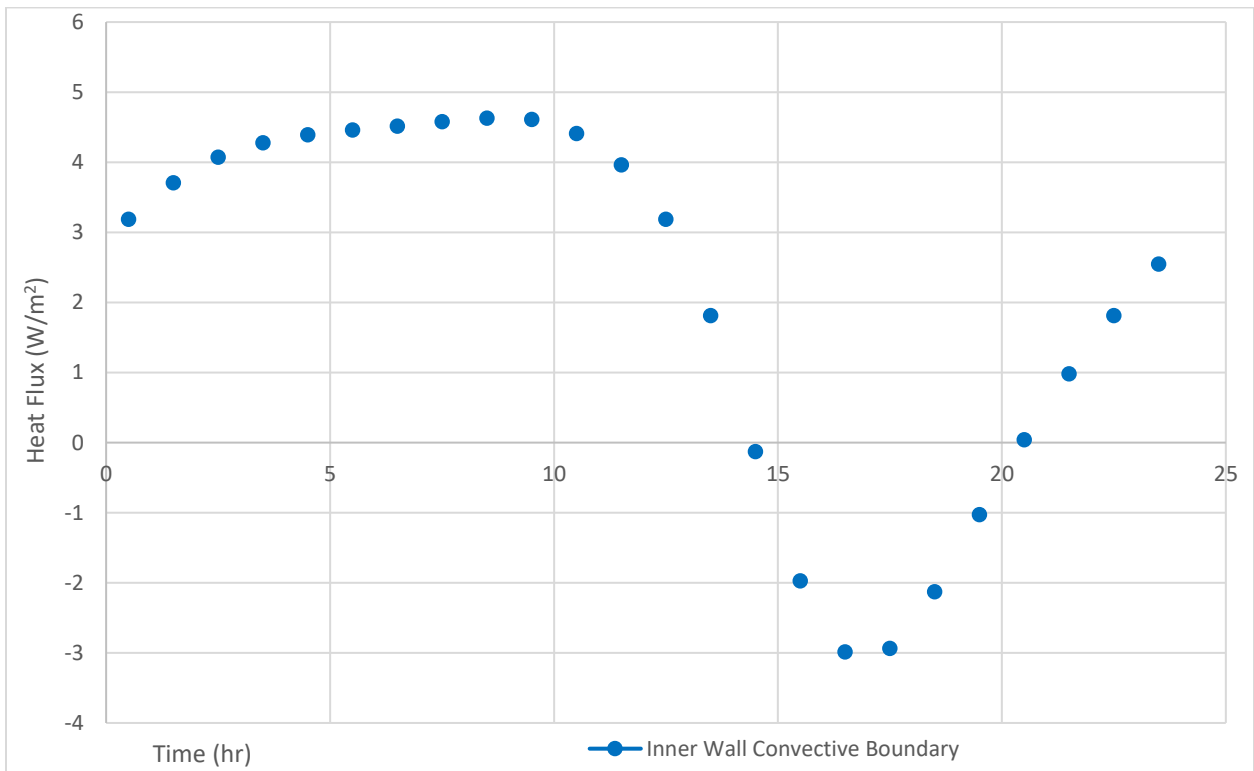


Figure 16. 24-hour heat flux profile at inner wall surface on a typical Winter day with inner wall convective boundary condition

Figure 17 shows the inner wall surface temperature profile during a representative Summer day. Between 0 hours and 8.5 hours the temperature drops from 299.3K to 296.4K. At 8.5 hours the temperature starts increasing and this is the effect of sunrise reaching the inner wall surface. Between 8.5 hours and 17.5 hours the inner wall surface temperature increases at a constant rate to 302K and this corresponds to the heat gained from the solar radiation traveling through the wall. Beyond 17.5 hours the temperature again starts dropping and reaches 299K at 24 hours. The trend is similar to what is seen during a representative Winter day but magnitudes of temperature fluctuation are different.

The heat flux on the outer wall surface during a representative Summer day is with the inner wall convective boundary condition is exactly the same as Figure 12. Figure 18 shows the inner wall surface heat flux profile during a representative Summer day. Between 0 hours and 1.5 hours the heat flux is negative and this indicates that the heat is entering the house from the walls. Between 1.5 hours to 8.5 hours the heat flux is positive and increasing indicating that heat from inside the house is entering the walls and beyond 8.5 hours the heat flux is still positive but now is decreasing in magnitude. At 8.5 hours the heat flux starts decreasing and the inner wall surface temperature starts increasing at the same time. Between 8.5 hours and 12 hours the heat flux is decreasing in magnitude. Between 12 hours to 18.5 hours the heat is negative and increasing in magnitude indicating that during this time more and more heat is entering the house from the walls. Beyond 18.5 hours to 24 hours the heat is still entering the house but the amount of heat entering is reducing with time. The goal of adding PCMs to the house in Summer is reducing the heat rejection into the house so that the cooler is turned for a less hours and less energy is expended in cooling.

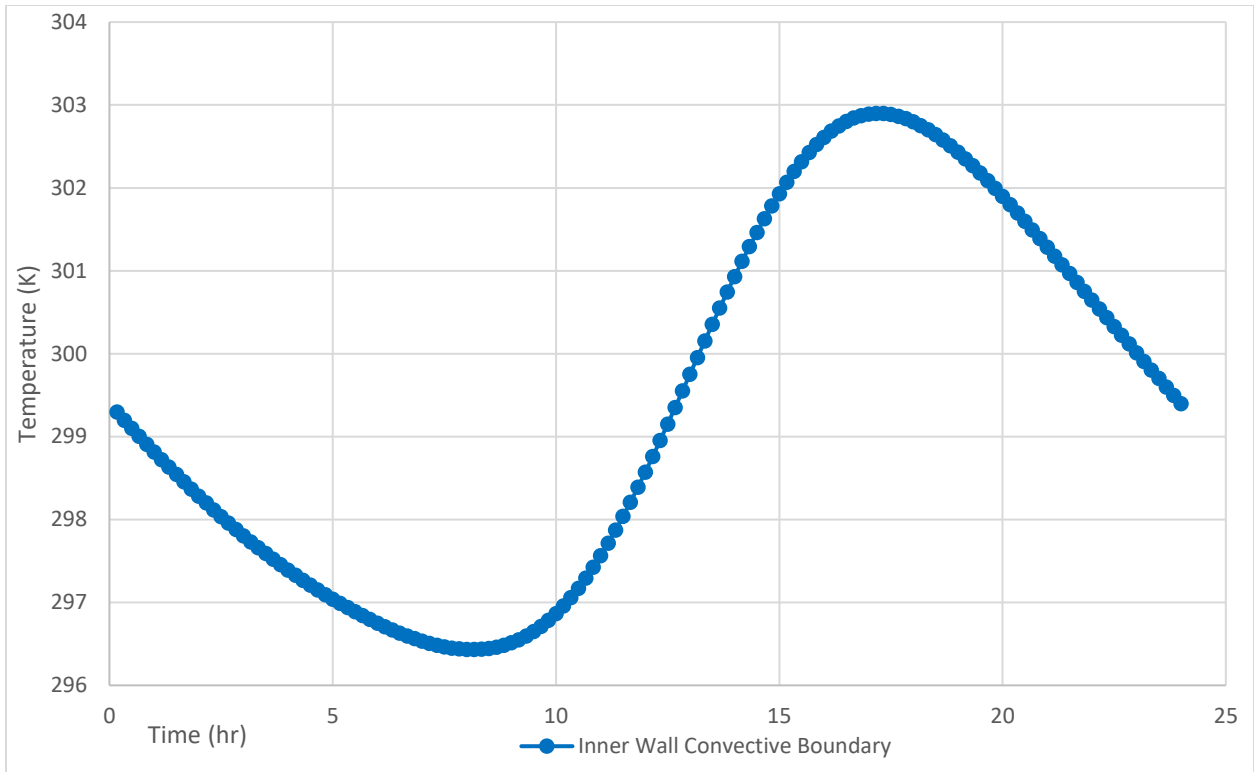


Figure 17. 24-hour temperature profile at inner wall surface on a typical Summer day with inner wall convective boundary condition

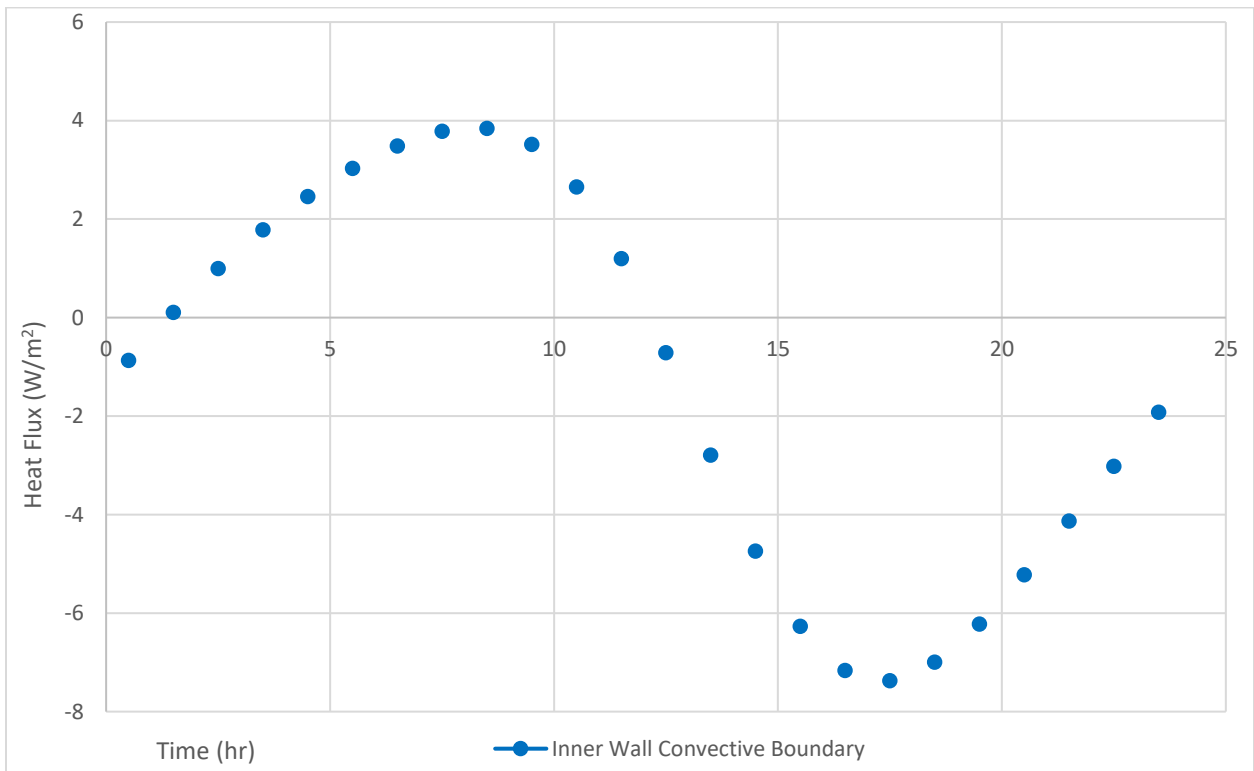


Figure 18. 24-hour heat flux profile at inner wall surface on a typical Summer day with inner wall convective boundary condition

Chapter 4: PCM 1 Simulations

PCM 1 Background

PCM 1 is a spackle-type product that can be applied to the inside wall surface in different thicknesses with the maximum thickness being limited to 9mm. PCM 1 consists of 53% of PCM that is encapsulated inside the spackle and when this mixture is applied over the wall surface it dries as a solid layer. The PCM is well-retained inside the spackle and thus, the PCM 1 product holds its form even when the encapsulated PCM is melted. The density and thermal conductivity specific heat capacity of PCM 1 were available for modeling as shown in Table 4. The specific heat capacity variation with temperature was available but no information of PCM 1's viscosity was available. Thus, PCM 1 was modeled as a solid with varying heat capacity. This approach allowed accounting for the absorption and release of energy during the melting and solidification processes.

Table 4. Thermophysical properties of PCM 1

| Thermophysical Property | Temperature Range | Value |
|------------------------------|-------------------|-------|
| Density (kg/m ³) | 273.15K-400K | 970 |
| Thermal Conductivity (W/mK) | 273.15K-400K | 0.1 |

The specific heat capacity vs. temperature curve was provided by the manufacturer as shown in Figure 19. The melting region consists of two peaks and the range of this region is approximately from 280K (6.85°C) to 300K (26.85°C). The two peaks indicate that PCM 1 contains a blend of 2 different PCM materials and this contributes to the width of the melting region. The width of the melting region for PCM 1 is significantly larger than PCM 2 for which the melting range is from 294.15K (21°C) to 295.95K (21.8°C). This large melting range meant that it needed PCM 1 temperature to increase or decrease by 20K (20 °C) in a single 24-hour cycle and this was challenging considering the small temperature range in

which the inner wall surface temperature varied for the No PCM cases. Another observation that can be made is the difference in the magnitude of the two peaks indicate that the 2 PCMs blended have different latent heats of fusion.

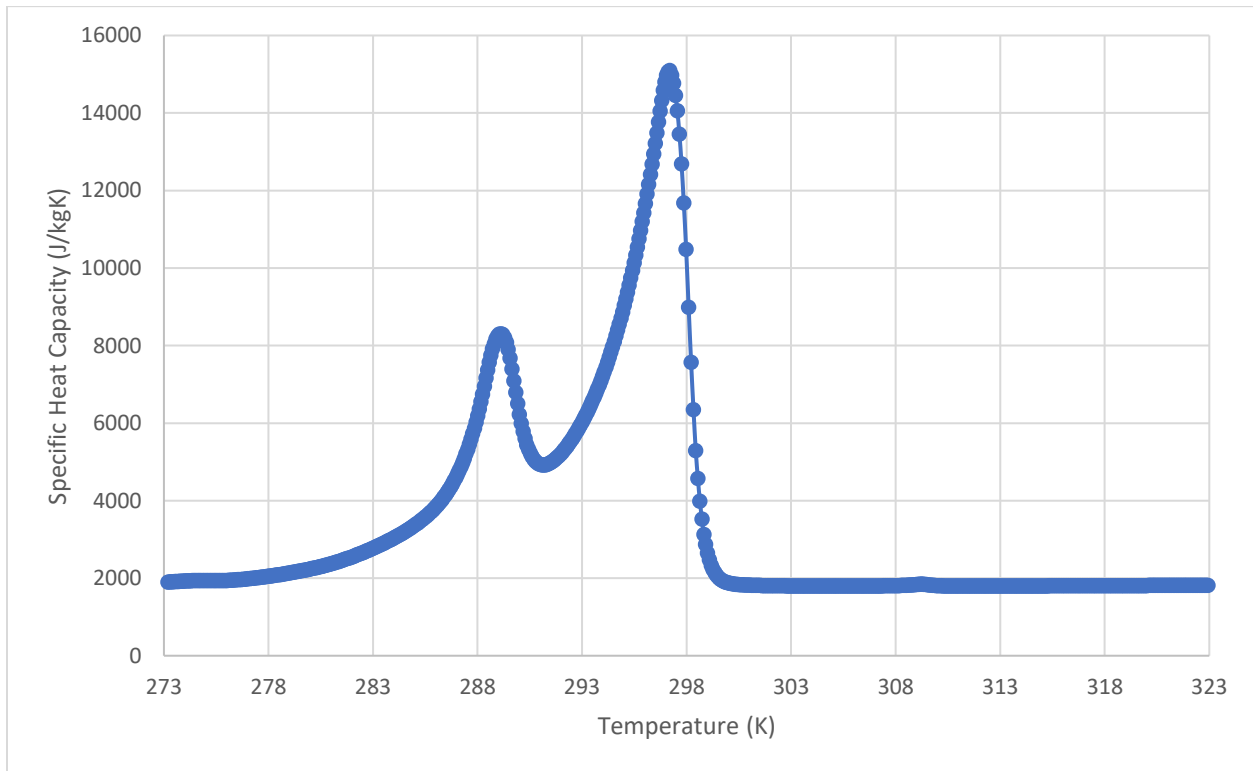


Figure 19. Specific heat versus temperature curve for PCM 1

Modeling Approach for PCM 1

Based on the limitations of ANSYS Fluent in assigning material properties and to accurately capture the variation of the specific heat capacity with temperature a user-defined function (UDF) was used to model the specific heat capacity of PCM 1. Initially, the curve was broken into 8 smaller curves using the 6th order polynomial interpolation and the equation for each curve was obtained by using MS-Excel. These equations were then assembled to recreate the specific heat capacity vs. temperature curve of PCM 1 using a simple code in C to generate the UDF. The results from the simulation using this UDF

showed unrealistic PCM 1 behavior. ANSYS Fluent rounds of the coefficients of the 6th order polynomial to 7 significant digits. This round-off error limits the ability of the UDF to replicate the specific heat capacity vs. temperature curve. Thus, the curve was broken into 17 smaller curves using 2nd order polynomials. While creating the smaller curves it was ensured that the coefficients when rounded off to 7 significant digits will not cause large round-off errors. The UDF generated with equations from the 2nd order polynomial combined accurately captured the behavior in ANSYS Fluent and this was reflected in the realistic behavior of the PCM 1. Table 5 shows the different temperature ranges in which the curve is broken into and the 2nd order polynomial or linear equations for each curve. For temperatures above and below the range in Table 5 the specific heat capacity of PCM 1 has a constant value of 1825 J/kgK.

Table 5. Specific heat equation for different temperature ranges for PCM 1

| Range (K) | Equation (J/kgK) |
|-------------------|---|
| 270.031 - 272.944 | $C_p=1.85455*(T^2) - 963.4818*(T) + 126716.6$ |
| 273.027 - 274.942 | $C_p=-8.7484*(T^2) + 4819.147*(T) - 661719.7$ |
| 275.026 - 275.942 | $C_p=8.38721*(T^2) - 4623.529*(T) + 639134.5$ |
| 276.025 - 280.931 | $C_p=10.3844*(T^2)-5698.913*(T)+783803$ |
| 281.014 - 285.98 | $C_p=31.37585*(T^2) - 17510.48*(T) + 2445373$ |
| 286.062 - 287.928 | $C_p=363.4688*(T^2) - 207497.3*(T) + (2.961781*(10^7))$ |
| 288.008 - 288.638 | $C_p=2516.566*(T) - 718618.2$ |
| 288.717 - 289.555 | $C_p=-2929.693*(T^2) + 1693904*(T) - (2.448392*(10^8))$ |
| 289.645 - 290.698 | $C_p=1522.384*(A2^2) - 885740.9*(A2) + (1.288386*(10^8))$ |
| 290.783 - 292.272 | $C_p=385.4055*(T^2) - 224423.6*(T) + (3.267569*(10^7))$ |
| 292.354 - 295.957 | $C_p=297.8632*(T^2) - 173622.9*(A2) + (2.530626*(10^7))$ |
| 296.035 - 296.802 | $C_p=3482.385*(T) - 1019278$ |
| 296.879 - 297.464 | $C_p=-6644.557*(T^2) + 3948950*(T) - (5.867135*(10^8))$ |
| 297.557 - 298.097 | $C_p=-7307.384*(T^2) + 4343271*(T) - (6.453597*(10^8))$ |
| 298.215 - 298.635 | $C_p=8168.112*(T^2)-4883675*(T)+(7.299846*(10^8))$ |
| 298.73 - 299.432 | $C_p=2529.154*(T^2) - 1514824*(T) + (2.268262*(10^8))$ |
| 299.517 - 300.104 | $C_p=329.9978*(T^2) - 198138.7*(T) + (2.97437*(10^7))$ |

The amount of PCM applied on the inner wall surface plays a significant role in maximizing the energy savings and affects the cost of retrofitting. If the PCM applied on the inner wall surface is less than the

optimal amount then the energy absorbed by the PCM layer will also be less and thus, the effectivity of PCM in reducing energy consumption will be lowered. To better understand the impact of the PCM 1 quantity on energy savings and cost of retrofitting three different cases with 3mm, 6mm, and 9mm thick PCM 1 layers were simulated, and their performance was compared.

Modeling Domain

The modeling domain for the PCM 1 simulations was exactly like the Blended Wall model for the No PCM cases but with an additional layer of PCM 1 on top of the gypsum layer. The PCM 1 layer had different thickness of 3 mm, 6mm, or 9 mm depending on case being run. Figure 20 shows cross sectional view Blended Wall model for PCM 1.

Wall Material Properties

The thermophysical properties of gypsum, stucco, and plywood are given in Table 2. The thermophysical properties of the blended layer are calculated based on the mass-weighted thermophysical properties of the insulation and the stud and are given in Table 3. The density and thermal conductivity of PCM 1 are provided in Table 4 and the specific heat capacity variation with temperature is captured using the UDF and the details of it are provided in Table 5.

Boundary Conditions

The boundary conditions applied on the PCM 2 cases were exactly like the boundary conditions imposed on the No PCM cases. As shown in Figure 3, the insulated boundary condition was imposed on Surfaces

1 and 2, the symmetry boundary condition was imposed on Surfaces 3 and 4, Inner Wall surface temperature profile obtained from EnergyPlus on Surface 5, and Outer Wall surface temperature profile obtained from EnergyPlus on Surface 6. The only difference was that the profiles obtained from EnergyPlus for the PCM 1 cases were different than the No PCM cases. Additionally, there were slight differences in the temperature profiles of the 3mm, 6mm, and 9mm PCM 1 cases.

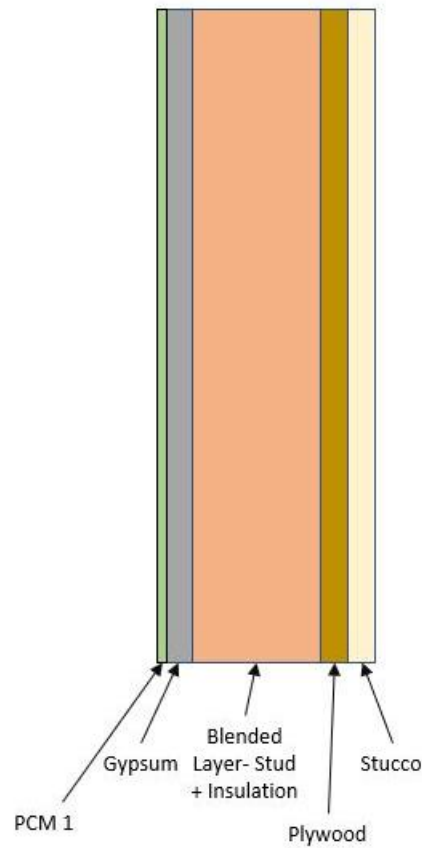


Figure 20. Blended wall model with PCM 1 layer next to Gypsum layer

Initial Conditions and Simulation Time

The initial conditions and simulation time for the PCM 1 cases were exactly like the No PCM cases. The 24-hour temperature profiles are run consecutively for 3 days. The identical heat flux profiles of day 2

and day 3 that obtained as an output were used to ensure that the simulation results were independent of the initial condition.

Solver Settings and Mesh Quality

The SIMPLE scheme was used for pressure-velocity coupling. A second-order implicit scheme was used for the transient formulation. The use of an implicit scheme ensured there is no possibility of the calculations becoming unstable and this also provided greater flexibility in selecting the time step size. The time step used in these simulations was 300 seconds and the solutions were recorded after every 2-time steps. The total number of elements in the mesh was 462500, maximum skewness of the mesh was 1.3×10^{-10} , and average skewness of the mesh was 1.3×10^{-10} .

PCM 1 Winter Results

Based on the conclusions drawn in the previous section regarding the differences between the Fluent Blended Wall and the Fluent Complete Wall the simulations henceforth with the PCM located at the inner surface were carried out using the Fluent Blended Wall geometry.

Figure 21 and Figure 22 show the surface temperature boundary conditions applied to the Fluent Blended Wall model, based on EnergyPlus simulations of a typical winter day in Climate Zone 9 in California. Figure 21 shows the different inner wall surface temperatures throughout 24-hours for a typical Winter day. It can be observed that the maximum temperature and minimum temperature at this location occurs with the No PCM case. This is expected as adding the PCM layer adds to the thermal mass of the wall section. The PCM 1 3mm case shows the highest diurnal temperature variation amongst the PCM cases and the PCM 1 9mm case shows the lowest temperature variation amongst the

PCM cases. This too can be explained using the argument of added thermal mass. The temperature of PCM 1 varies from 291K to 293.5K at the inner wall surface in the Winter day simulations. As PCM 1 has a wide melting range the effect of latent heat cannot be observed clearly as a plateau in temperature of the inner wall. The time at which the highest temperature at the inner wall surface occurs is shifted from 15.5 hours in the No PCM case to 17.5 hours in the PCM 1 9mm case. Figure 22 shows the different outer wall surface temperatures throughout 24-hours for a typical Winter day. It can be observed that the outer wall surface temperature is the same for all the cases. The outer wall temperature starts to increase at the 8.5-hour mark and the rate of increase becomes steeper after the 10-hour mark. The effect of this is observed at the inner wall surface temperature.

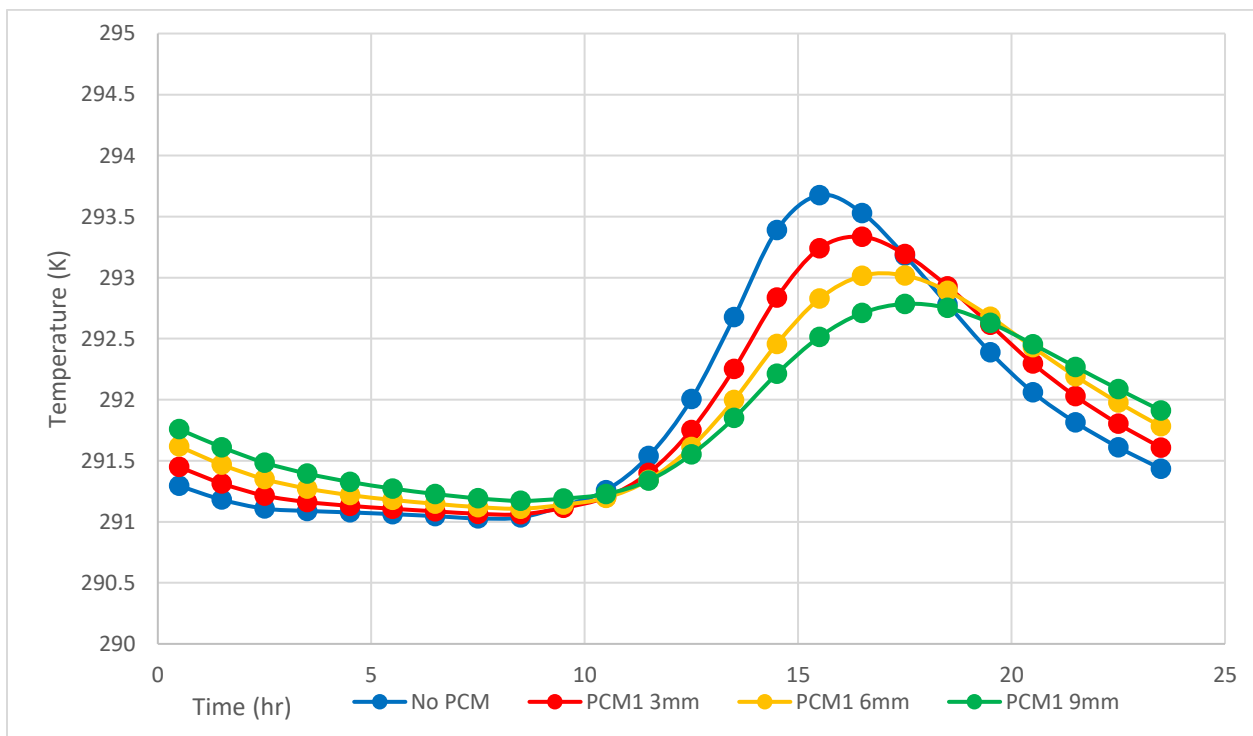


Figure 21. Comparison of inner wall surface temperature profiles for No PCM, 3mm PCM 1 layer, 6mm PCM 1 layer, and 9mm PCM 1 layer for a Winter day

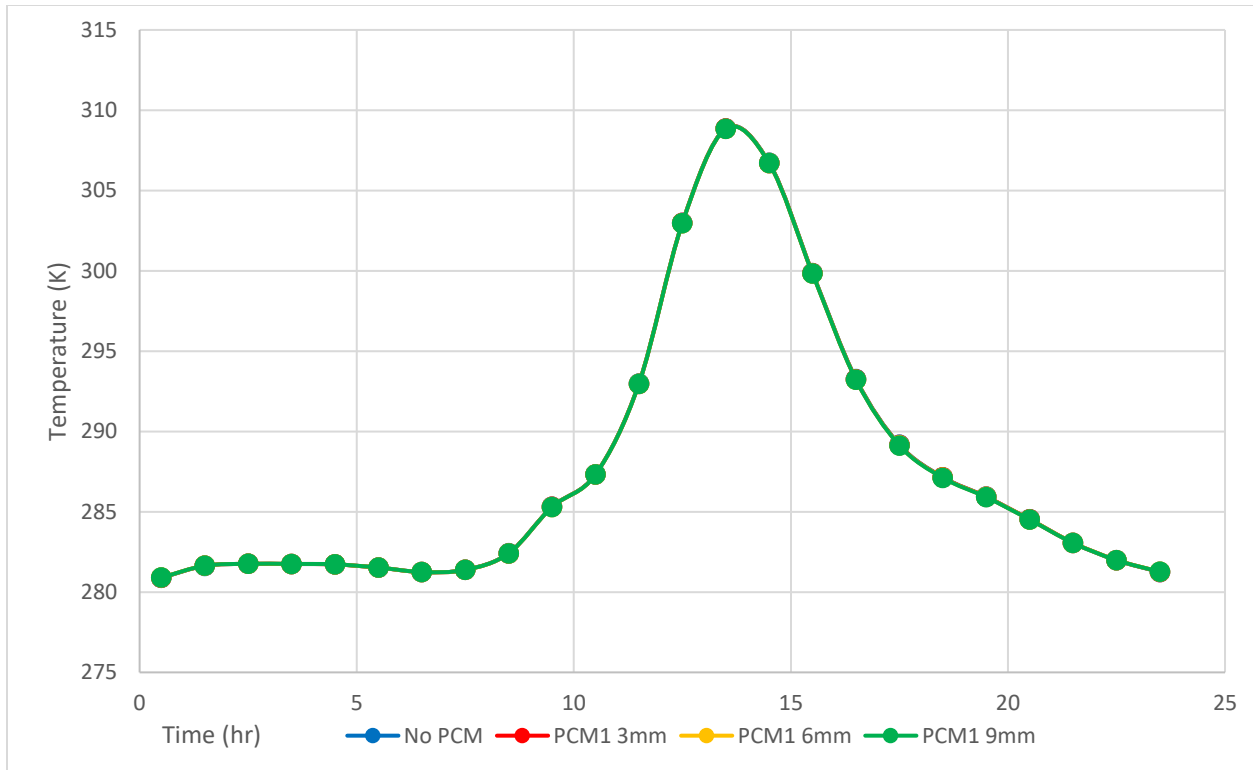


Figure 22. Comparison of outer wall surface temperature profiles for No PCM, 3mm PCM 1 layer, 6mm PCM 1 layer, and 9mm PCM 1 layer for a Winter day

The temperature at the inner wall surface for the PCM cases ranges between 291K and 293.5K. Although this is not the mass averaged temperature of PCM 1 it gives an approximate understanding of how the specific heat capacity varies during these simulations. Between 290K and 295K the specific heat capacity of PCM 1 varies approximately from 4900 J/kgK to 8000 J/kgK as seen in Figure 19. The change in specific heat capacity in this range is not significant enough to have a strong impact on the heat transfer characteristics of the wall and this can be observed from the heat flux profiles of the inner wall .

Figure 23 shows the heat flux profiles at the inner wall surface over the 24-hour duration for a typical Winter day. From 0 hours to 10 hours the heat flux does not change very much and lies in the 4-6 W/m². During this time the heat flux of the different PCM 1 cases and the No PCM case is almost the same. Between 10-14 hours the heat flux is highest for the No PCM case and reduces in magnitude as the PCM quantity increases. This indicates that the addition of the PCM reduces the heat flux leaving the house and this heat is stored in the PCM. The decrease in the heat flux at the inner wall surface occurs at the

same time as the outer wall temperature starts to rapidly increase. Between 14.5-20 hours the heat flux changes direction and the heat starts entering the house from the outside and thus, the heat flux at the inner wall surface is negative. Between 15-20 hours the magnitude of heat flux differs between the No PCM and different PCM cases. With the highest heat flux occurring in the No PCM case and the lowest heat flux occurring in the PCM 1 9 mm case. The cumulative heat flux over the 24 hour period to the inner wall surface from inside the house is $196,478.9 \text{ J/m}^2$ for the No PCM case, $193,084 \text{ J/m}^2$ for the PCM 1 3mm case, $189,917 \text{ J/m}^2$ for the PCM 1 6mm case, and $186,813 \text{ J/m}^2$ for the PCM 1 9mm case. These values show that adding PCM has very minor impacts (< 2% reduction in heat flux) on the heat entering the inner wall surface from inside the house. PCM 1 shows the difference in the heat flux profiles only from 10-20 hours and the differences in magnitude at each time are also very small. The time at which the changes in direction of the heat flux occurs are also closely aligned and thus, adding PCM 1 does not make a huge difference in this climate zone in winter. Figure 24 shows the heat flux profiles at the outer wall surface over the 24-hour duration for a typical Winter day. The heat flux profiles exactly overlap each other and thus, no effect of adding PCM 1 is observed at the outer wall surface. It is important to observe that the magnitudes of the heat fluxes at the inner wall surface and outer wall surface differ significantly.

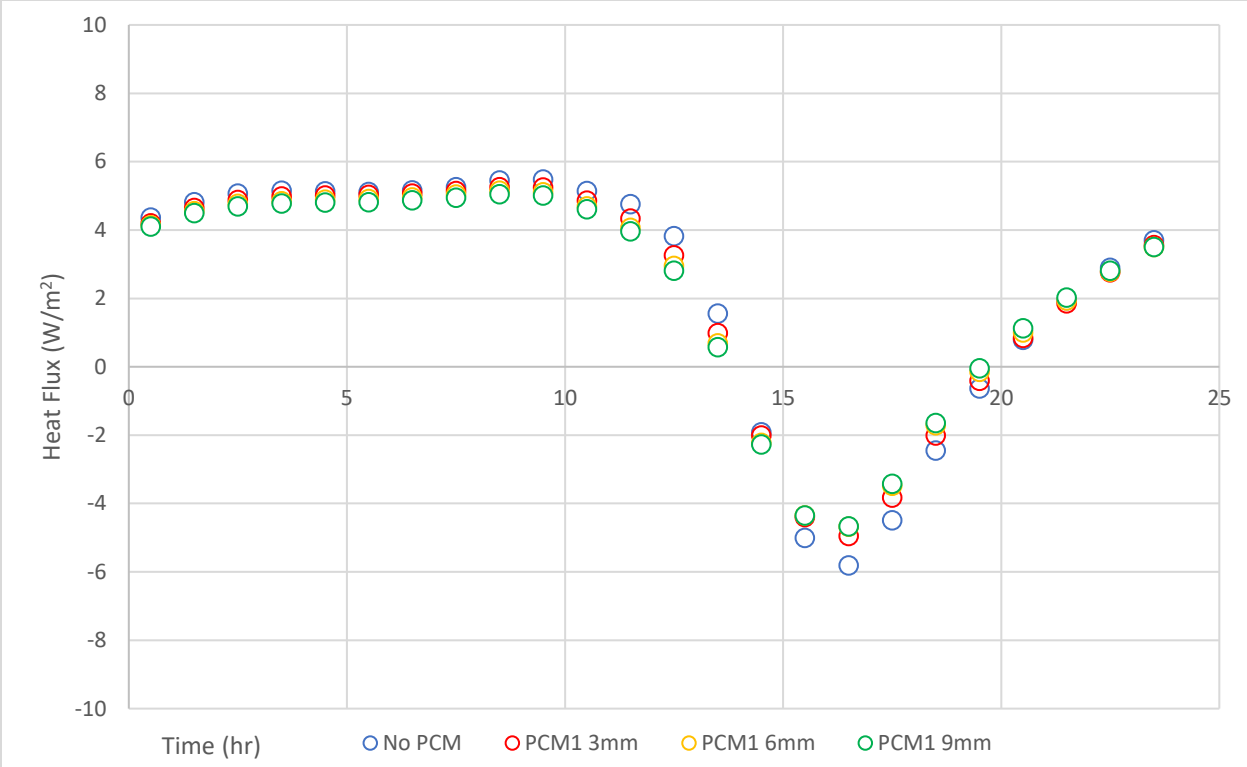


Figure 23. Comparison of inner wall surface heat flux profiles for No PCM, 3mm PCM 1 layer, 6mm PCM 1 layer, and 9mm PCM 1 layer for a Winter day

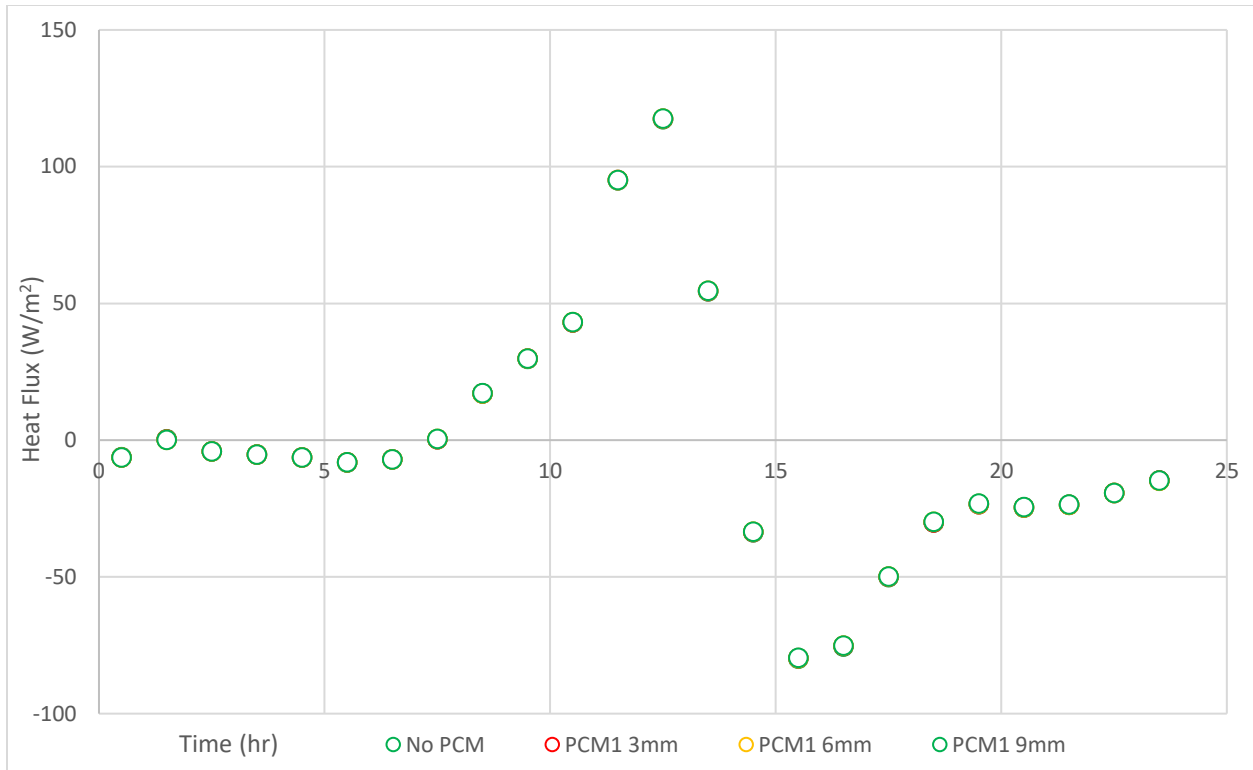


Figure 24. Comparison of outer wall surface heat flux profiles for No PCM, 3mm PCM 1 layer, 6mm PCM 1 layer, and 9mm PCM 1 layer for a Winter day

PCM 1 Summer Results

Figure 25 shows the different inner wall surface temperatures throughout 24-hours for a typical Summer day obtained from EnergyPlus simulations. As expected, the temperature range for a typical Summer day is much higher than the Winter day and this impacts the behavior of PCM 1. Similar to the Winter day the maximum variations in temperature are observed for the No PCM case and the variations reduce in magnitude as the quantity of PCM at the inner wall surface increases. This can be explained as the effect of increase the thermal mass of the wall. At the inner wall surface, PCM 1 temperature varies approximately from 298K to 301.5K. This consists of only a small portion of the melting range of PCM 1 and thus, the effect of the latent heat cannot be significantly observed in these simulations. Figure 26 shows the different outer wall surface temperatures throughout 24-hours for a typical Summer day. The outer wall temperature profile exactly overlaps each other. For the No PCM

case the inner wall temperature decreases sharply up to the 5.5-hour mark and after this, it increases strongly. This corresponds to the sudden increase in the outer wall surface temperature occurring beyond the 5-hour mark.

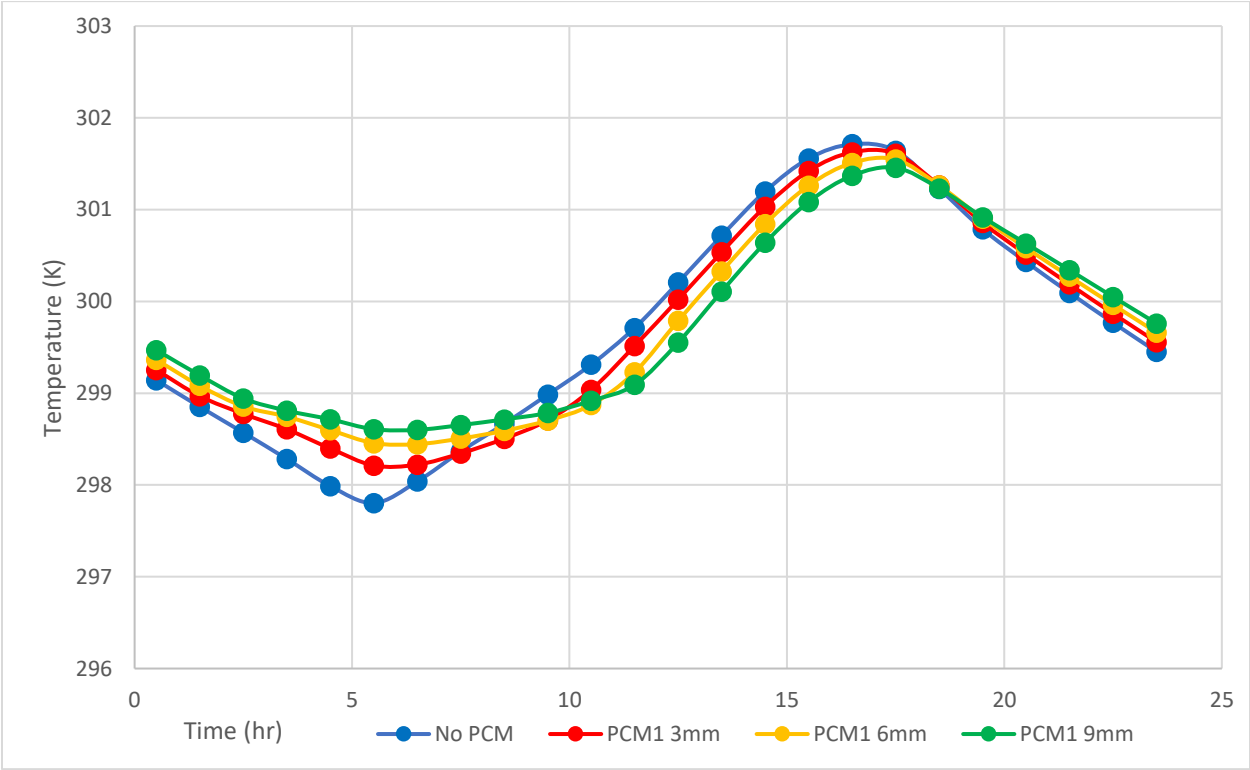


Figure 25. Comparison of inner wall surface temperature profiles for No PCM, 3mm PCM 1 layer, 6mm PCM 1 layer, and 9mm PCM 1 layer for a Summer day

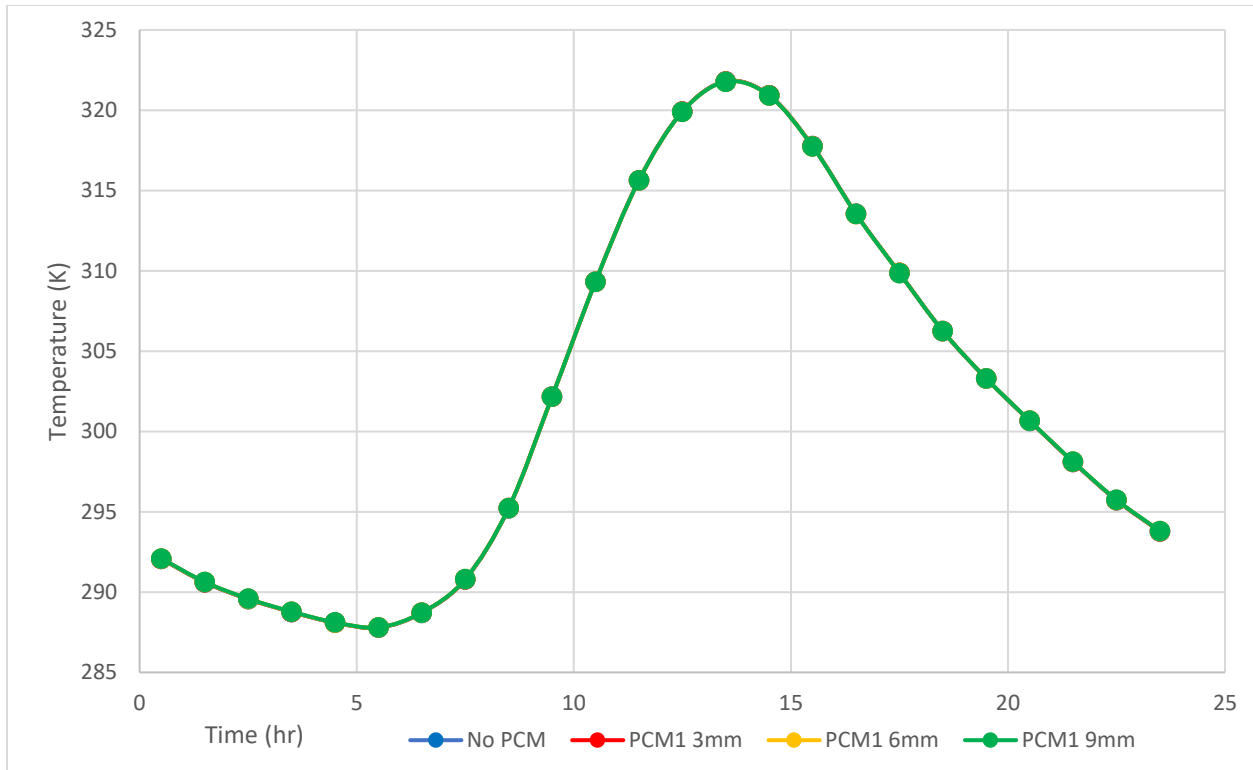


Figure 26. Comparison of outer wall surface temperature profiles for No PCM, 3mm PCM 1 layer, 6mm PCM 1 layer, and 9mm PCM 1 layer for a Summer day

The inner wall surface temperature varies from 298 K to 301.5 K. Although this is not the mass averaged temperature of PCM1, it gives an approximate understanding of the temperature range within which the PCM 1 temperature varies during the 24-hour cycle. Between 298 K and 301.5 K the specific heat capacity of PCM 1 goes from approximately 10,500 J/kg-K to 2,000 J/kg-K as seen in Figure 19. It is worth noting that between 298K and 299K the specific heat capacity reduces from 10500J/kgK to 2500J/kgK and this indicates that the specific heat capacity hardly varies between 299K and 301.5K. This variation is greater than in the Winter day but still not strong enough to significantly alter the heat transfer characteristics of the wall. The maximum temperature difference between the No PCM and the PCM 1 9mm case occurs at the 5.5-hour mark and this temperature corresponds to the highest specific heat capacity of PCM 1. The temperatures at other times have a smaller difference and this can be explained using the lower specific heat capacity of PCM 1.

Figure 27 shows the heat flux profiles at the inner wall surface over the 24-hour duration for a typical Summer day. From 0 hours to 2.5 hours and from 19.5 hours to 23.5 hours the heat flux at the inner wall surfaces are clustered very close to each other and during these times no effect of adding PCM 1 can be noticed in the heat flux profiles. From 6.5 hours to 18.5 hours the behavior of the No PCM case and the different PCM cases is different. With the No PCM case showing the highest heat flux values and the PCM 1 9mm case showing the lowest heat flux values between 6.5 hours and 9.5 hours and between 13.5 hours and 18.5 hours. Even with the PCM 1 9mm case, the difference in the heat flux magnitudes is not significant, and the time at which the heat flux changes direction also does not change by much. The cumulative heat leaving the inner wall surface and entering the house $-95,248 \text{ J/m}^2$ for the No PCM case, $-92,729 \text{ J/m}^2$ for the PCM 1 3mm case, $-90,796 \text{ J/m}^2$ for the PCM 1 6mm case, and -88949 J/m^2 for the PCM 1 9mm case. These values indicate that there is a drop of 6.7% in the cumulative heat leaving the inner wall surface and entering the house in the PCM 1 9mm case compared to the No PCM case. .

Figure 28 shows the heat flux profiles at the outer wall surface over the 24-hour duration for a typical Summer day. The heat flux profiles exactly overlap each other and thus, no effect of adding PCM 1 is observed at the outer wall surface.

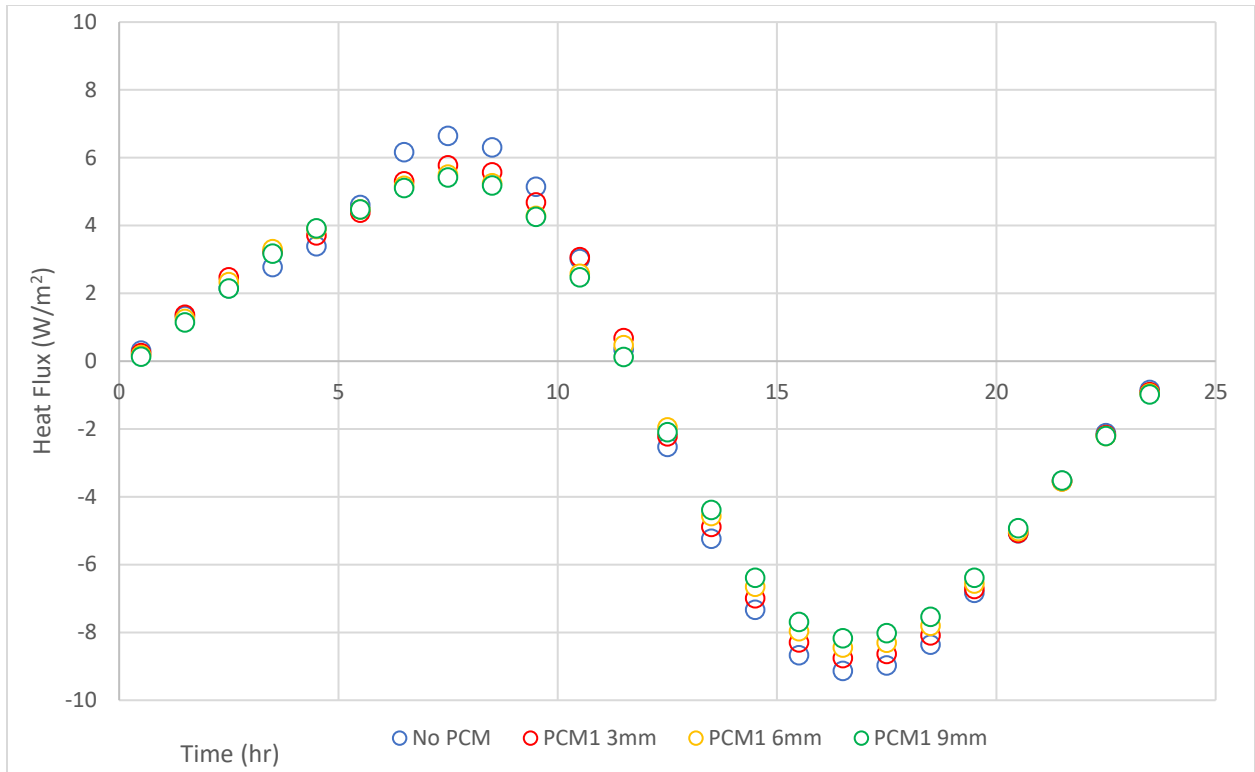


Figure 27. Comparison of inner wall surface heat flux profiles for No PCM, 3mm PCM 1 layer, 6mm PCM 1 layer, and 9mm PCM 1 layer for a Summer day

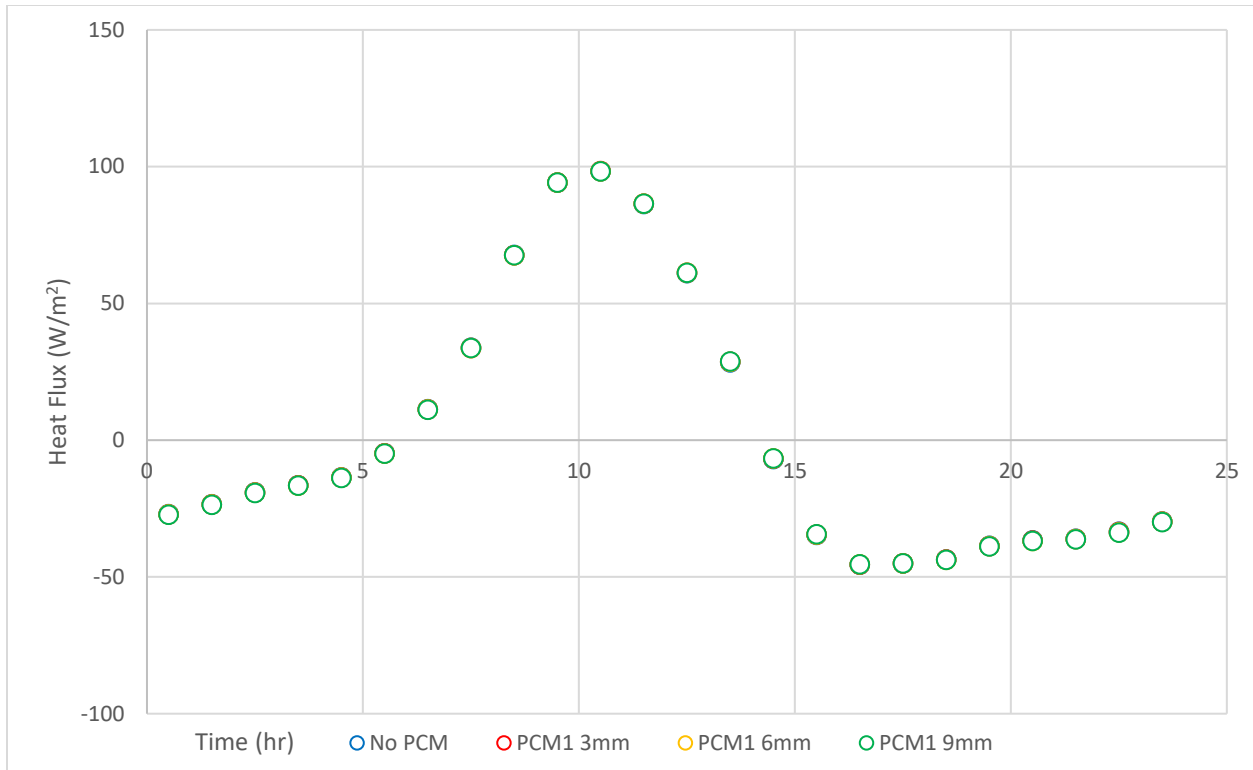


Figure 28. Comparison of outer wall surface heat flux profiles for No PCM, 3mm PCM 1 layer, 6mm PCM 1 layer, and 9mm PCM 1 layer for a Summer day

PCM 1 Shoulder Results

Figure 29 shows the different inner wall surface temperatures throughout 24-hours for a typical Shoulder day. Between 0-6 hours the temperature at the inner wall surface decreases for all the cases which are followed by an increase in the temperature up to 293.5 for the No PCM case and between 292.8K to 293.2K for the different PCM cases. This increase in temperature at the inner wall surface corresponds to an increase at the outer wall surface layer occurring between 6.5-10.5 hours. The maximum temperature fluctuation at the inner wall surface can be observed in the No PCM case and the minimum temperature fluctuation at the same location can be observed in the PCM 1 9 mm case. These trends are consistently seen in the Winter, Summer, and Shoulder days and can be explained using the increase in the thermal mass of the wall section by the addition of PCM 1. The highest temperature at the inner wall surface occurs at 13.5 hours in the No PCM case and shifts to 15.5 hours in the PCM 1 9 mm case. The temperature range of the inner wall surface temperature for the different PCM cases is

from 291 K to 293.2 K. Figure 30 shows the different outer wall surface temperatures throughout 24-hours for a typical Shoulder day. The temperature profiles of the outer wall surface temperature exactly overlap each other and this is consistently observed in the other representative days as well.

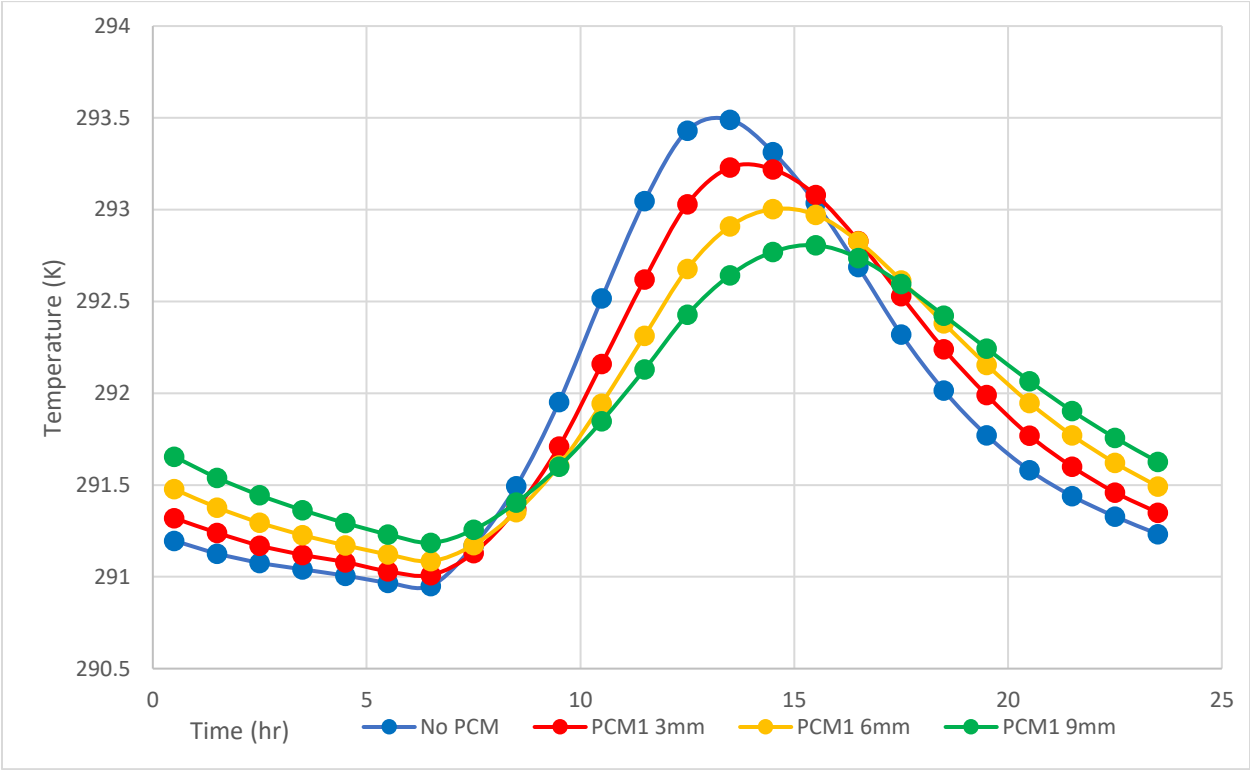


Figure 29. Comparison of inner wall surface temperature profiles for No PCM, 3mm PCM 1 layer, 6mm PCM 1 layer, and 9mm PCM 1 layer for a Shoulder day

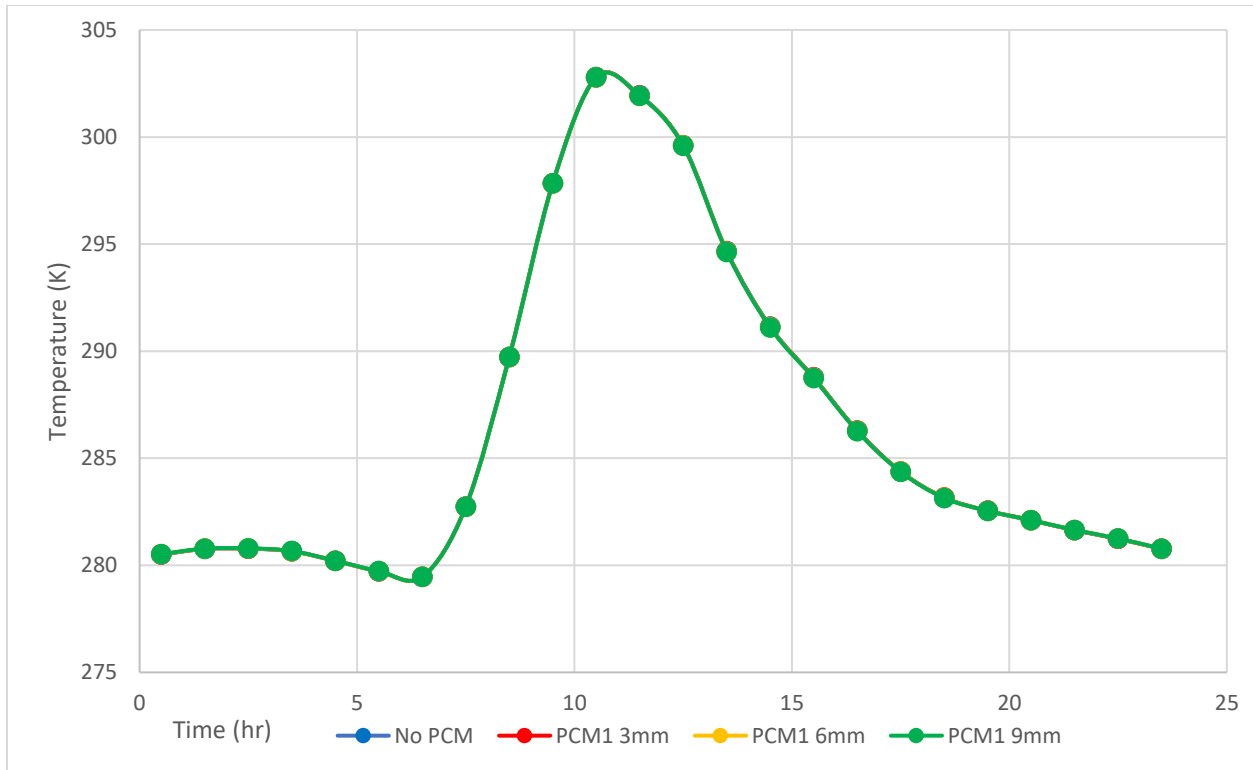


Figure 30. Comparison of outer wall surface temperature profiles for No PCM, 3mm PCM 1 layer, 6mm PCM 1 layer, and 9mm PCM 1 layer for a Shoulder day

The inner wall surface temperature for the different PCM cases varies between 291K and 293.5K. This is not exactly the mass averaged temperature of PCM 1 but it gives an approximate understanding of the temperature variations occurring within PCM 1 located at the inner wall. In this temperature range, the specific heat capacity of PCM 1 varies from 4,900 J/kg-K to 6,200 J/kg-K as seen in Figure 19. This change in the specific heat capacity is not strong enough to significantly affect the heat transfer characteristics of the wall section and this can be observed in Figure 31.

Figure 31 shows the heat flux profiles at the inner wall surface over the 24-hour duration for a typical Shoulder day. Between 0-6.5 hours and between 18.5-23.5 hours the heat fluxes at the different instances in time are clustered together and no effect of adding PCM 1 can be observed at these times. Starting at 7.5 hours the heat flux in the No PCM starts to rise rapidly than all the different PCM 1 cases. Around 11.5 hours heat flux at the inner wall surface changes direction and between 11.5-16.5 hours the heat flux is negative indicating that the heat is entering the house from the outside. Between 7.5-

10.5 hours and between 13.5-16.5 hours the No PCM has the highest heat flux magnitude at the inner wall surface and the PCM 1 9 mm case has the lowest heat flux magnitude at the inner wall surface. Similar trends occurring at different times are observed during the Winter and Summer days as well. The cumulative heat entering the inner wall surface from inside is 259,771 J/m² for the No PCM case, 255,848 J/m² for the PCM 1 3mm case, 252,222 J/m² for the PCM 1 6 mm case, and 249,102 J/m² for the PCM 1 9 mm case. This very small change in the cumulative heat and no time shift occurring due to the addition of PCM 1 shows that it has no significant impact on the wall heat transfer throughout the 24-hours. Figure 32 shows the heat flux profiles at the outer wall surface over the 24-hour duration for a typical Shoulder day and the heat flux profile of the different cases exactly overlap each other.

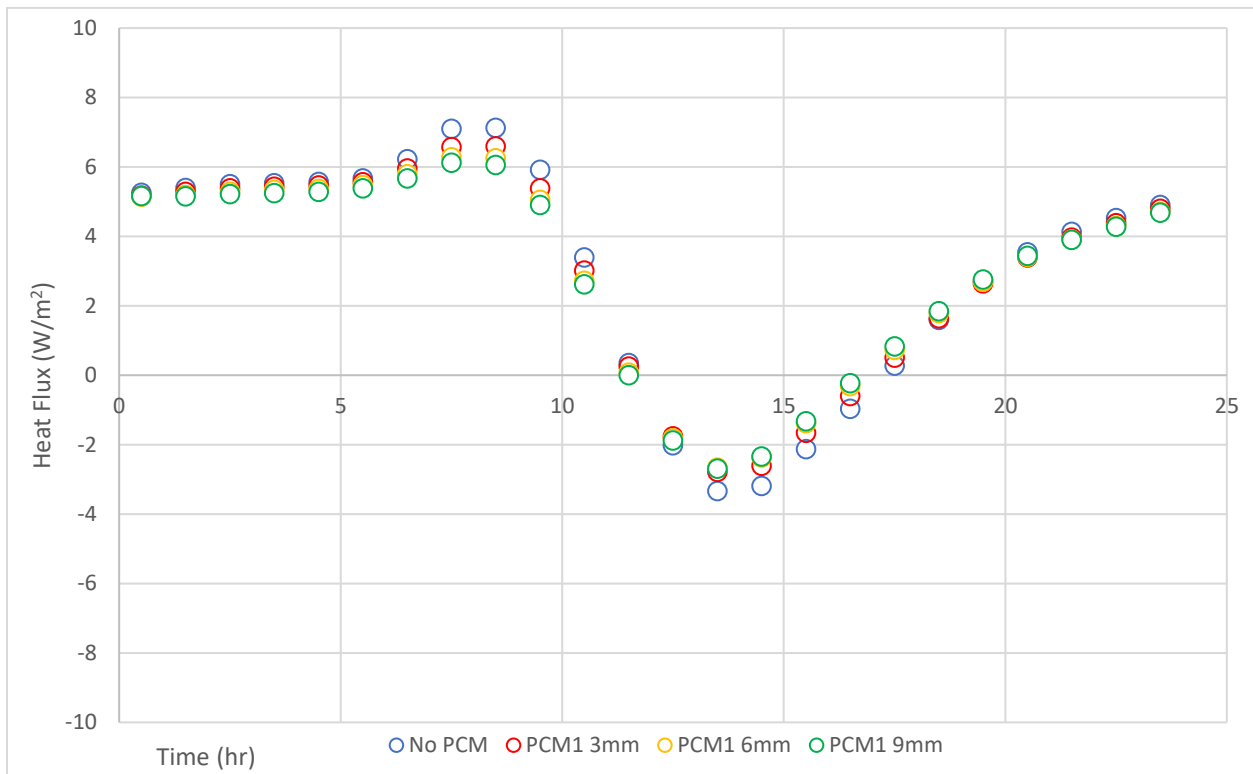


Figure 31. Comparison of inner wall surface heat flux profiles for No PCM, 3mm PCM 1 layer, 6mm PCM 1 layer, and 9mm PCM 1 layer for a Shoulder day

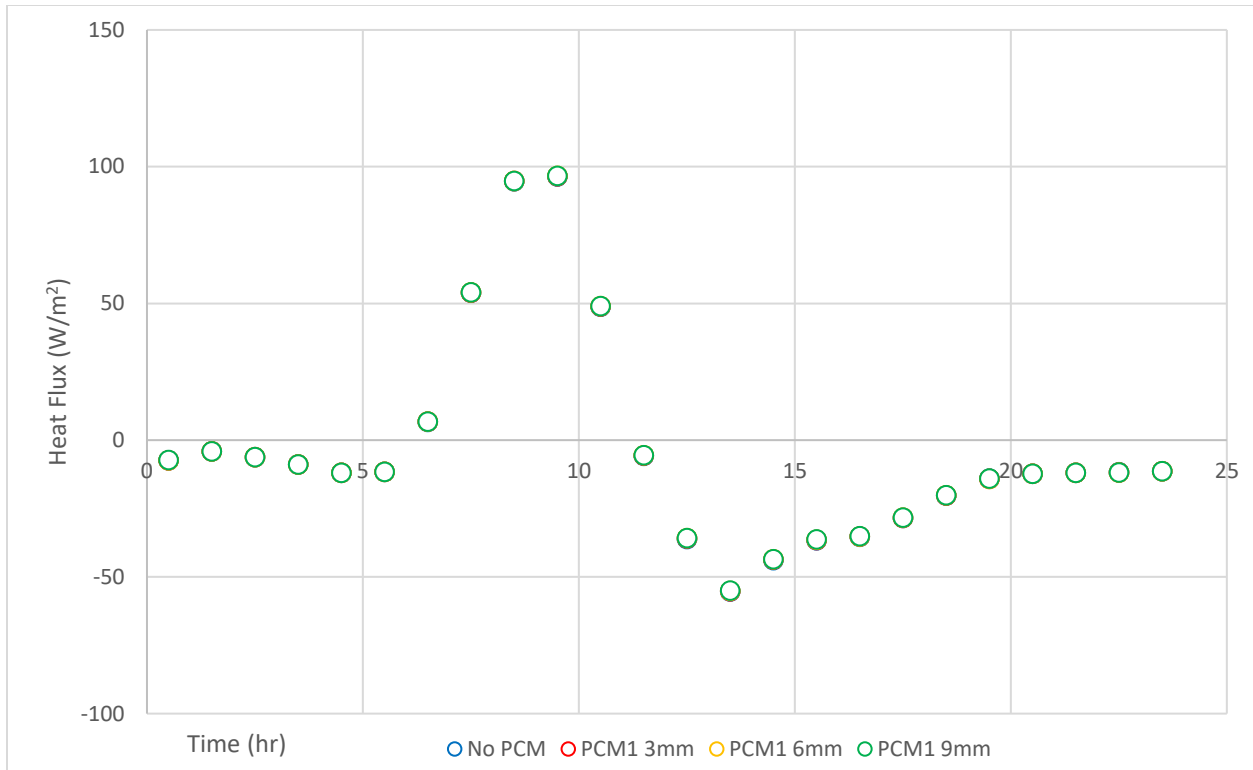


Figure 32. Comparison of outer wall surface heat flux profiles for No PCM, 3mm PCM 1 layer, 6mm PCM 1 layer, and 9mm PCM 1 layer for a Shoulder day

The different thicknesses of PCM 1 applied to the inner wall surface and their behavior under different representative days has been analyzed. Before going in any further it is important to look at the inner wall surface temperature ranges for the different representative days and overlap them with the PCM 1 specific heat versus temperature curve as shown below. For Winter the inner wall surface temperature range is 291-293.6K and for Shoulder the inner wall surface temperature range is 290.9-239.5K. In this temperature range, the specific heat reaches the trough at 4930 J/kgK and then increases to around 6700 J/kgK. Thus, there is not a huge change in the specific heat in these temperature ranges and thus, adding PCM 1 shows no significant impact in Winter and Shoulder. For Summer the inner wall surface temperature ranges from 297.8-301.6K and this corresponds to significant drop in the specific heat of PCM 1. At 297.8K the specific heat of PCM 1 is around 12000 J/kgK and it rapidly drops to 1986 J/kgK at 299.6K. Between 299.6-301.6K the specific heat of PCM 1 remains almost constant. This steep gradient

in the specific heat of PCM 1 in the Summer inner wall surface temperature range is beneficial in reducing the energy consumption of cooling. Its impact is reflected by a 6.7% drop in the cumulative heat leaving the inner wall surface and entering the house. From these observations it is clear that for reducing energy consumption the specific heat of the PCM must significantly change in the temperature range of a particular representative day.

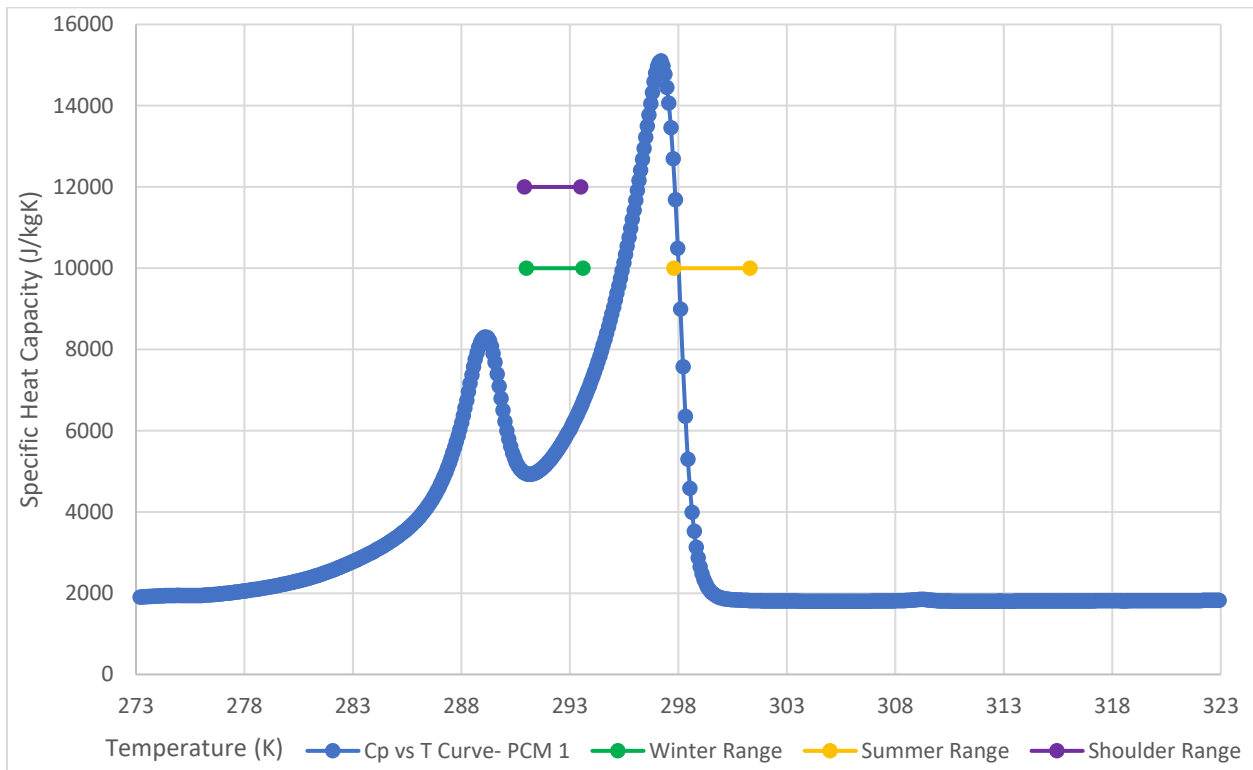


Figure 19. Specific heat versus temperature curve for PCM 1

EnergyPlus vs Fluent Results

The primary goal of trying to use PCM in the wall sections is reducing the energy consumption and this is possible if the addition of PCMs causes desirable time shifts. For example, during the Winter months if the heat flux at the inner wall surface remains negative till later in the day compared to the No PCM case it signifies that heat from outside is entering the house. This means a delay in turning ON the

heater during the winter months. This delay indicates that the PCM was able to store energy when it was heated during the day and then released this energy into the house keeping it warm during the evening and night.

Unfortunately, no such delays were observed with the PCM 1 simulations carried out using ANSYS Fluent for the Winter day. Figure 23, Figure 27, and Figure 31 show the inner wall surface heat flux profiles obtained from EnergyPlus during the Winter day, Summer day, and Shoulder day respectively. These profiles differ significantly from the ones obtained from ANSYS Fluent. From Figure 33, Figure 34, and Figure 35 it is observed that the EnergyPlus profiles show the desired time delays occurring in each case as well as impacts on the magnitudes of the heat fluxes at different instances in time. Thus, it was necessary to carefully study the simulations and try to find out the reason for the disagreement between the heat flux profiles at the inner wall surface between the EnergyPlus and ANSYS Fluent results.

The EnergyPlus PCM model is known to show oscillatory behavior for coarse grids around the analytical solution when the temperature of the PCM is suddenly increased [8]. To avoid this oscillatory behavior a fine mesh is needed to properly simulate the propagation of heat through the PCM.

Assuming 1D heat diffusion with no source terms, for simplicity and integrating the governing equation over the length of the control volume, leads to the following equation:

$$k \left(\frac{dT}{dx} \right) = \rho C_p \left(\frac{dT}{dt} \right) \Delta x$$

where k is the thermal conductivity, T is the temperature, ρ is the density, C_p is the specific heat capacity, and Δx is the length of the control volume. This equation shows that:

$$\left(\frac{\partial T}{\partial x} \right) \propto C_p \left(\frac{\partial T}{\partial t} \right)$$

For PCM 1 the modeling approach adopted was the solid PCM with Cp curve and thus, the Cp value of the PCM was significantly higher than the other wall materials. Thus, when C_p changes drastically in a given interval of time it will cause spatial temperature gradient to show a drastic change as well. Thus, a mesh with poor resolution will not be able to accurately capture the temperature gradient within the PCM and thus, there was a need for a finer mesh inside PCM 1.

Additionally, during these simulations, the PCM 1 was discretized with the default mesh in EnergyPlus and thus, a study using a finer mesh was carried out. For this simulation, the PCM 1 6mm case was re-run but with the 6mm PCM 1 layer being split into 6 1mm thick PCM 1 layers. The comparison of the results of these cases was necessary to understand which of these simulations was generating reliable results.

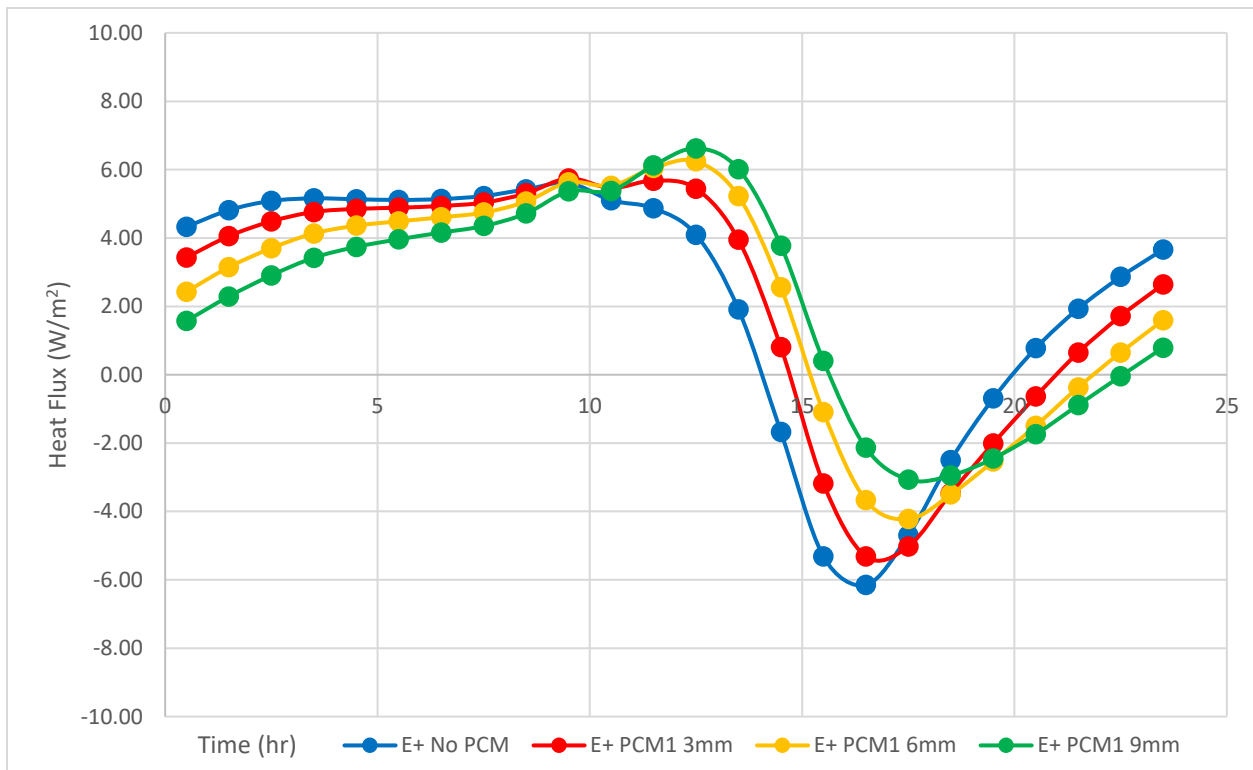


Figure 33. Comparison of inner wall surface heat flux profiles obtained from EnergyPlus (E+) for No PCM, 3mm PCM 1 layer, 6mm PCM 1 layer, and 9mm PCM 1 layer for a Winter day

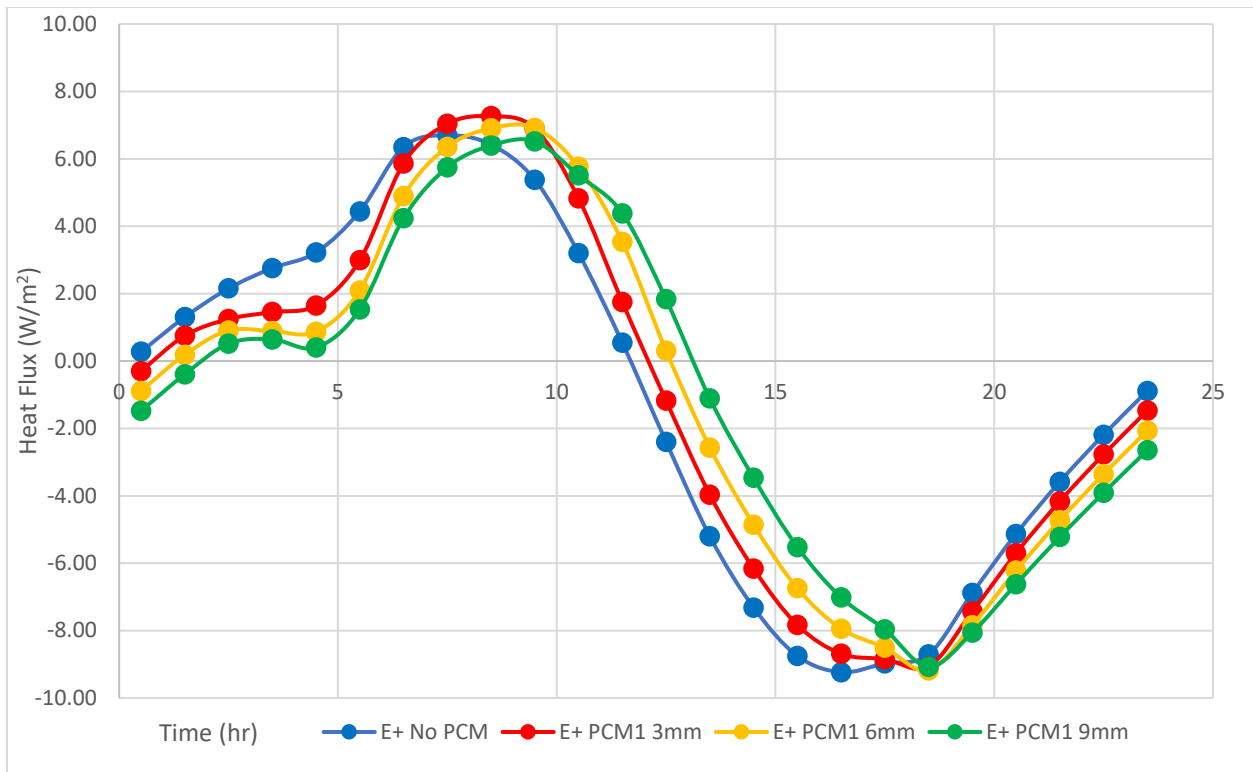


Figure 34. Comparison of inner wall surface heat flux profiles obtained from EnergyPlus (E+) for No PCM, 3mm PCM 1 layer, 6mm PCM 1 layer, and 9mm PCM 1 layer for a Summer day

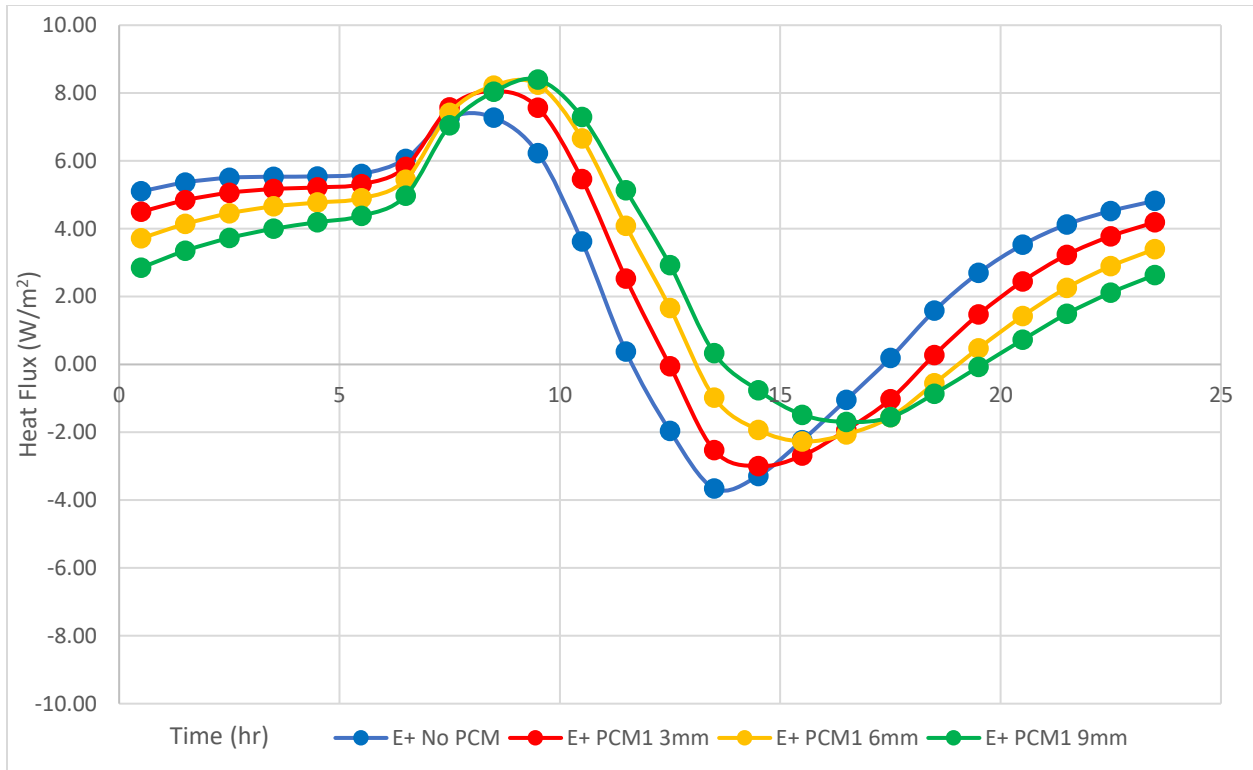


Figure 35. Comparison of inner wall surface heat flux profiles obtained from EnergyPlus (E+) for No PCM, 3mm PCM 1 layer, 6mm PCM 1 layer, and 9mm PCM 1 layer for a Shoulder day

Comparison between PCM 1 6mm Case and PCM 1 6 x 1mm Case

The results for the PCM 1 6mm case were already available for all three representative days but additional simulations were run for the PCM 1 6x1mm case using both ANSYS Fluent and EnergyPlus. The EnergyPlus model helped in the generation of temperature boundary conditions to be used for the ANSYS Fluent model. It is important to know that no changes were made to the ANSYS Fluent model except for changed boundary conditions obtained from EnergyPlus. Whereas the EnergyPlus had one major change and it was the way PCM in the domain was modeled. In the previous simulations, the 6mm PCM 1 layer was one single layer with the default mesh but in the new model, the PCM 1 layer was broken into 6 1mm layers with the default mesh. This leads to a higher mesh density inside the PCM 1 layer.

The key differentiating feature that can be observed in the EnergyPlus results is the time shift that is evident in the inner wall surface heat fluxes that cannot be seen in the ANSYS Fluent results. The inner wall surface heat fluxes are clustered together for most of the day but show a slight difference in magnitude at some times but no shift in time is evident. Figure 36, Figure 37, and Figure 38 show the inner wall surface heat fluxes of the different EnergyPlus models under the conditions of the Winter day, Summer day, and Shoulder day respectively. In Figure 36 it can be observed that PCM 1 6x1mm inner wall surface heat flux profile lies intermediately between the No PCM and PCM 1 6mm profiles. The time shift between the No PCM case and the PCM 1 6x1mm case is smaller than the time shift between the No PCM and the PCM 1 6mm case. The peak values of the heat fluxes of the PCM 1 6x1mm case have also drifted towards the No PCM case. Figure 37 shows that the PCM 1 6x1mm case lies intermediately between the No PCM and PCM 1 6mm case but this is observed only between the 5-10 hours. In the Summer case, the peak values are not affected and they are consistent in all the cases. Figure 38 shows trends similar to that are observed during the Winter day and this can be attributed to the similar temperature ranges of the Winter and Shoulder day.

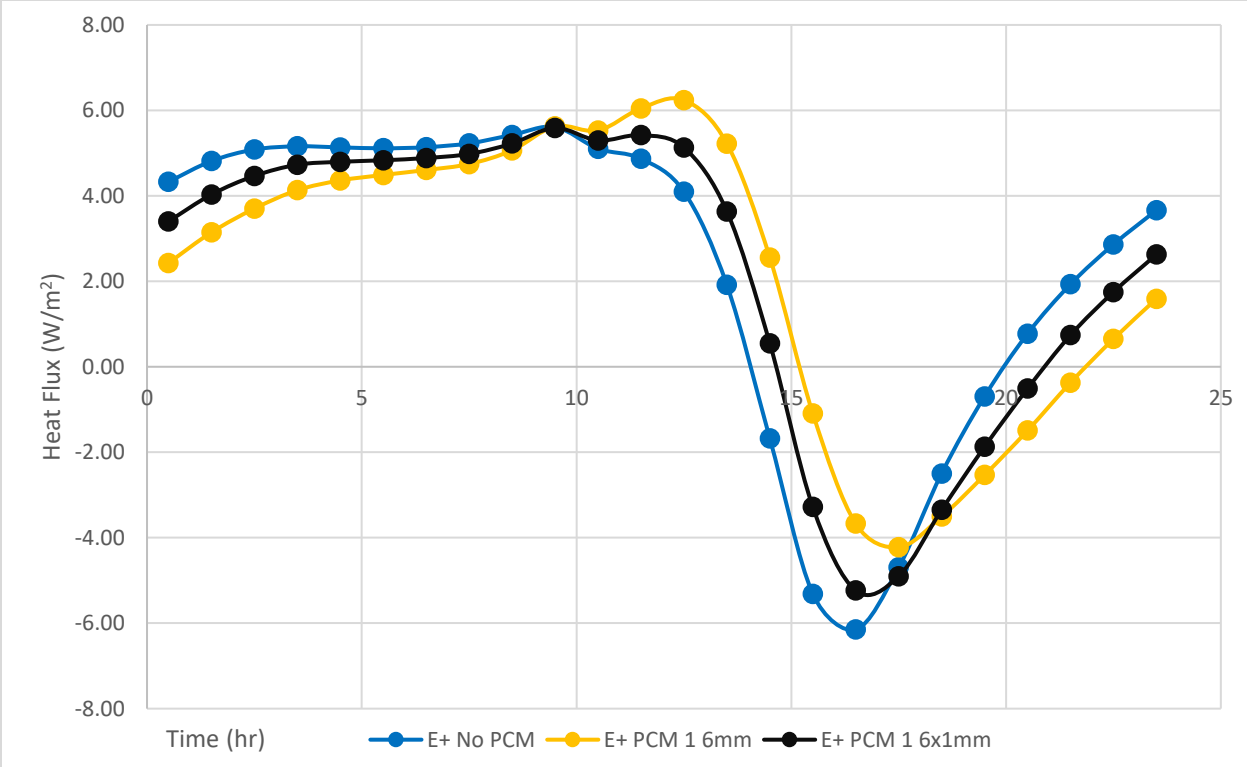


Figure 36. Comparison of inner wall surface heat flux profiles obtained from EnergyPlus (E+) for No PCM, 6mm PCM 1 layer, and 6 x 1mm PCM 1 layers for a Winter day

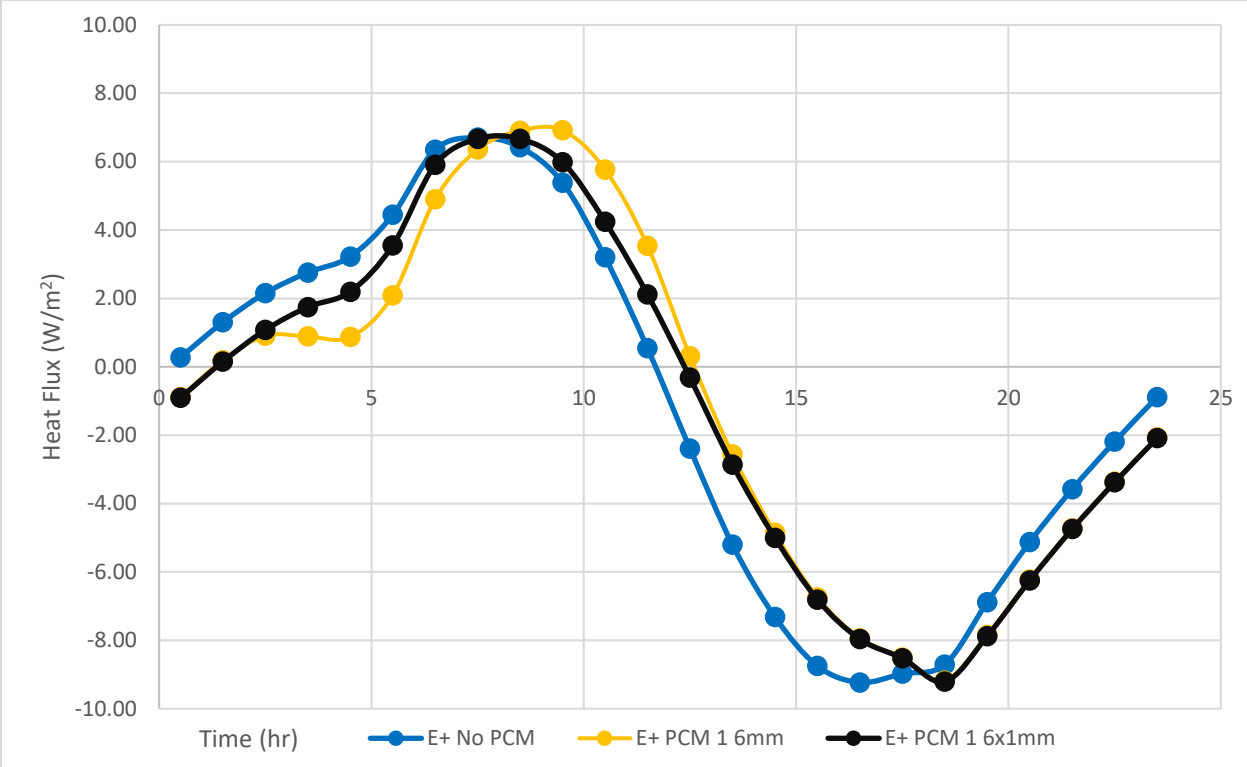


Figure 37. Comparison of inner wall surface heat flux profiles obtained from EnergyPlus (E+) for No PCM, 6mm PCM 1 layer, and 6 x 1mm PCM 1 layers for a Summer day

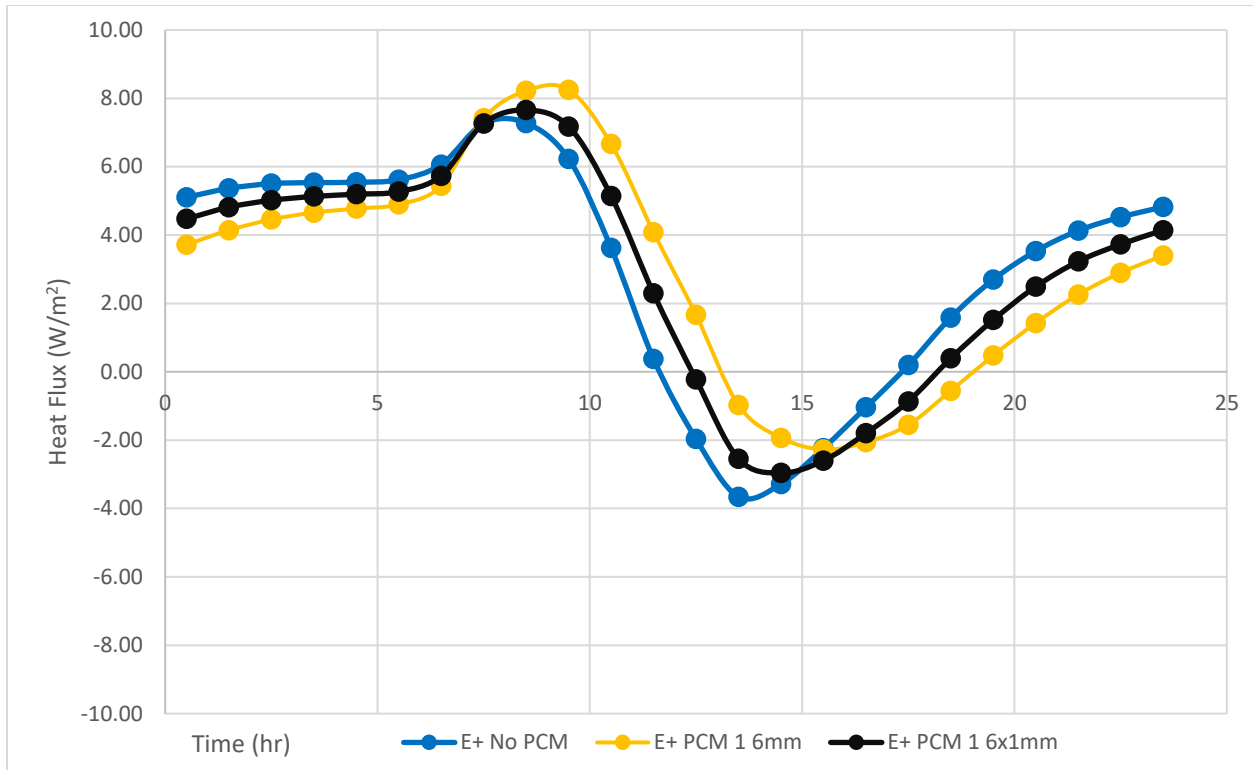


Figure 38. Comparison of inner wall surface heat flux profiles obtained from EnergyPlus (E+) for No PCM, 6mm PCM 1 layer, and 6 x 1mm PCM 1 layers for a Shoulder day

From Figure 36, Figure 37, and Figure 38 it is evident that improving the mesh inside PCM 1 domain has affected the results of EnergyPlus and shifted the inner wall surface heat flux behavior towards the No PCM case. The ANSYS Fluent results already show that no time shift can be observed by using PCM 1. Based on the inner wall surface heat flux profiles obtained from ANSYS Fluent for the No PCM case and the different PCM cases there is only a slight change in magnitude with no change in times at which the heat flux changes direction. The changes in the inner wall surface heat flux profile obtained from EnergyPlus show that improving the mesh is beneficial for the model to obtain reliable results. Thus, it can be concluded that the reason for the disagreement between the ANSYS Fluent and EnergyPlus results is the poor mesh resolution in PCM 1 used in the EnergyPlus model.

Chapter 5: PCM 2 Simulations

Difference between PCM 1 and PCM 2

As discussed in the previous chapter, PCM 1 is a spackle product and can be applied over the inner wall surface in layers up to 9mm thickness. PCM 1 is not a pure PCM product but consists of approximately 53% PCM inside the spackle, which dries as a solid layer. Even when the melting of the PCM occurs it is well-retained inside the spackle. Material properties of PCM 1 available are its density, thermal conductivity, and specific heat capacity varying as a function of temperature for the PCM plus spackle combination. This limits the modeling approach that can be used for PCM 1 as a solid with varying heat capacity to account for the absorption or release of huge amounts of energy depending on the latent heat of fusion.

PCM 2 is a PCM product where the salt-based PCM is encapsulated inside panels of a plastic material. The microencapsulation provides structural integrity to PCM 2 when the salt-based PCM contained inside goes through the solidification and melting cycles. PCM 2 is designed to have a total thickness of 6.3 mm when installed on the interior wall surface. The material properties of the salt-based PCM of PCM 2 available are the density, thermal conductivity, specific heat capacity, and latent heat of fusion as shown in Table 6. For reducing the computational effort and to minimize the complexities in the geometry PCM 2 was modeled as a 6.3mm thick layer of pure PCM on the inner wall surface. This simplification was possible because the plastic wall thickness is small and hence can be ignored. To model this using the enthalpy porosity model, the viscosity value was needed to be known; however, this property was unavailable from the manufacturer. Based on the assumption that PCM 2 is a $CaCl_2$ -based PCM the order of magnitude of the viscosity can be estimated.

Table 6. Thermophysical Properties of PCM 2

| Thermophysical Property | Temperature Range | Value |
|--------------------------------|--------------------------|--------------|
| Density (kg/m^3) | 273.15K-400K | 1550 |

| | | |
|--|-----------------|-----------|
| Specific Heat Capacity (J/kgK) | 273.15K-400K | 3140 |
| Thermal Conductivity (W/mK) (Solid) | 273.15K-294.15K | 1.09 |
| Thermal Conductivity (W/mK) (Liquid) | 294.95K-400K | 0.54 |
| Latent Heat of Fusion (J/kg) | 294.15K-294.95K | 200000 |
| Viscosity (assuming CaCl ₂ in kg/ms) | 294.95K-400K | 0.0059295 |

Modeling Approach for PCM 2

The solid-liquid phase change problems with a moving boundary are typically more challenging than the heat transfer problems because the position of the solid-liquid interface as a function of time is unknown. The accurate prediction of the interface motion depends on the quantity and the location of the material that has already melted or solidified by a certain instant in time and this gives the information about the heat stored or released by the PCM [34]. The effective heat capacity approach simplifies this problem to heat conduction and involves solving only the energy where the latent heat of fusion is incorporated within the specific heat capacity over the melting range.

The enthalpy porosity method is widely used in PCM simulations because it does not require the explicit tracking of the phase interface [34]. Additionally, the enthalpy porosity method can be used in cases when melting or solidification occurs over a range of temperature. In the melting range, the PCM is a combination of the solid PCM and liquid PCM where the liquid fraction is dependent on the temperature. In this method, the energy conservation equation for constant thermophysical properties is as follows [20]:

$$\frac{\partial(\rho H)}{\partial t} + \nabla \cdot (\rho V H) = k \nabla^2 T$$

where H is the total volumetric enthalpy, which is the sum of the sensible and latent heats:

$$H = h + \Delta H$$

where h is the sensible heat, ρ_l is the liquid density, β is the liquid fraction, and L_{fus} is the latent heat of fusion. The liquid fraction β is defined as:

$$\beta = \frac{L_{fus}}{T_{liquidus} - T_{solidus}} = \begin{cases} 0 & \text{if } T < T_{solidus} \\ \frac{T - T_{solidus}}{T_{liquidus} - T_{solidus}} & \text{if } T_{liquidus} < T < T_{solidus} \\ 1 & \text{if } T > T_{liquidus} \end{cases}$$

The latent heat is given as follows:

$$\Delta H = \beta L$$

The system of equations for this problem is completed with the continuity and momentum equations that are coupled with the energy equation above.

Continuity:

$$\frac{\partial \rho}{\partial t} + \nabla \cdot (\rho V) = 0$$

Momentum:

$$\frac{\partial(\rho V)}{\partial t} + \nabla \cdot (\rho V) = -\nabla p + \mu \nabla^2 V + \rho g + S$$

The term (S) indicates a momentum sink and is given by

$$S = -A(\beta)V$$

As the mushy zone is a combination of solid PCM and liquid PCM the flow of the liquid PCM is obstructed by the solid PCM. This obstruction of the flow is represented by the momentum sink term and thus, its value depends on the liquid fraction. When the PCM inside a cell is fully liquid there is no momentum sink term as the liquid fraction becomes 1. To mimic the flow of liquid through a porous

medium the enthalpy porosity method uses the Carman-Kozeny equation. This is derived from Darcy law for flow through porous media and with some modifications it becomes:

$$A(\beta) = \frac{A_{mush}(1 - \beta)^2}{\beta^3 + 0.001}$$

The term A_{mush} is known as the mushy zone constant and has a significant impact on the solidification and melting simulations. A higher mushy zone constant means a larger momentum sink term and this large sink term dampens the motion in the liquid region. In the case where gravity is present the natural convection in the liquid region is strongly dampened by increasing the mushy zone constant. The mushy zone constant impacts the heat transfer and flow characteristics during the solidification and melting of the PCM. The mushy zone constant ranging from 10^3 - 10^8 has been suggested in manuals of commercial software. Higher values of the mushy zone constant lead oscillations in the solution. The typical approach that has been followed in recent studies is to develop a numerical model of an actual experiment and then change the mushy zone constant to match the experimental results. This approach is used because there is no analytical way to find out the value of the mushy zone constant.

Analytical Solution

The analytical solution for solidification and melting of materials is based on some simplifications that make the Stefan problem analytically solvable. One such solution has been provided in [21]. The solution investigates the solidification of a semi-infinite slab of water into ice that is bounded by a stationary wall at ($z_2 = 0$ m). The fluid under consideration is incompressible and gravity is ignored in the solution. The water block is initially at a temperature of $T_0 = 278K$ at this temperature the complete slab is liquid and at time, $t = 0$ seconds the temperature of the stationary wall ($z_2 = 0$ m) is changed to $T_1 = 268K$ which is below the melting temperature of $T_M = 273K$. Thus, for $t > 0$ seconds the semi-infinite water

slab starts freezing and the melt front or the solid-liquid interface starts moving in the upward direction. It is also assumed that the melting and solidification processes are isothermal and there is no hysteresis in the process. Thus, there is a singular melting and freezing temperature, $T_M = 273K$ and this is the temperature of the solid-liquid interface. The vertical location of the solid-liquid interface as a function of time is displayed in Figure 39 and this location can be calculated using the following equation:

$$h = \lambda \sqrt{4\alpha^{(B)}t}$$

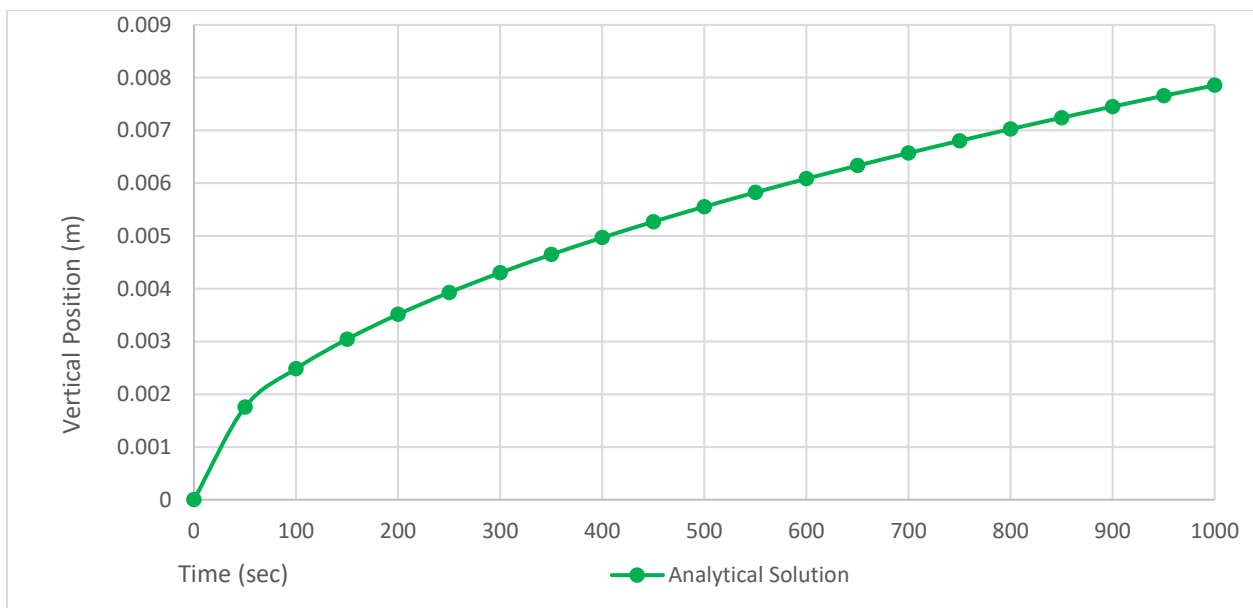


Figure 39. Solid-liquid (ice-water) interface location as a function of time from analytical solution

where, h is the solid-liquid interface location, $\alpha^{(B)}$ is the thermal diffusivity of ice and t is time elapsed since the temperature of the stationary wall is changed to T_1 , and λ is a constant that depends on material properties and the initial and boundary conditions. For the material properties of water and ice, and the description of the physics provided above, $\lambda = 0.1159$. For further information related to calculation of λ and the overall analytical solution method please refer to [21].

ANSYS Model for Analytical Validation

To better understand the implementation of the enthalpy-porosity method using ANSYS Fluent a simulation to validate the model was carried out. The model replicated the material properties, initial condition, and the boundary conditions as described in the analytical solution discussed above. To compare the performance of the simulation against analytical solution the location of the mushy zone was tracked and it was compared to the solid-liquid interface location provided by the analytical solution. The mushy zone is a region where the liquid fraction changes from 0 to 1. Thus, the both edges of the mushy zone were manually tracked at different instances of time and for the model to be validated against the analytical solution it is expected that the solid-liquid interface location calculated using the analytical should be inside the mushy zone. In comparison to the complete domain of simulation only a small region has a liquid fraction greater than 0 but less than 1, which is the mushy zone. The mushy zone does not exist in the analytical solution as it assumes the melting and solidification processes are isothermal but the enthalpy porosity method needs different solidus and liquidus temperatures. The solidus temperature is the temperature at which the melting begins and liquidus temperature is the temperature at which the melting ends. Thus, another way that was used to gauge the performance of the simulation was converting the area weighted liquid fraction into height occupied by the ice at any moment in time. It was expected that this height will be slightly lower than the solid-liquid interface location provided by the analytical solution.

Material Properties

The material properties provided in the analytical solution were used but with a slight alteration. The enthalpy porosity method needs distinct solidus and liquidus temperatures because when these two are set equal to each other the simulation starts generating errors as it leads to division by zero in certain terms. Thus, to make the simulation closely replicate the analytical solution the solidus temperature ($T_{solidus}$) was set to 273K and the liquidus temperature ($T_{liquidus}$) was set to 273.1K. The mushy zone in this case lies between 273K and 273.1K and the thermophysical properties in this region were linearly

interpolated based on the temperature. The Piecewise Linear functionality in ANSYS Fluent was used in assigning temperature dependent thermophysical properties. The thermophysical properties used in this simulation are provided in Table 7.

Table 7. Thermophysical properties of water and ice

| Thermophysical Property and Phase | Value |
|---|------------------------|
| Thermal Conductivity – Water ($k_{water}, W/mK$) | 0.6028 |
| Thermal Conductivity – Ice ($k_{ice}, W/mK$) | 2.219 |
| Density – Water ($\rho_{water}, kg/m^3$) | 1000 |
| Density – Ice ($\rho_{ice}, kg/m^3$) | 920 |
| Specific Heat Capacity – Water ($Cp_{water}, J/kgK$) | 4187 |
| Specific Heat Capacity – Ice ($Cp_{ice}, J/kgK$) | 2100 |
| Thermal Diffusivity – Water ($\alpha_{water}, m^2/s$) | 1.44×10^{-7} |
| Thermal Diffusivity – Ice ($\alpha_{ice}, m^2/s$) | 1.148×10^{-6} |
| Latent Heat of Fusion ($\Delta H, J/kg$) | 3.338×10^5 |

Domain and Meshing

The domain of interest in the analytical solution is a semi-infinite slab of water and to replicate this a 2D domain of size 0.05m x 0.05m was generated and appropriate boundary conditions were added. A structured mesh with a high mesh density was used to accurately capture the motion of the solid-liquid interface. The mesh was generated using the Meshing tool in ANSYS Workbench. The total number of cells in the domain were 22500, maximum skewness was 1.3×10^{-10} , and average skewness was 1.3×10^{-10} . Figure 40 shows the mesh that was generated for the analytical validation.

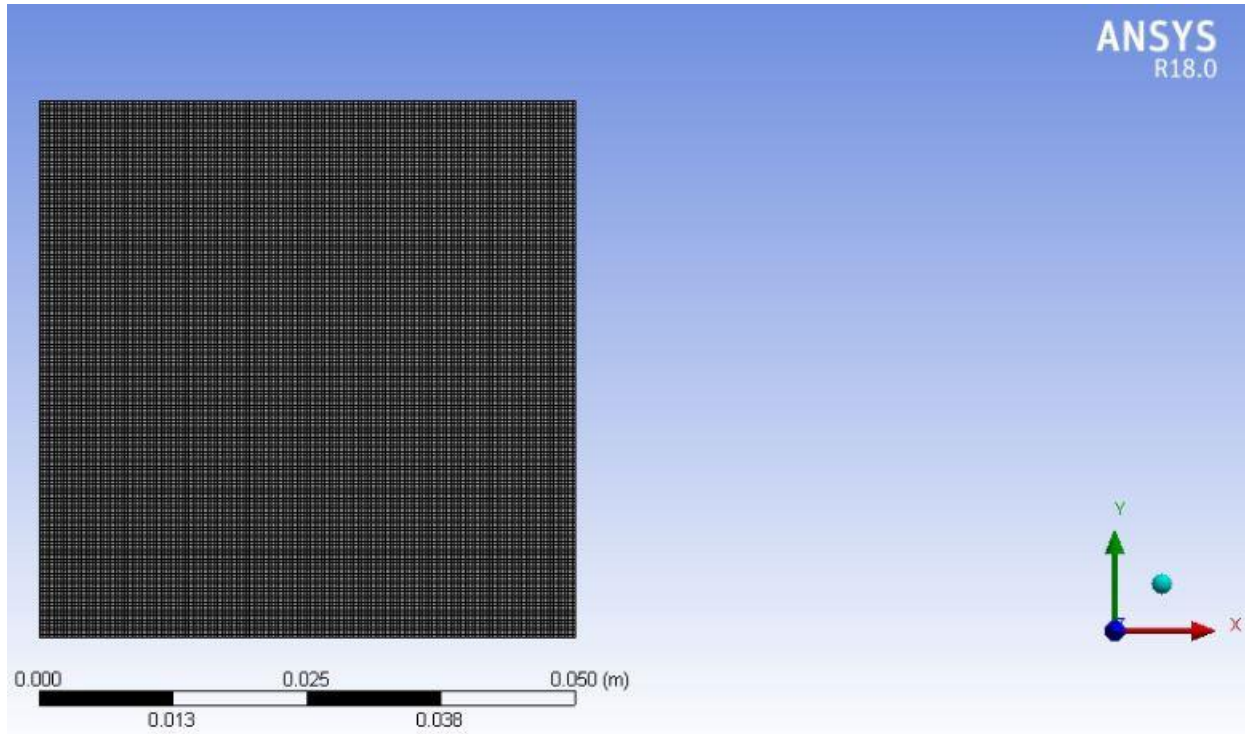


Figure 40. Mesh generated for water freezing simulation

Boundary and Initial Conditions

The bottom wall was a stationary wall with no slip condition and with a fixed temperature of $T_{bottom} = 268K$ for times, $t \geq 0$ and this was set equal to T_1 from the analytical solution. The left, right, and top boundaries were assigned symmetry boundary conditions. For times, $t < 0$ the semi-infinite block of water was at a temperature of $T_{domain,0} = 278K$ and this was set equal to T_0 from the analytical solution. The different boundary conditions and their locations are represented in Figure 41.

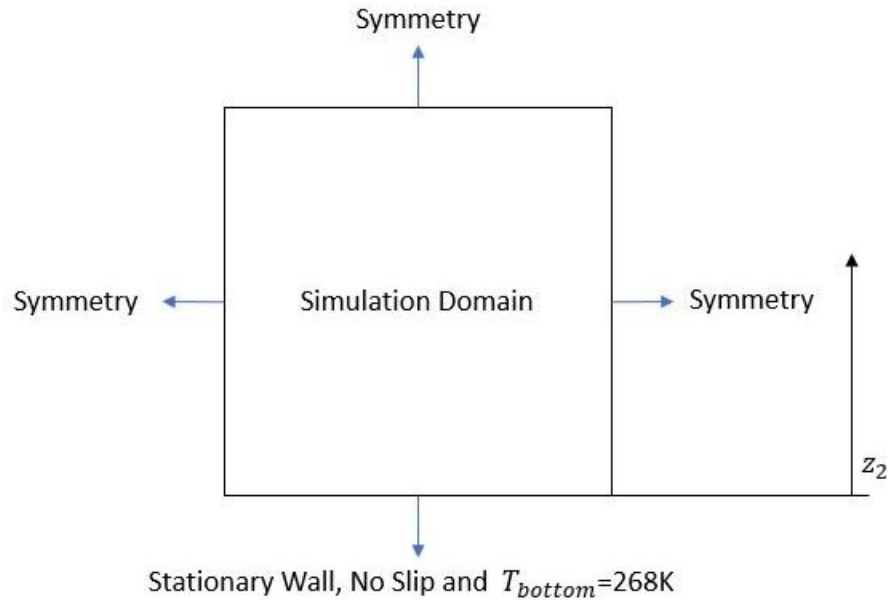


Figure 41. Boundary conditions for water freezing simulation

Solver Settings

For this simulation the Solidification and Melting module was turned ON and the default value of 10^5 was used for the mushy zone parameter (A_{mush}). The simulation was transient and impacts of gravity were not considered. The pressure-velocity coupling scheme used was SIMPLE, the convective interpolation schemes used were 2nd order upwind schemes, the diffusion term used a 2nd order central difference scheme, and the 2nd order implicit scheme is used for the unsteady term. A time step size of 1sec was used. The under-relaxation factors used were 0.3 for pressure, 0.7 for momentum, 0.9 for liquid fraction update and the default value of 1 was used for density, body forces, and energy. A total of 1000 time steps were executed in the simulation, the heat flux at the bottom surface and the area weighted liquid fraction was recorded after every time step but the contours of the liquid fraction were recorded after every 50 time steps.

Results

The analytical solution provides the vertical location of the solid-liquid interface (h) as a function of time and simulation provides the vertical locations of the lower limit and upper limit of the mushy zone as a function of time. The main goal of this analytical study is to verify if vertical location of the solid-liquid interface (h) as provided by the analytical solution lies inside the mushy zone predicted by the simulation. A visual representation of the lower and upper limits of the mushy zones and the vertical location of the solid-liquid interface after every 50 seconds is provided in Figure 42. It can be observed that for all time steps between 0 seconds to 1000 seconds the solid-liquid interface lies within the mushy zone. This validates the simulation against the analytical solution.

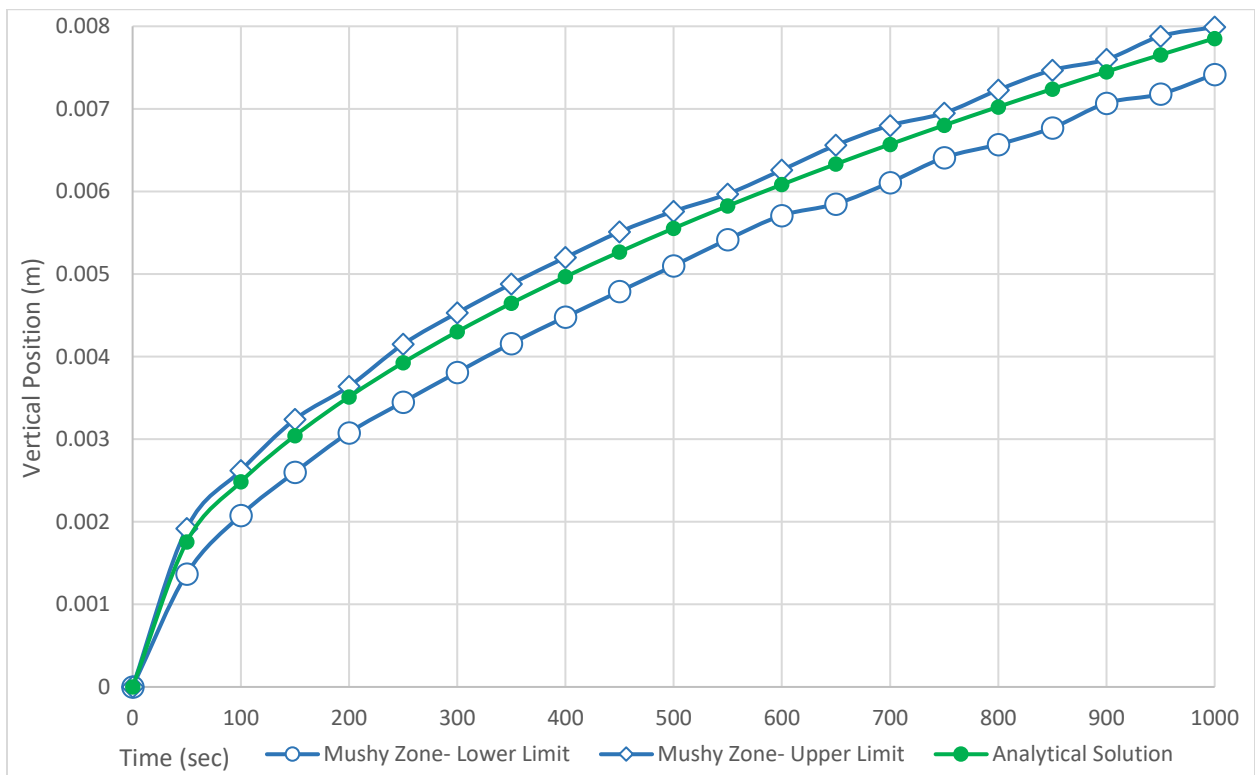


Figure 42. Comparison of mushy zone location from simulation and solid-liquid interface from analytical solution

As previously mentioned, another way to gauge the performance of the simulation against the analytical solution was by calculating the height occupied by the ice layer. The ice layer height was calculated

based on the area weighted liquid fraction and its comparison against the analytical solution is provided in Figure 43. The data for this graph was collected after every 1 second from both the simulation and the analytical solution. The mean average error between the analytical solid-liquid interface location and the simulation-based height occupied by ice layer was 1.9×10^{-4} m. This completes the analytical validation study and it can be concluded that the simulation was able to accurately predict the freezing of the ice to water. The same model with appropriate changes can now be used to predict the melting and solidification processes of PCM 2 with confidence provided the thermophysical properties are reliable.

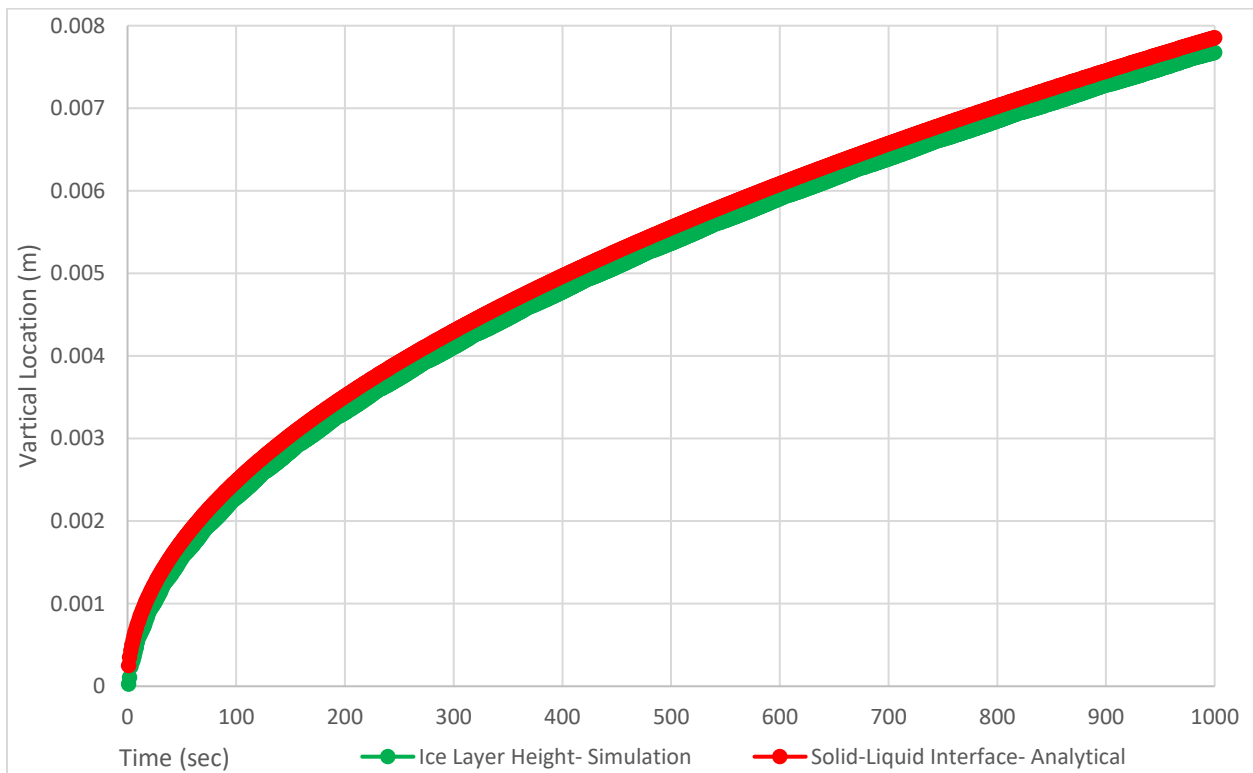


Figure 43. Comparison of ice layer height from simulation and solid-liquid interface from analytical solution

PCM 2 2D Simulations: Enthalpy Porosity Approach vs Cp Curve Approach

Due to the lack of viscosity and experimental data for PCM 2, it was decided to use the solid Cp curve simulation approach and then use those results to fine-tune the mushy zone constant for PCM 2. Also, it

was decided based on the presumed composition of PCM 2 that the dynamic viscosity should be in the order of magnitude of ~ 0.001 kg/ms. The solid Cp curve simulations were followed by the enthalpy porosity simulations on the same domain with the appropriate material properties and refined mesh to capture the melting process accurately. To replicate the physics of the solid Cp curve simulation gravity was turned off during the enthalpy porosity method simulations.

The solid Cp curve method requires the construction of the Cp curve in the melting region. The curve was constructed such that the area under the curve from the solidus temperature ($T_{solidus}$) to the liquidus temperature ($T_{liquidus}$) was equal to the latent heat of fusion of PCM 2. The curve was constructed as a trapezium where the length of the larger parallel side was known but the distance between the parallel sides and the length of the shorter parallel side was determined to obtain the desired area under the curve. The Cp curve in the range 290K-300K is shown in Figure 44.

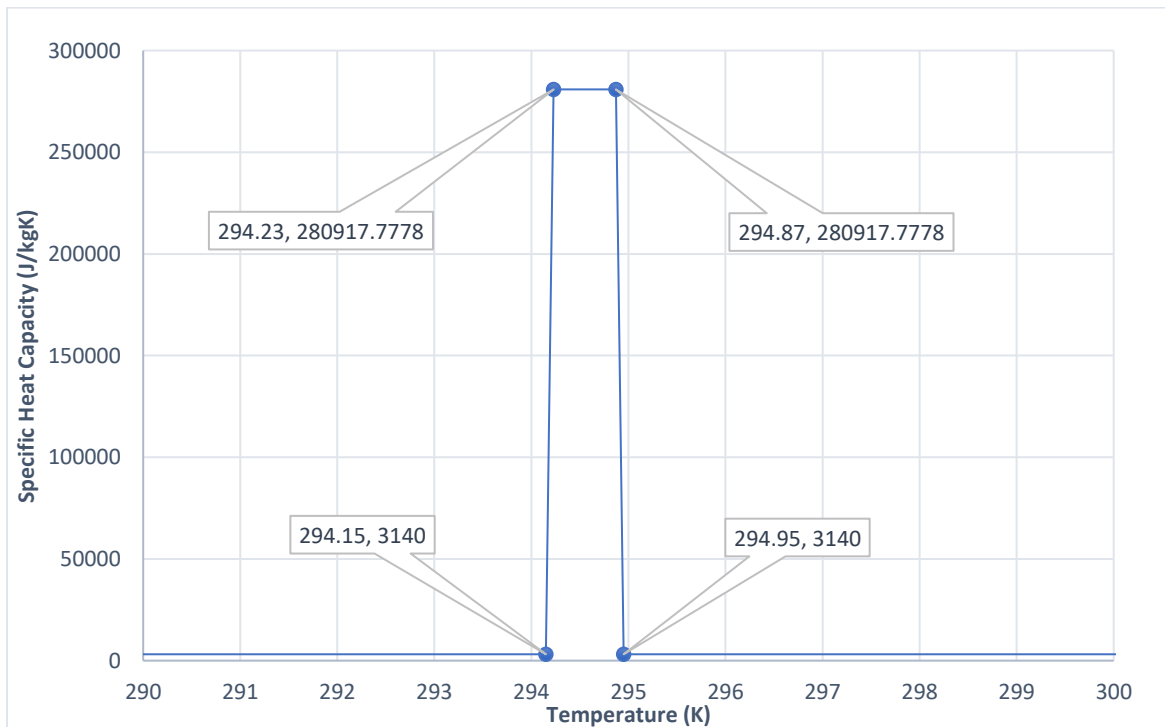


Figure 44. Constructed curve of specific heat (C_p) as a function of temperature for PCM 2

Modeling Domain and Mesh

The modeling domain for both the solid Cp curve simulation and the enthalpy porosity simulations was a 2D rectangular cavity that is 609.6mm tall and 6.3mm wide. These dimensions are used because this was the cross-section of the PCM layer applied on the inner wall surface.

Material Properties

The thermophysical properties of PCM 2 used in these simulations are given in Table 6. The thermal conductivity changes between the solid and liquid phases. Thus, the variation of the thermal conductivity in the temperature range from the solidus temperature ($T_{s,PCM 2} = 21^{\circ}\text{C}$) to the liquidus temperature ($T_{l,PCM 2} = 21.8^{\circ}\text{C}$) is unknown and thus, linear interpolation in this range was used. The equations were generated using MS Excel and they are provided in Table 8.

Table 8. Thermal conductivity of PCM 2 in melting temperature range as a function of temperature

| Thermophysical Property | Temperature-Dependent Equation in Melting Temperature Range |
|-----------------------------|---|
| Thermal Conductivity (W/mK) | $k_{mushy} = -0.6875 T + 203.318$ |

Boundary Conditions

The boundaries on the top, bottom, and the left had a no-slip boundary condition ($u = v = 0$) imposed for the momentum equation and an adiabatic boundary condition ($\frac{\partial T}{\partial n} = 0$) imposed for the energy equation as shown in Figure 45. The right boundary had a no-slip boundary condition ($u = v = 0$) and an isothermal boundary condition ($T = 27^{\circ}\text{C}$) imposed for the momentum and energy equation respectively. At the start of the simulation, the entire domain was at $T = 17^{\circ}\text{C}$ and this initial condition was important because it impacts the total melting time of PCM 2.

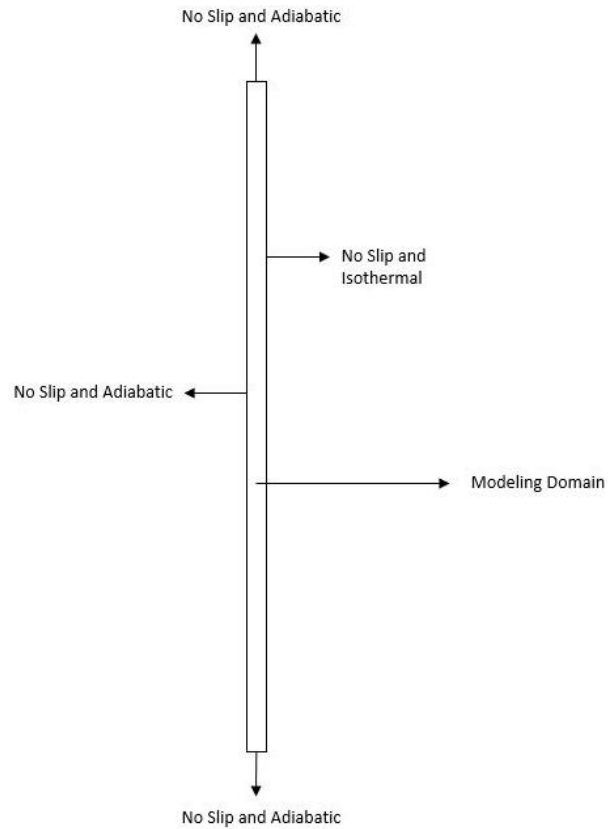


Figure 45. Boundary conditions for comparison of PCM 2 melting using enthalpy porosity approach and solid Cp curve approach

Solver Settings and Mesh Quality

The pressure-velocity coupling scheme used was SIMPLE, the convective interpolation scheme used was the 2nd order upwind scheme, the diffusion term used a 2nd order central difference scheme, and the 2nd order implicit scheme was used for the unsteady term. A time step size of 0.2 s was used for the enthalpy porosity simulations and a time step size of 5 sec was used for the solid Cp curve simulations.

The mushy zone constant used during the PCM 2 simulations was 4×10^5 . A structured grid was generated using the Meshing tool in ANSYS Workbench. The total number of cells in the domain were 30000, maximum skewness of the mesh was 2.14×10^{-8} , and the average skewness of the mesh was 2.14×10^{-8} .

Results

The temperature inside the PCM was extracted at 3 different locations with 1-minute intervals between consecutive data points. The temperature was extracted at 2mm, 4mm, and 6.3mm from the right wall where the isothermal boundary condition was imposed. The time taken for the different locations to reach 300K is different between the solid Cp curve method and the enthalpy porosity method. Based on Figure 46, Figure 47, and Figure 48 it can be observed that reaching 300K takes a longer time in the Solid Cp curve approach than the enthalpy porosity approach. Comparing the temperatures within the same approach it is observed that the 2mm plane is the first to reach 300K and the 6.3mm plane is the last to reach 300K as expected as shown in Figure 46 and Figure 48. Also, it can be observed that after 23 minutes for the enthalpy porosity approach and after 33 minutes for the solid Cp curve approach the increase in the temperatures is rapid and because after these points in time the PCM is completely melted and thus, the heat capacity of the PCM is less than it is during the melting zone.

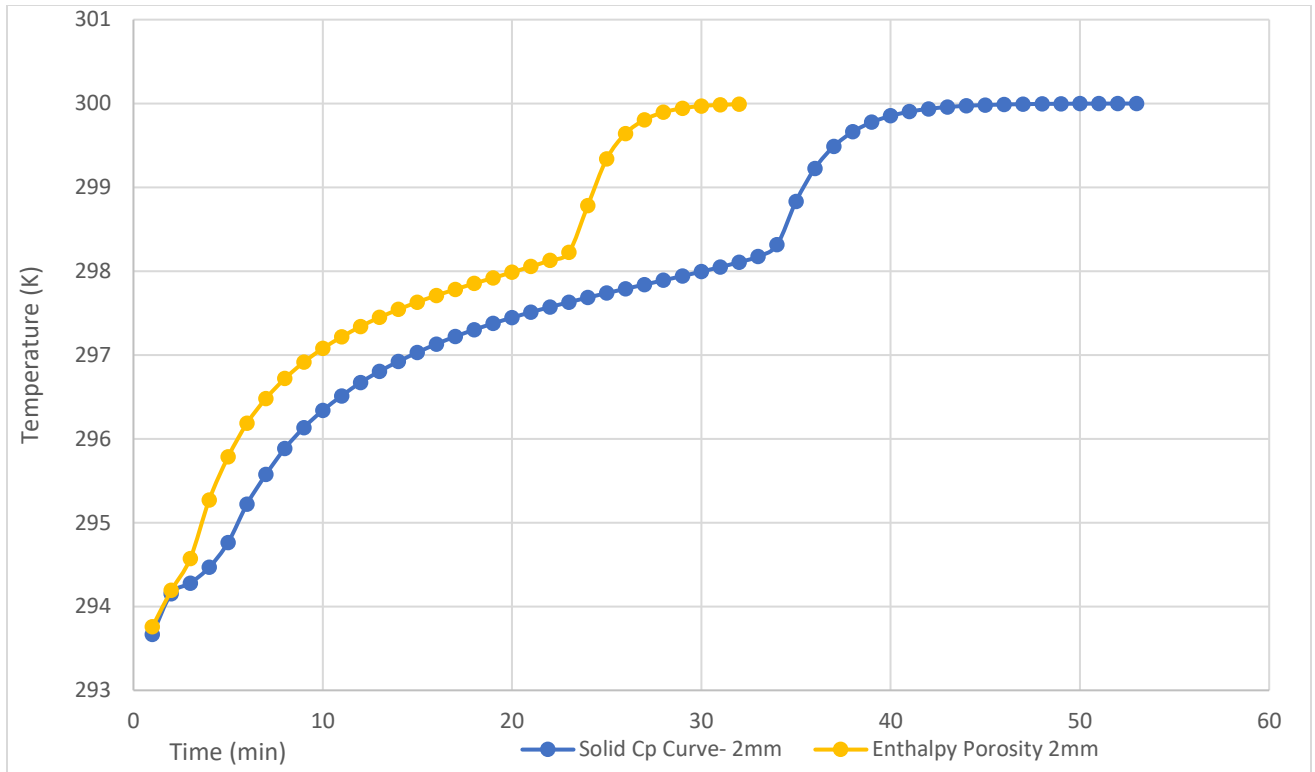


Figure 46. Comparison of temperature as a function of time at 2mm from isothermal boundary between the enthalpy porosity approach and solid Cp approach

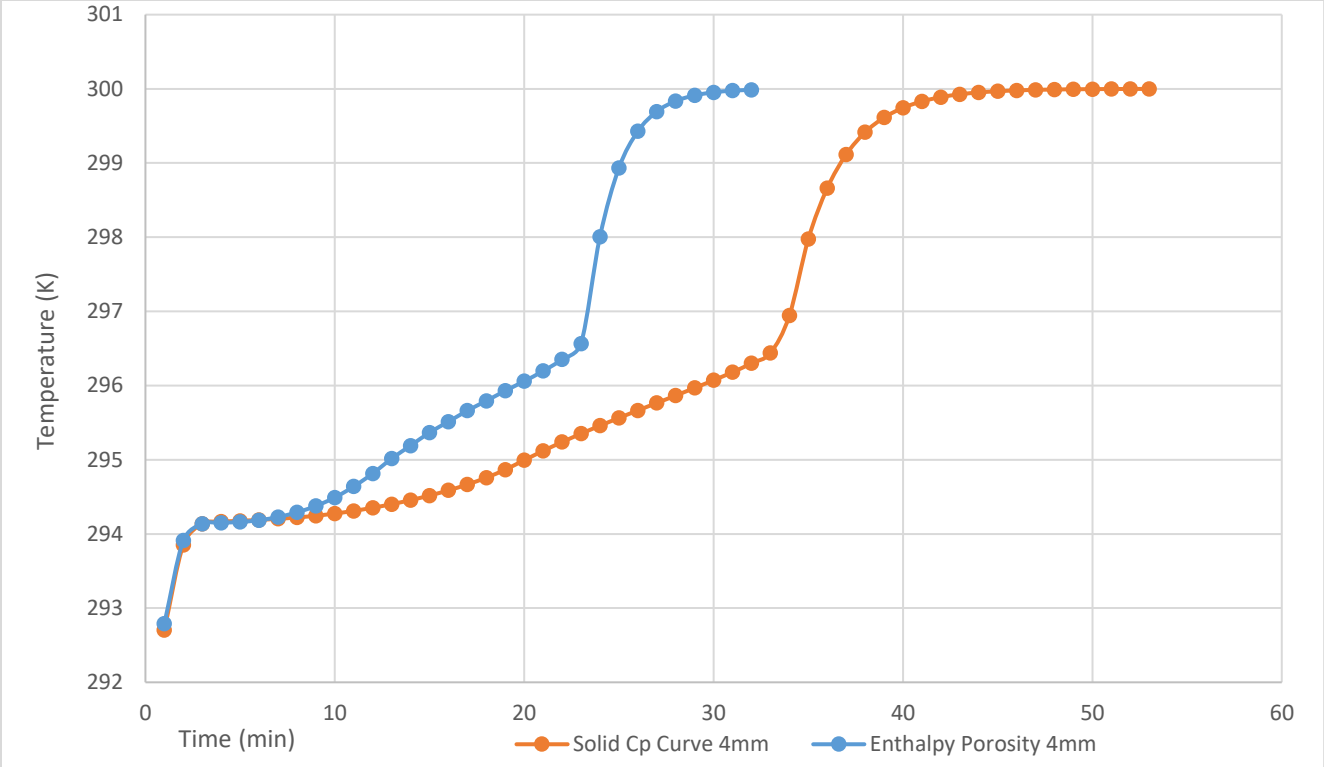


Figure 47. Comparison of temperature as a function of time at 4mm from isothermal boundary between the enthalpy porosity approach and solid Cp approach

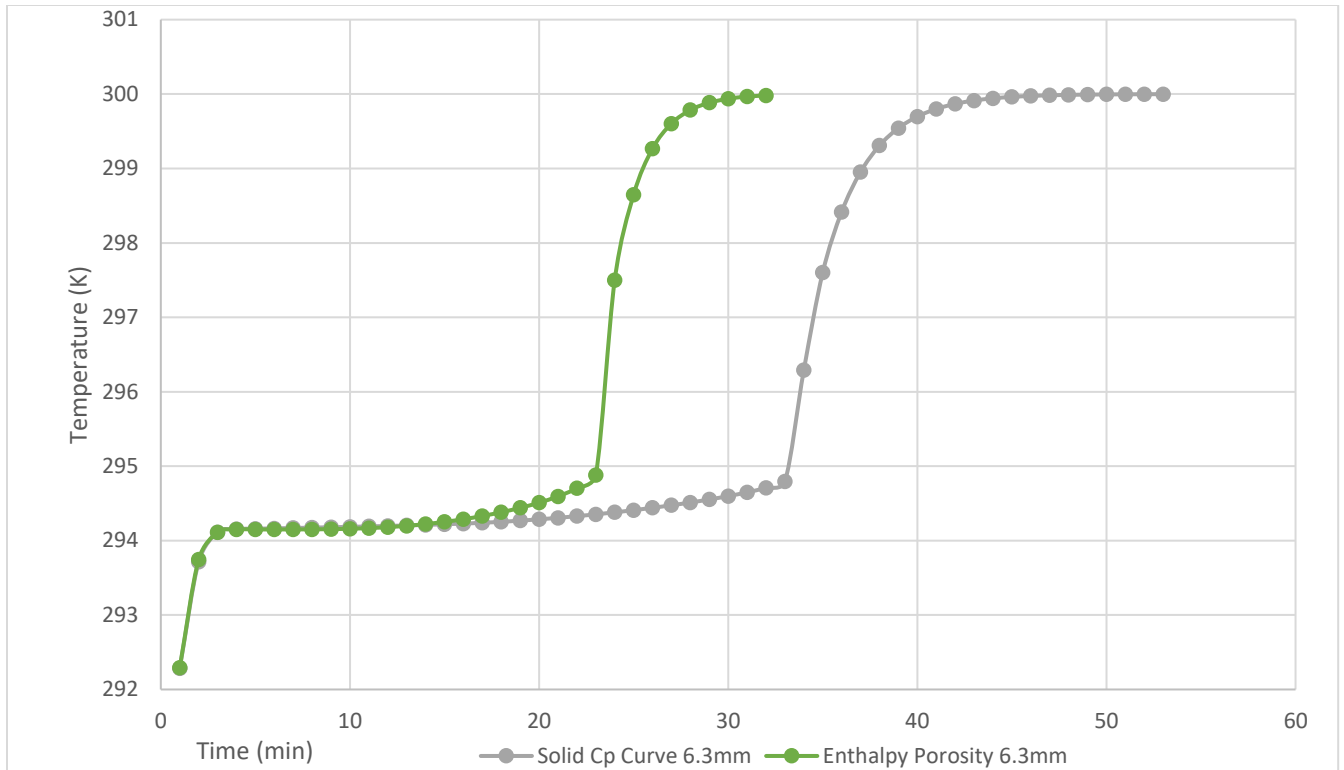


Figure 48. Comparison of temperature as a function of time at 6.3mm from isothermal boundary between the enthalpy porosity approach and solid Cp approach

The heat flux at the right wall is averaged over the entire surface and consecutive data points are extracted with a 1-minute interval in between. Initially, the heat flux is very high about $\sim 3500 \text{ W/m}^2$ and then drops quickly into the $1500\text{-}500 \text{ W/m}^2$ range where the rate of heat flux change is significantly smaller as shown in Figure 49. At the 23-minute mark in the enthalpy porosity approach, and at the 33-minute mark in the solid Cp curve approach, there is a sudden change in the heat flux which indicates that the entire PCM has melted as shown in Figure 49. At the 30-minute mark in the enthalpy porosity approach and the 41-minute mark in the solid Cp curve approach the heat flux drops to zero and this corresponds to the temperature at the 6.3 mm wall reaching thermal equilibrium with the entire domain as shown in Figure 48 and Figure 49.

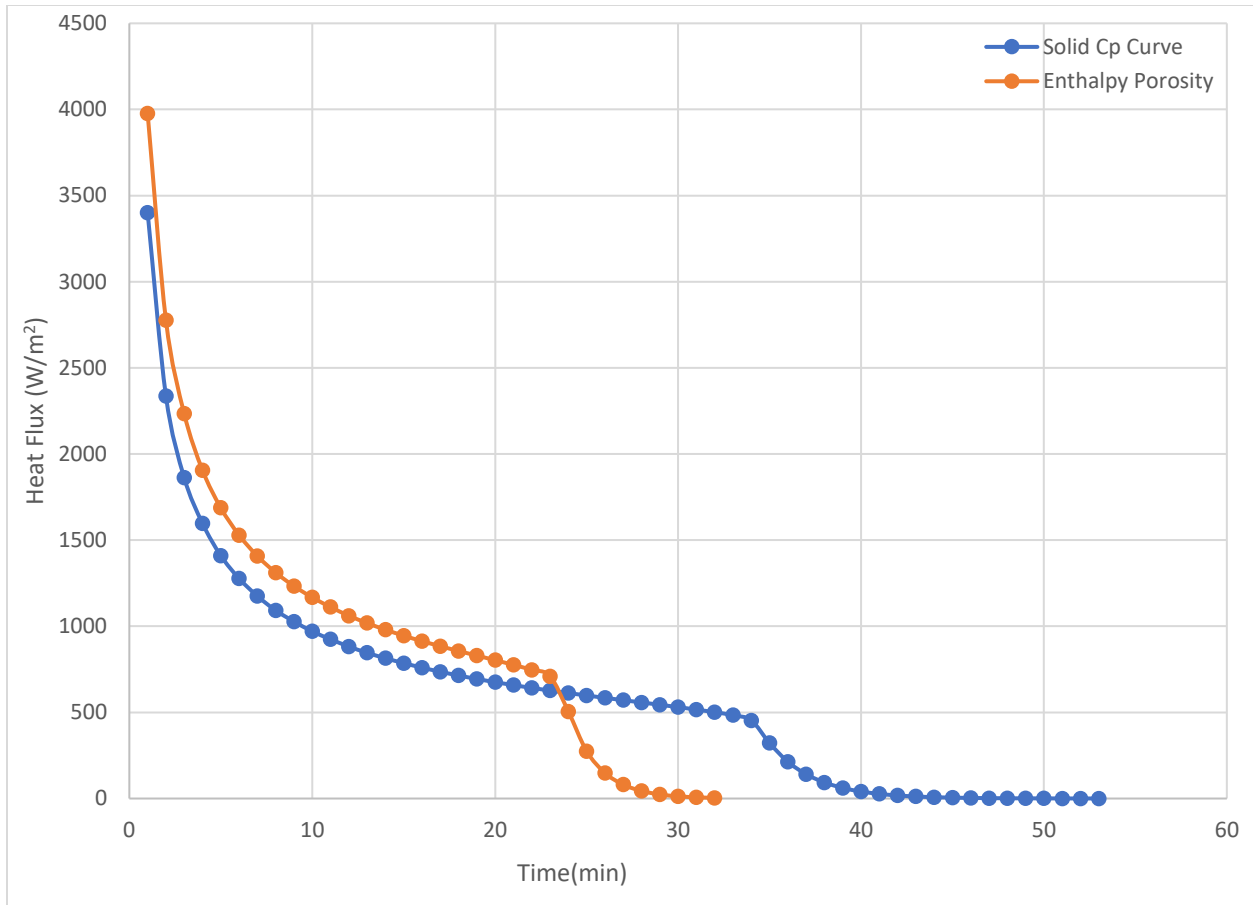


Figure 49. Comparison of heat flux as a function of time at the isothermal boundary between the enthalpy porosity approach and solid Cp approach

Analyzing these graphs, the trends of both approaches look similar, but the time taken by the solid PCM is longer. To explore the reason for this mismatch between the approaches, two exploratory simulations were carried out. Firstly, the solid Cp curve was modified to have a triangular form as opposed to the trapezium-like form. The comparison of the heat flux on the right wall and the temperatures at different depths inside the PCM show that changing the Cp curve shape to triangular does not have any impact on the melting time and the overall behavior of PCM 2 modeled as a solid. Secondly, the mushy zone constant can affect the flow characteristics and heat transfer by changing the magnitude of the sink term in the momentum equation, and therefore, the different mushy zone constants were used to study the impact on the melting time. The mushy zone constant (A_{mush}) was set to 5×10^6 and 10^9 for the simulations but no change in melting time, heat flux at right wall, and

temperatures at different depths was observed. Therefore, it can be concluded that in this case PCM 2 melting behavior is independent of mushy zone constant and that the viscosity value used for PCM 2 is not the correct fit. Thus, due to lack of viscosity data and experimental data it was decided to use the Solid Cp curve approach for PCM 2 as well.

PCM 2 Blended Wall Simulations with Inner Wall Convective Boundary Condition

Modeling Domain

The modeling domain for the PCM 2 simulations was exactly like the Blended Wall model for the No PCM cases but with an additional layer of PCM 2 on top of the gypsum layer. The PCM 2 layer had a thickness of 6.3mm. Figure 50 shows cross sectional view Blended Wall model for PCM 2.

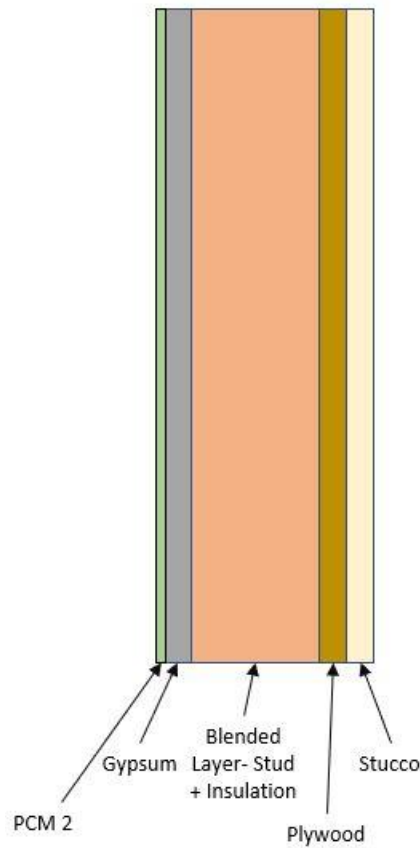


Figure 50. Blended wall model with PCM 2 layer next to Gypsum layer

Wall Material Properties

The thermophysical properties of gypsum, stucco, and plywood are given in Table 2. The thermophysical properties of the blended layer were calculated based on the mass-weighted thermophysical properties of the insulation and the stud and are given in Table 3. The density of PCM 2 is provided in Table 6 and the specific heat capacity variation with temperature was modelled using piecewise linear profiles as shown in Figure 44. The thermal conductivity of solid PCM 2 (273.15K-294.15K) and of liquid PCM 2 (294.95K-400K) is given in Table 6. The variation of thermal conductivity with temperature in the mushy zone (294.15K-294.95K) is modelled using the equation given in Table 8.

Boundary Conditions

The boundary conditions applied on the PCM 2 cases were exactly like the boundary conditions imposed on the No PCM with Inner Wall Convective Boundary Condition cases. As shown in Figure 2, the insulated boundary condition was imposed on Surfaces 1 and 2, the symmetry boundary condition was imposed on Surfaces 3 and 4, the convective boundary condition was imposed on Surface 5, and Outer Wall surface temperature profile obtained from EnergyPlus on Surface 6. For PCM 2 Blended Wall Simulations with Inner Wall Convective Boundary Condition 4 cases for Winter were run and they were Winter 1 No PCM, Winter 1 PCM 2, Winter 2 No PCM, and Winter 2 PCM 2. Similar cases were executed for Summer as well and for PCM 2 no Shoulder cases were executed. For all the Winter and Summer cases the outer wall temperature profiles imposed as a boundary condition were all the same for the same season. The inner wall convective boundary conditions for the different cases have been summarized in the Table 9.

Table 9. Different cases run for PCM 2 and their inner wall surface boundary conditions

| Case | Convective Heat Transfer Coefficient (W/m ² K) | Free Stream Temperature (K) |
|-----------------|---|-----------------------------|
| Winter 1 No PCM | 1.744 | 292.65 |
| Winter 1 PCM 2 | 1.744 | 292.65 |
| Winter 2 No PCM | 1.744 | 294.5 |
| Winter 2 PCM 2 | 1.744 | 294.5 |
| Summer 1 No PCM | 1.744 | 298.65 |
| Summer 1 PCM 2 | 1.744 | 298.65 |
| Summer 2 No PCM | 1.744 | 294.8 |
| Summer 2 PCM 2 | 1.744 | 294.8 |

Initial Conditions and Simulation Time

The initial conditions and simulation time for the PCM 2 cases were exactly like the No PCM cases. The 24-hour temperature profiles were run consecutively for 3 days. The identical heat flux profiles of day 2 and day 3 that obtained as an output were used to ensure that the simulation results were independent of the initial condition.

Solver Settings and Mesh Quality

The SIMPLE scheme was used for pressure-velocity coupling. A second-order implicit scheme was used for the transient formulation. The use of an implicit scheme ensured that there was no possibility of the calculations becoming unstable and this also provides greater flexibility in selecting the time step size. The time step used in these simulations was 300 seconds and the solutions were recorded after every 2-time steps. The total number of elements in the mesh was 525000, maximum skewness of the mesh was 1.3×10^{-10} , and average skewness of the mesh was 1.3×10^{-10} .

Results

PCM 2 Winter

Comparing the inner wall surface temperatures of Winter 1 No PCM with Winter 1 PCM 2 and Winter 2 No PCM with Winter 2 PCM 2 the No PCM cases show a higher temperature fluctuation than the corresponding PCM 2 cases as shown in Figure 51. Winter 1 had an indoor air temperature of 292.65K and this was lower than the solidus temperature of PCM 2 which was 294.15 K and thus, PCM 2 never melted or even reached the solidus temperature. The maximum temperature PCM 2 in Winter 1 PCM 2 case was 293K. Thus, the reduced temperature fluctuation of Winter 1 PCM 2 as compared to Winter 1 No PCM is purely due to the added thermal mass. For Winter 2 the freestream temperature was 294.5K and this was selected to ensure that PCM 2 started melting during the 24-hour cycle. The maximum

temperature of the inner wall surface was 294.18K and thus, PCM 2 entered the mushy zone but did not completely. From Figure 46, Figure 47, Figure 48, and Figure 49 it can be concluded that PCM 2 completely melts approximately at 33-34 minutes in the simplified 2D simulation using when using the Solid Cp curve approach. The heat flux values range from 453-3401 W/m² between 0-34 minutes as shown in Figure 49 and these are significantly higher than the heat flux values at the inner wall surface in the Blended Wall model. Thus, the amount of energy needed to melt PCM 2 was not available from the inner wall surface heat flux and this lead to the temperatures showing no change between 17-20.67 hours for Winter 2 PCM 2 case. Between 0-10 hours the inner wall surface temperatures for all cases was decreasing and this corresponded to the nighttime and early morning times. For Winter 1 No PCM and Winter 2 No PCM the inner wall surface temperature started increasing slightly before 10 hours and peaked at around 16.5 hours. This corresponds to the time between sunrise to sunset. But the for the PCM 2 cases the temperature started rising a little later in time.

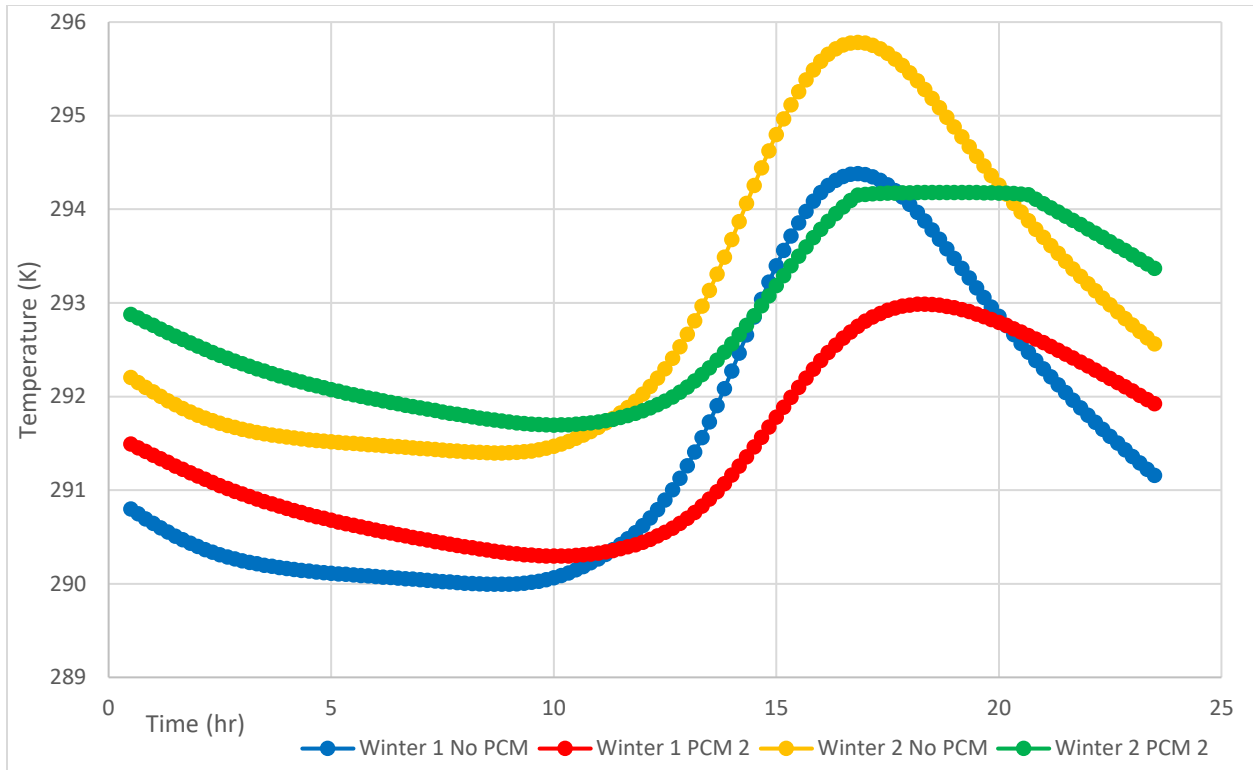


Figure 51. Comparison of inner wall surface temperature profiles between Winter 1 No PCM, Winter 1 PCM 2, Winter 2 No PCM, and Winter 2 PCM 2

Like the inner wall surface temperatures, the higher fluctuations in the inner wall surface heat flux are observed in the No PCM cases as shown in Figure 52. For a Winter day, the goal of adding PCM to the wall envelope is to ensure that PCM melts during the day and at night releases this energy to the inside of the house and keeps it warm. This delays turning ON the heater and reduces the energy consumption of heating the house. Thus, it is expected that for the PCM to be effective the heat flux should be negative for a longer period than the No PCM case in the evening and should have a higher or comparable negative heat flux in the evening. But for Winter 1 PCM 2 it is observed that the highest negative heat flux is less than -1 W/m^2 and this is significantly smaller than the -3 W/m^2 that is observed in the Winter 1 No PCM case. Thus, the heat entering the house from the inner wall surface is much smaller in the Winter 1 PCM 2 case. The time duration for which the heat is entering the house is also much smaller. For Winter 1 No PCM case it is between 14.5-20.5 hours and for the Winter 1 PCM 2 case

it is between 16.5-20.5 hours. For the Winter 1 case no effect of PCM melting was seen and thus, for Winter 2 the freestream temperature of 294.5K was chosen to ensure that PCM 2 at least partially melted. The Winter 2 No PCM case showed that a higher freestream temperature meant that more heat left the house between 0-10 hours than the Winter 1 No PCM case. The overall trend of Winter 2 No PCM is similar to Winter 1 No PCM but with a higher positive heat flux between 0-10 hours and lower negative heat flux between 14.5-20 hours. Winter 2 PCM 2 case shows a similar trend where more heat leaves the house between 0-5.5 hours than the Winter 1 PCM 2 case. The heat flux never changes direction and at no point during the 24-hours the heat enters the house from the inner wall surface. Thus, changing the freestream temperature to 294.5K did not have the desired impact. The inner wall surface heat flux for Winter 2 PCM 2 is almost constant between 17.5-20.5 hours and this corresponds the time during which PCM 2 temperature is above the solidus temperature. The heat flowing through the wall was not enough to melt the PCM during the day and thus, the benefit of heat released during PCM solidification was not extracted in this configuration. Throughout the 24-hour cycle the heat flux is positive for longer periods of time than it is negative and thus, in a cumulative sense this means a wall configuration with lower value of heat flux integrated over the 24-hour cycle is a more energy efficient option. The total heat entering the inner wall surface from inside the house over the 24-hour cycle was 179,138 J/m² for Winter 1 No PCM, 185,281 J/m² for Winter 1 PCM 2, 246,151 J/m² for Winter 2 No PCM, and 254,367 J/m² for Winter 2 PCM 2. Thus, in the Winter 1 PCM 2 case the total heat entering the inner wall surface from inside the house is 3.4% higher than in the Winter 1 No PCM case. Similarly, in the Winter 2 PCM 2 case the total heat entering the inner wall surface from inside the house is 3.3% higher than in the Winter 2 No PCM case. These numbers indicate that more heat will leave the house in order to maintain the corresponding freestream temperatures, and this will require the heating system to spend more energy in the case when PCM 2 is added at the inner wall. Because more heat travels from

inside the house to the inner wall surface when PCM 2 is added and to compensate for this loss of heat the heating system will end up consuming more energy.

The outer wall surface heat flux variation throughout the 24-hour cycle is shown in Figure 53 and it is exactly same in all the cases. The heat flux is flowing from inside the house to outside during the night and at 7.5 hours the heat flux changes direction. The change in direction corresponds to solar radiation incident on the outer wall surface and the impact of the solar radiation can be seen on the inner wall surface temperature at 10 hours. The outer wall surface heat flux remains positive only between 7.5-14.5 hours.

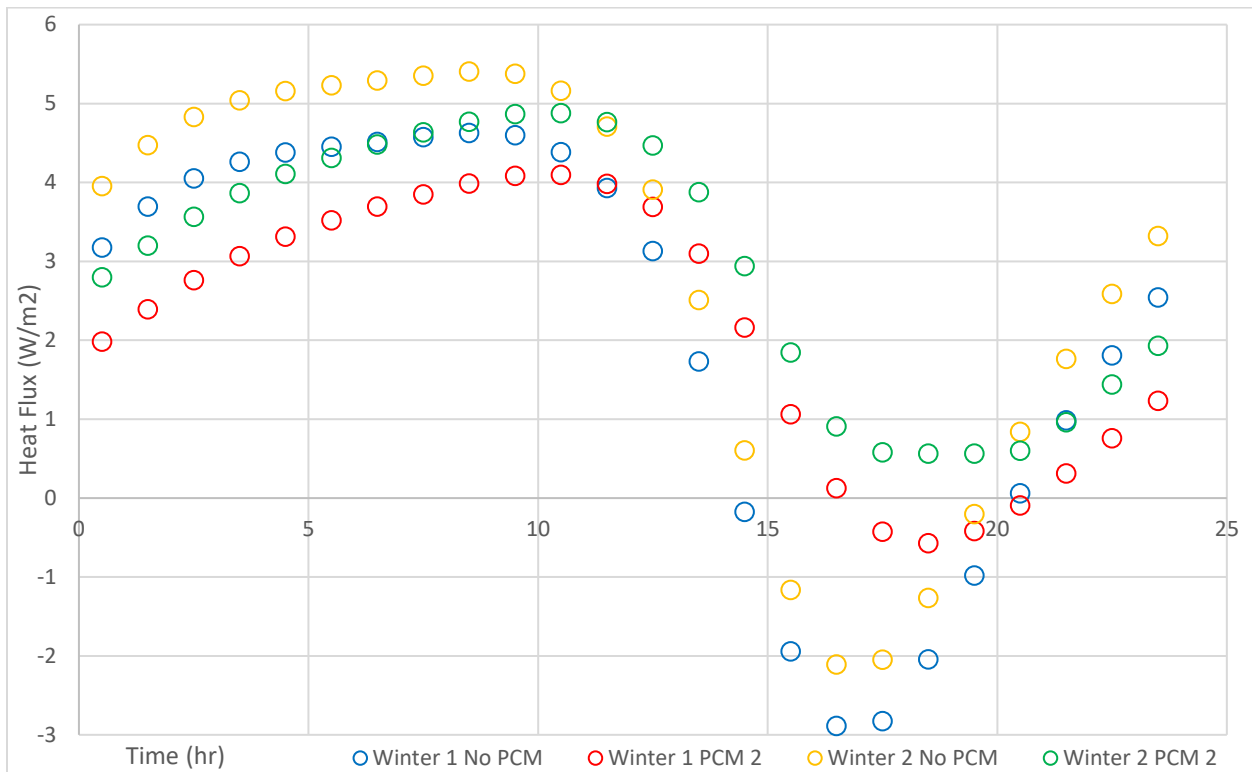


Figure 52. Comparison of inner wall surface heat flux profiles between Winter 1 No PCM, Winter 1 PCM 2, Winter 2 No PCM, and Winter 2 PCM 2

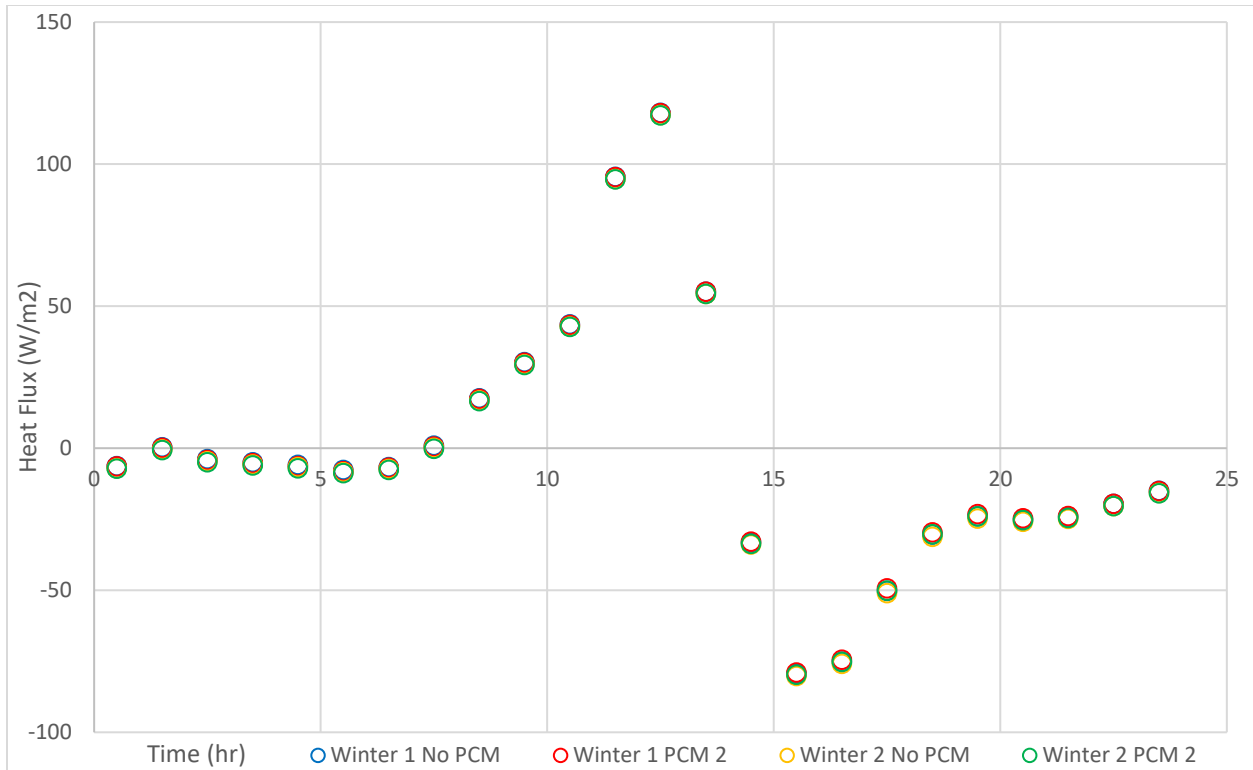


Figure 53. Comparison of outer wall surface heat flux profiles between Winter 1 No PCM, Winter 1 PCM 2, Winter 2 No PCM, and Winter 2 PCM 2

PCM 2 Summer

Summer 1 No PCM and Summer 2 No PCM show the exact same trends and behavior throughout the 24-hour cycle and the only change is they are displaced in temperature as shown in Figure 54. This is expected because the only different between these cases is the freestream temperature values.

Comparing Summer 1 No PCM with Summer 1 PCM 2 and Summer 2 No PCM with Summer 2 PCM 2 the No PCM cases have a higher temperature fluctuation. This can be attributed to the added thermal mass in the PCM 2 cases. The inner wall surface temperature is always above the liquidus temperature (294.95K) in the Summer 1 PCM 2 case and this indicates that PCM 2 was always a liquid in this case and there was no phase change that took place. Thus, no benefit of adding the PCM was seen as the freestream temperature was 298.65K. To ensure that PCM at least partially started solidifying the

freestream temperature was set to 294.8K which is lower than the liquidus temperature for Summer 2 cases. The inner wall surface temperature remains constant between 6.5-12.67 hours but it never drops significantly in the mushy zone region. The lowest temperature during this time is 294.90K which indicates that only a small fraction of PCM 2 has solidified partially. PCM 2 does not lose enough heat to solidify the PCM significantly. The temperature of inner wall surface drops constantly from 0-8 hours and then increases between 8-17 hours for the No PCM cases. For the PCM 2 cases there are delays in the time until which the temperature drops and delays in the time until which the temperature rises.

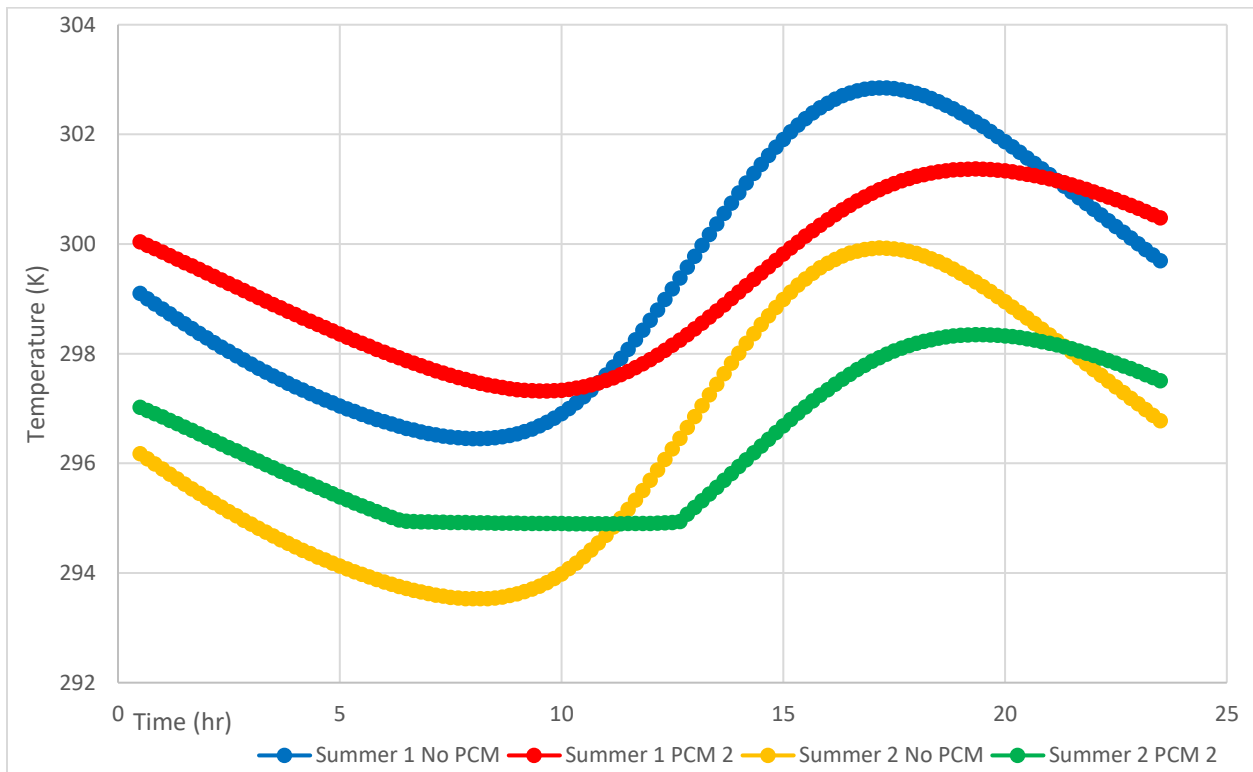


Figure 54. Comparison of inner wall surface temperature profiles between Summer 1 No PCM, Summer 1 PCM 2, Summer 2 No PCM, and Summer 2 PCM 2

For a Summer day, the goal of adding PCM is to reduce the amount of heat entering inside the house and thus, reducing the energy consumption of cooling the house. The heat leaving the inner wall surface and entering the house has a negative value. Thus, when analyzing the graph a wall configuration that has a smaller negative value of total heat over the 24-hour duration is a more energy efficient option.

For Summer 1 No PCM the inner wall surface heat flux is negative between 0-1.5 hours and this indicates that the heat entering the house from the inside wall surface as shown in Figure 55. Between 1.5-12.5 hours the inner wall surface heat flux is positive indicating that the heat is leaving the house and during this time the heat flux first increases till 8.5 hours and then decreases. Between 12.5-24 hours the inner wall surface heat flux is negative indicating that heat is continuously entering the house during these times. For the Summer 1 PCM 2 case the heat flux is negative between 0-4.5 hours and this indicates that the heat is entering the house for longer time period than the No PCM case. Between 4.5-13.5 hours the inner wall surface heat flux is positive but the magnitude of heat leaving the house is much smaller than the No PCM case and this is not desirable. Beyond 13.5 hours the inner wall surface heat flux is negative but lower in magnitude than the No PCM case and thus, lower amount of heat enters the house. Summer 2 No PCM shows similar trends to Summer 1 No PCM but with differing magnitudes and time shift. For the Summer 2 No PCM case the amount of heat leaving the house is lower than both Summer 1 cases but the heat entering the house is greater than all the cases. For the Summer 2 PCM 2 case the inner wall surface heat flux is negative throughout the 24-hour cycle and this indicates that the heat is continuously entering the house and this does not contribute towards reducing the cooling energy consumption. The cumulative heat entering the house from the inner wall surface was -109292 J/m^2 for Summer 1 No PCM, -104868 J/m^2 for Summer 1 PCM 2, -248264 J/m^2 for Summer 2 No PCM, and -241179 J/m^2 for Summer 2 PCM 2. In the Summer 1 PCM 2 case the total heat entering the house from the inner wall surface is 4% less than in the Summer 1 No PCM case. Similarly, in the Summer 2 PCM 2 case the total heat entering the house from the inner wall surface is 2% less than in the Summer 2 No PCM case. Thus, as less heat enters inside the house when PCM 2 is placed at the inner wall surface less energy will be spent in cooling the house to maintain the appropriate freestream temperatures. These numbers clearly indicate that adding PCM 2 had some impact on reducing the cooling energy consumption.

As observed in the outer wall surface heat fluxes of all the Winter cases the outer wall surface heat fluxes of all the Summer cases also overlapped each other and there was no significant difference between any cases as shown in Figure 56. Comparison of outer wall surface heat flux profiles between Summer 1 No PCM, Summer 1 PCM 2, Summer 2 No PCM, and Summer 2 PCM 2. Between 0-5.5 hours and 14.5-24 hours the outer wall surface heat flux is negative indicating that the heat is traveling from the outer wall surface to the outdoor environment. Only between 5.5-14.5 hours the heat is entering from the outdoor environment to the outer wall surface.

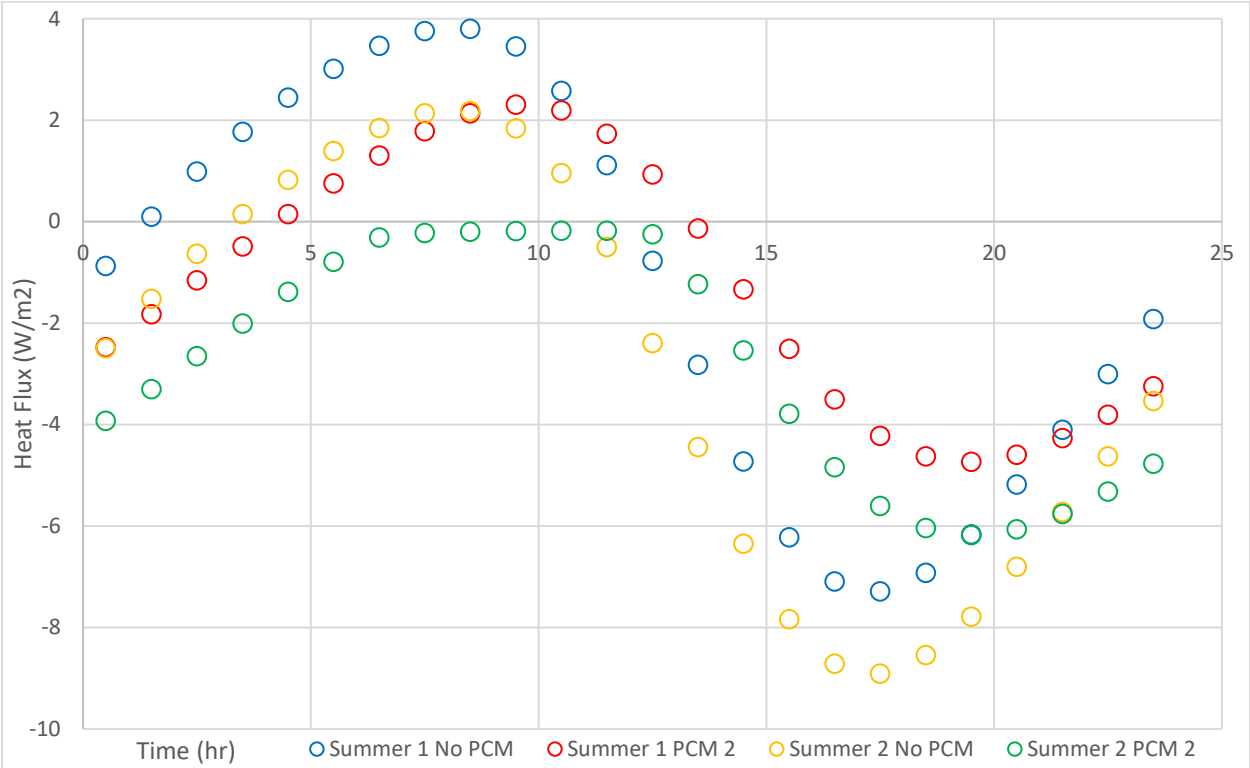


Figure 55. Comparison of inner wall surface heat flux profiles between Summer 1 No PCM, Summer 1 PCM 2, Summer 2 No PCM, and Summer 2 PCM 2

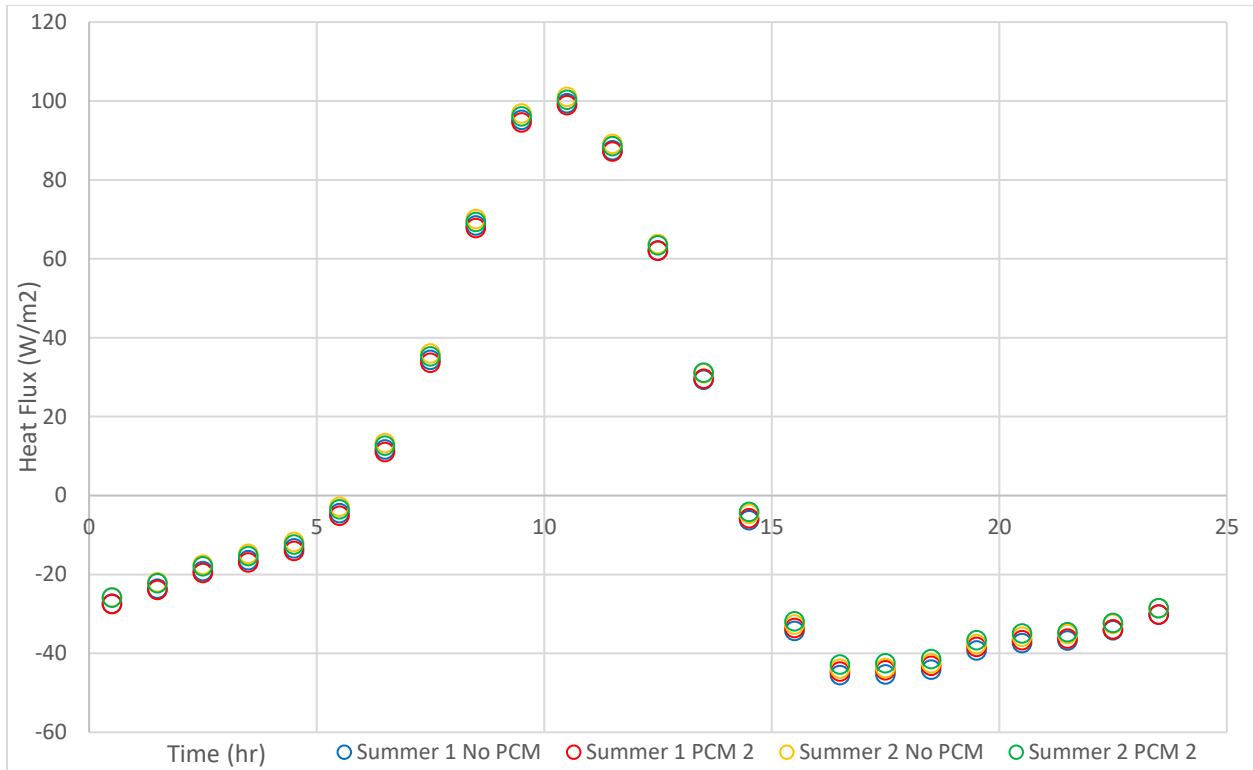


Figure 56. Comparison of outer wall surface heat flux profiles between Summer 1 No PCM, Summer 1 PCM 2, Summer 2 No PCM, and Summer 2 PCM 2

The inner wall surface temperature range for Winter 1 is from 290.3-293K and for Winter 2 is from 291.7-294.1K. Thus, in both the cases the inner wall surface temperature never enters the melting range of PCM 2 which is begins from 294.15K. The inner wall surface temperature in Winter 2 remains constant at 294.1K as the huge amount of energy is required for melting PCM 2. This much energy is not available at the inner wall surface and thus, only a very small fraction of PCM 2 melts. To reduce the energy consumption in Winter the inner wall surface temperature and the inner wall surface heat flux must be such that it at least partially melts a significant portion of the PCM. If this were the case, then high specific heat of PCM 2 can be leveraged to reduce the energy consumption. The inner wall surface temperature range for Summer 1 is from 297.3-301.3K and for Summer 2 is from 294.9-298.3K. In Summer 1 the inner wall surface temperature is such that PCM 2 is always in a liquid state but for Summer 2 between the range of 294.95-294.9K PCM 2 solidifies slightly. It is interesting to note that

although PCM 2 never melts in Summer 1 case the total heat entering house from the inner wall surface reduces by 4% but in the Summer 2 case where PCM 2 melts slightly the reduction in the heat entering the house from the inner wall surface is only 2%. This indicates that solidification of PCM 2 in Summer might not have the desired impact.

Chapter 6: Different PCM Locations

PCM Distributed Inside Insulation + Stud Layer

The PCM behavior when located at the inner wall surface is strongly affected by the indoor conditions but the impact of outdoor conditions is weak. To completely utilize the benefits of PCM in reducing energy requirements the PCM must be located at a position where it can interact with both the indoor and outdoor environments [35]. Prior to starting this project, the idea of locating PCM inside the insulation was rejected because the poor thermal conductivity of the insulation will reduce the heat conduction to the PCM. As the heat conducted to the PCM is reduced, the large heat capacity offered by the PCM is not completely utilized and thus, this location was not tested.

The optimal location of the PCM in the building envelope is a function of the thermophysical properties of the PCM, and the indoor and outdoor conditions of the building. Different studies have identified different optimal locations for the PCM and this proves that in addition to being a function of the thermophysical properties of the PCM and the indoor and outdoor conditions, it also depends on the wall structure of the building. Jin et al. [36][37] found the optimal PCM location to be $1/5$ the cavity thickness from the inner wall surface. Lee et al. [19] found the optimal PCM location as $2/5$ the cavity thickness from the inner wall surface for the South facing wall and $1/5$ the cavity thickness from the inner wall surface for the West facing wall. Fateh et al. [38][39] found the optimal PCM location to be at the middle of the wall. Kishore et al. [35] found the optimal PCM location to be in the center of the insulation for different cities in the U.S. Based on these studies, an additional PCM location of PCM inside the insulation layer was tested.

Modeling Domain

In the PCM inside Insulation + Stud layer, PCM cubes were equally distributed throughout the blended wall in the insulation + stud layer. The volume of the PCM distributed was equal to the volume of the PCM contained in the PCM 1 6mm layer model. As the densities of PCM 1 and PCM 2 were different the mass of the PCM in these models was different as well but both had the same volume. The PCM was distributed in cubes of 2mm arranged in a staggered pattern with a pitch of 4.91mm. With the addition of cubes distributed inside the insulation + stud layer the meshing of the domain needed higher density of elements and thus, to reduce the computational effort the cross-sectional area of the domain used was 4.91mm x 4.91mm as shown in Figure 57. This was possible by imposing symmetry boundary conditions on the lateral faces.

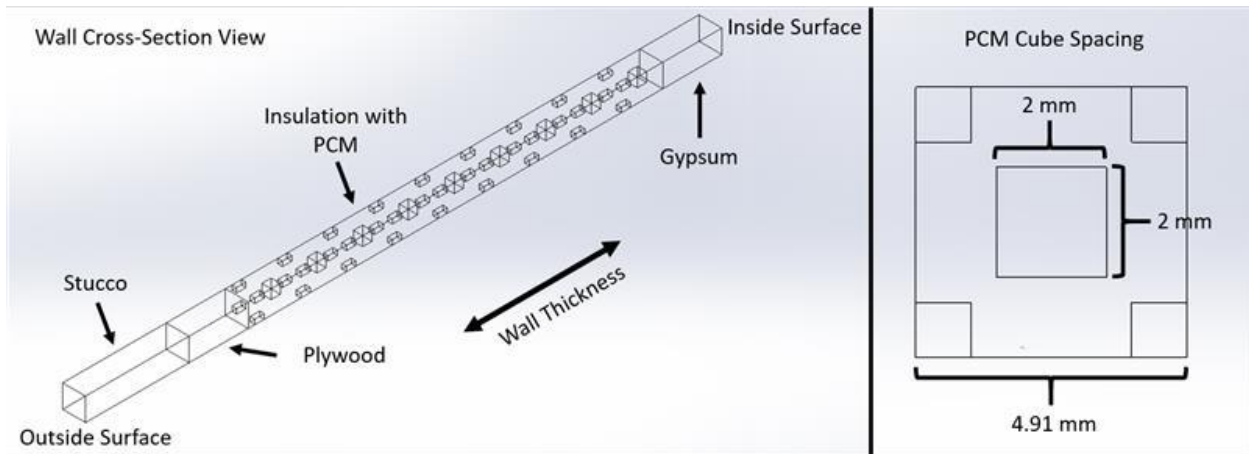


Figure 57. Wall model with PCM inside Insulation + Stud layer

Wall Material Properties

The thermophysical properties of gypsum, plywood, and stucco are given in Table 2. The thermophysical properties of the blended layer were calculated based on the mass-weighted thermophysical properties of the insulation and the stud and are given in Table 3. The density and thermal conductivity of PCM 1

are provided in Table 4 and the specific heat capacity variation with temperature was captured using the UDF and the details of it are provided in Table 5. The density of PCM 2 is provided in Table 6 and the specific heat capacity variation with temperature of PCM 2 was modelled using piecewise linear profiles as shown in Figure 44. The thermal conductivity of solid PCM 2 (273.15K-294.15K) and of liquid PCM 2 (294.95K-400K) is given in Table 6 The variation of thermal conductivity with temperature in the mushy zone (294.15K-294.95K) was modelled using the equation given in Table 8. Depending on the case the appropriate PCM material properties were used.

Boundary Conditions

The boundary conditions applied on the PCM inside Insulation + Stud layer cases were exactly like the boundary conditions imposed on PCM 2 and No PCM cases with Inner Wall Convective Boundary Condition cases. As shown in Figure 2, the symmetry boundary condition was imposed on Surfaces 1, 2, 3, and 4, the convective boundary condition was imposed on Surface 5, and Outer Wall surface temperature profile obtained from EnergyPlus on Surface 6. For PCM inside Insulation + Stud layer cases only Winter representative days were tested. The outer wall temperature profile imposed on all the cases was exactly same and only the inner wall convective boundary condition was changed. Table 10 summarizes the different boundary conditions imposed on the inner wall in the different cases.

Table 10. Different cases run for PCM inside Insulation + Stud layer and their inner wall surface boundary conditions

| Case | Convective Heat Transfer Coefficient (W/m ² K) | Free Stream Temperature (K) |
|-----------------|---|-----------------------------|
| Winter 1 No PCM | 1.744 | 292.65 |
| Winter 1 PCM 1 | 1.744 | 292.65 |
| Winter 1 PCM 2 | 1.744 | 292.65 |
| Winter 2 No PCM | 1.744 | 294.5 |
| Winter 2 PCM 1 | 1.744 | 294.5 |
| Winter 2 PCM 2 | 1.744 | 294.5 |

Initial Conditions and Simulation Time

The initial conditions and simulation time for the PCM Next to the Stud cases were exactly like the No PCM cases. The 24- hour temperature profiles were run consecutively for 3 days. The identical heat flux profiles of day 2 and day 3 that were obtained as an output were used to ensure that the simulation results were independent of the initial condition.

Solver Settings and Mesh Quality

The SIMPLE scheme was used for pressure-velocity coupling. A second-order implicit scheme was used for the transient formulation. The use of an implicit scheme ensured that there was no possibility of the calculations becoming unstable and this also provides greater flexibility in selecting the time step size. The time step used in these simulations was 300 seconds and the solutions were recorded after every 2-time steps. The total number of elements in the mesh was 8841643, maximum skewness of the mesh is 0.214, and average skewness of the mesh was 0.188.

Results

Figure 58 shows the outer wall surface temperature variation through the 24-hour cycle that was imposed on all the simulations of PCM inside Insulation + Stud layer. The outer wall surface temperature does not vary a lot between 0-7.5 hours and beyond this point the solar radiation starts hitting the outer wall surface. The impact of the solar radiation is that the outer wall surface temperature starts increasing and between 7.5-10.33 hours the temperature increases at certain rate but between the 10.33-13.33 hours the rate of outer wall surface temperature increase is even higher. After 13.33 hours

a decline in the outer wall surface temperature begins and this continues for the remainder of the 24-hour cycle.

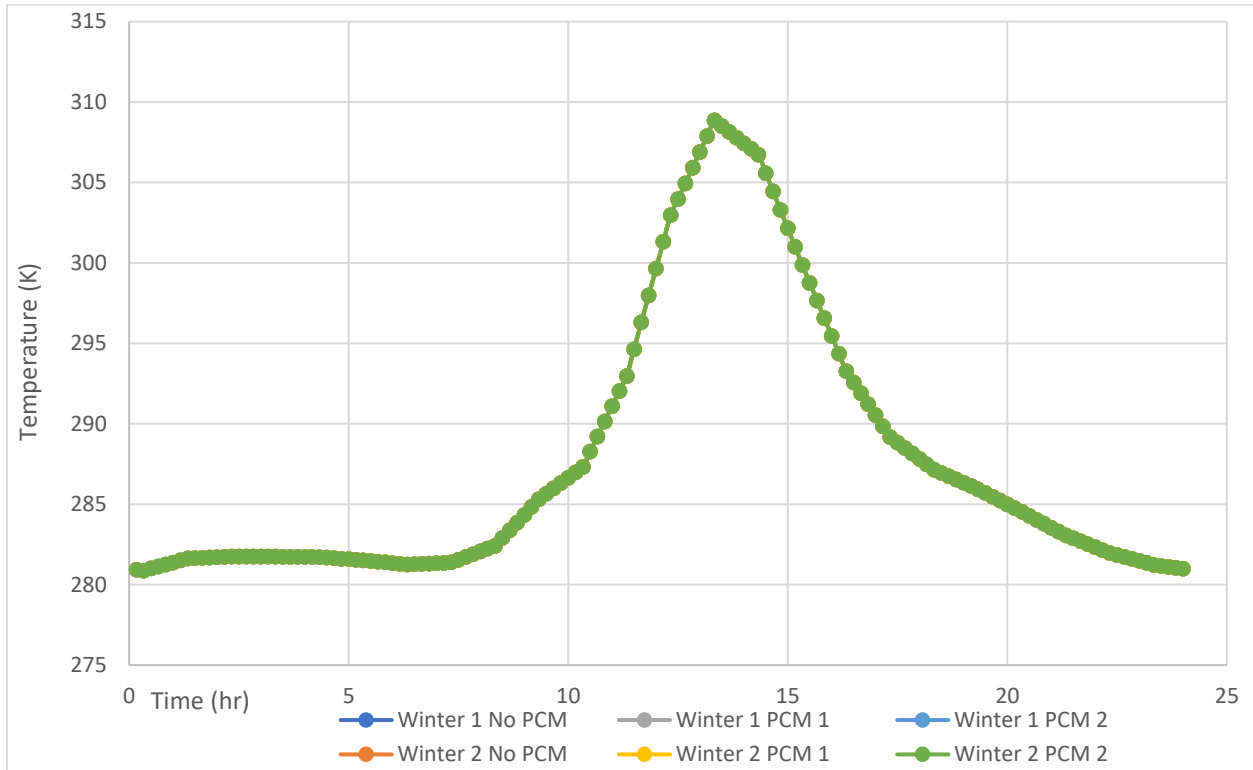


Figure 58. Comparison of outer wall surface temperature profiles between Winter 1 No PCM, Winter 1 PCM 1, Winter 1 PCM 2, Winter 2 No PCM, Winter 2 PCM 1, and Winter 2 PCM 2 with PCM inside Insulation + Stud layer wall model

The inner wall surface temperature variation through the 24-hour cycle for all the PCM inside Insulation + Stud layer are shown in Figure 59 and Figure 60 Comparison of the Winter 1 and Winter 2 cases shows that the general trends in both are very similar but have been displaced in temperature and this has been caused by the changed freestream temperature inside the house which for Winter 1 is 292.65K and for the Winter 2 is 294.5K. For the No PCM cases and the PCM 1 cases the temperatures slightly drop between 0-8.67 hours. The drop is even smaller in the PCM 1 cases. During the same time of 0-8.67 hours the PCM 2 cases shows a much higher drop in temperature and in these cases the drop continues till 9-hours. The solar radiation starts hitting the outer wall surface at 7.5 hours and the effect of the radiation on inner wall surface temperature is observed at around 10-hours. The inner wall surface

temperatures of the No PCM and PCM 1 cases start increasing slightly before 10-hours. For the No PCM cases the rise in temperature continues till 16.83 hours and for the PCM 1 cases it continues till 16-hours. Comparing the maximum temperature increase of the No PCM, PCM 1 and PCM 2 cases the maximum temperature increase occurs in the No PCM case followed by the PCM 1 case. This can be attributed to the additional thermal mass in the PCM cases compared to the No PCM cases. Beyond the peak in temperatures occurring at different times in the No PCM and PCM 1 cases the inner wall surface temperature decreases at a constant rate for the rest of the 24-hour cycle. For the PCM 2 cases the inner wall surface temperature continue rising until 23.5 hours in the Winter 1 case and 20.5 hours in the Winter 2 case.

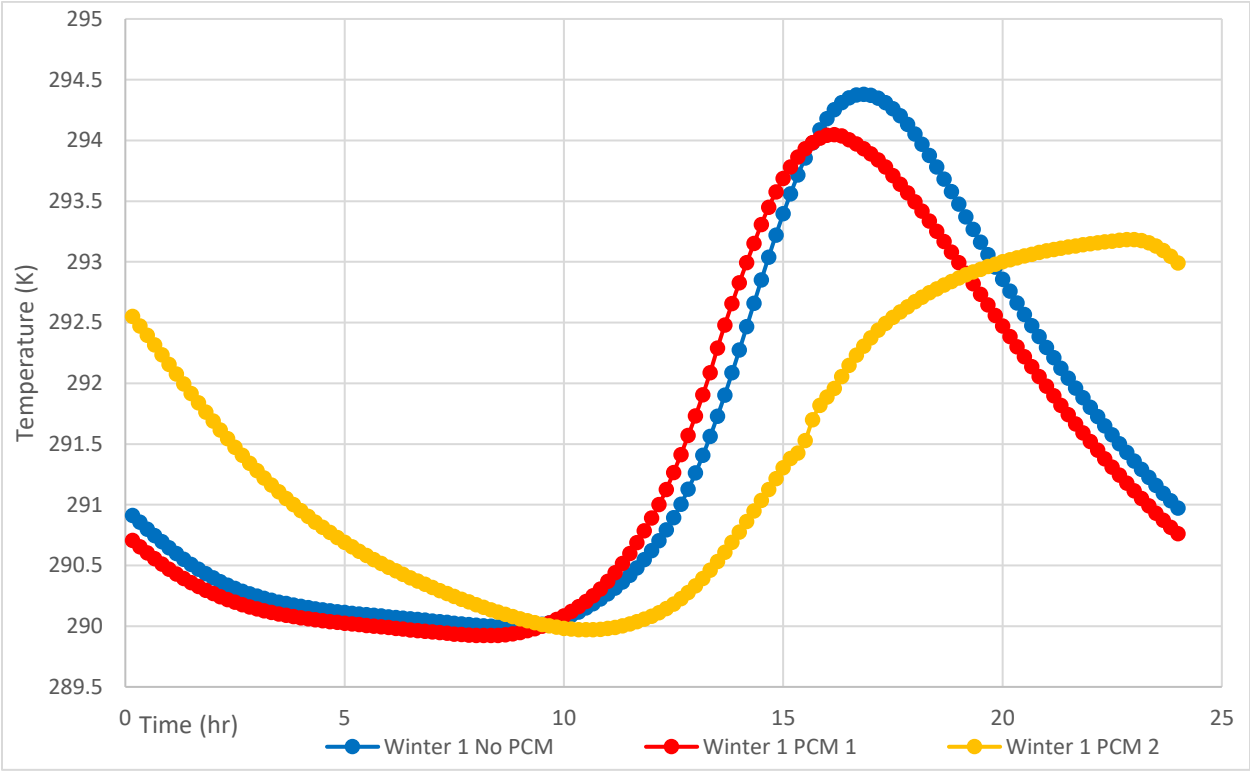


Figure 59. Comparison of inner wall surface temperature profiles between Winter 1 No PCM, Winter 1 PCM 1, and Winter 1 PCM 2 with PCM inside Insulation + Stud layer

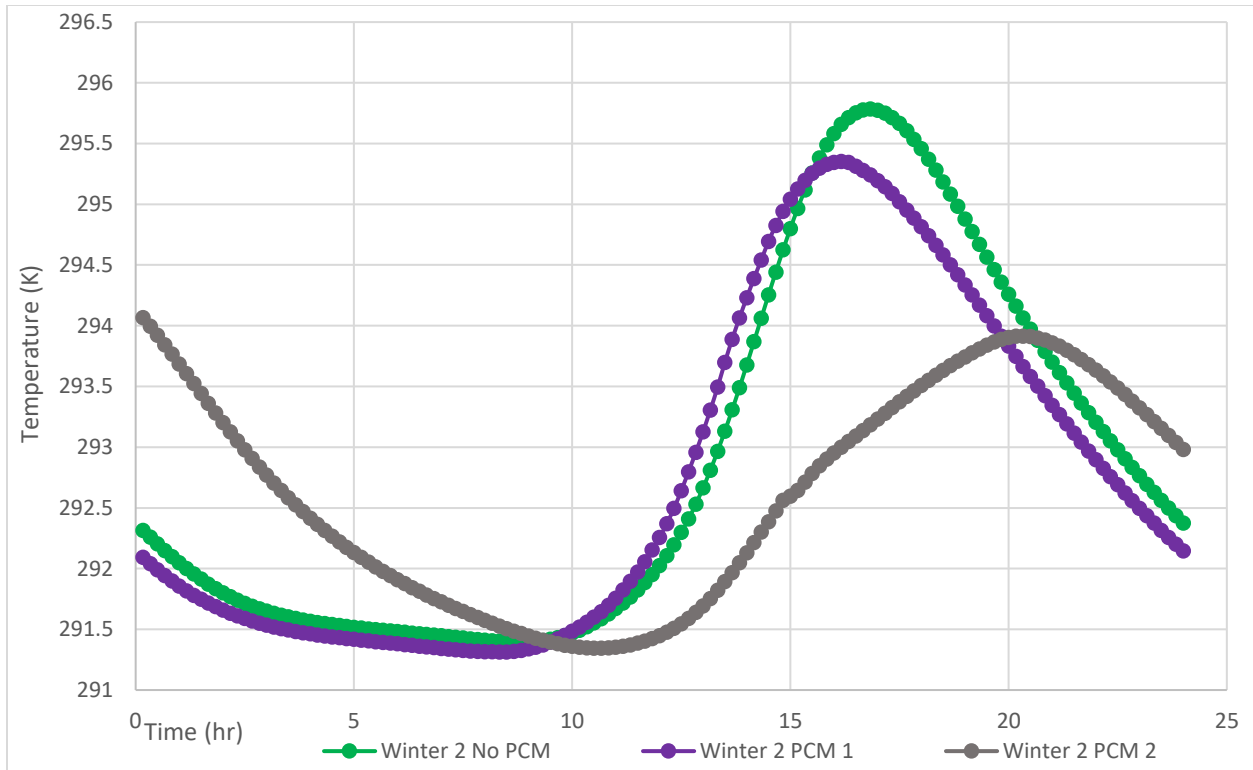


Figure 60. Comparison of inner wall surface temperature profiles between Winter 2 No PCM, Winter 2 PCM 1, and Winter 2 PCM 2 with PCM inside the Insulation + Stud layer

When the PCM is located inside insulation + stud layer the PCM is physically closer to the outdoor than when the PCM is located at the inner wall surface and thus, PCM inside insulation + stud layer can be affected by the outdoor conditions. Collecting the inner wall surface temperature does not provide an idea of the temperature of the PCM and thus, mass averaged PCM temperature was collected and has been shown in Figure 61. Clearly, the behavior of PCM 1 and PCM 2 is significantly different and this can be attributed to the difference in specific heat capacities of both PCMs. The PCM 1 mass averaged temperature shows a similar variation through the 24-hour cycle as the inner wall surface temperature in the same case but there is a time shift and the magnitudes are different as this location is closer to the outdoor conditions. The PCM 1 mass averaged temperature starts rising at around 7.83-hours and starts dropping back at 14.83-hours. The PCM 2 mass averaged temperature also shows a similar trend to the inner wall surface temperatures in the same case as well with a time shift and different

magnitude. It worth noting that the PCM 2 mass averaged temperature never really goes beyond 294K and this indicates that on a mass averaged scale the PCM 2 never enters the melting temperature range of 294.15k-294.95K.

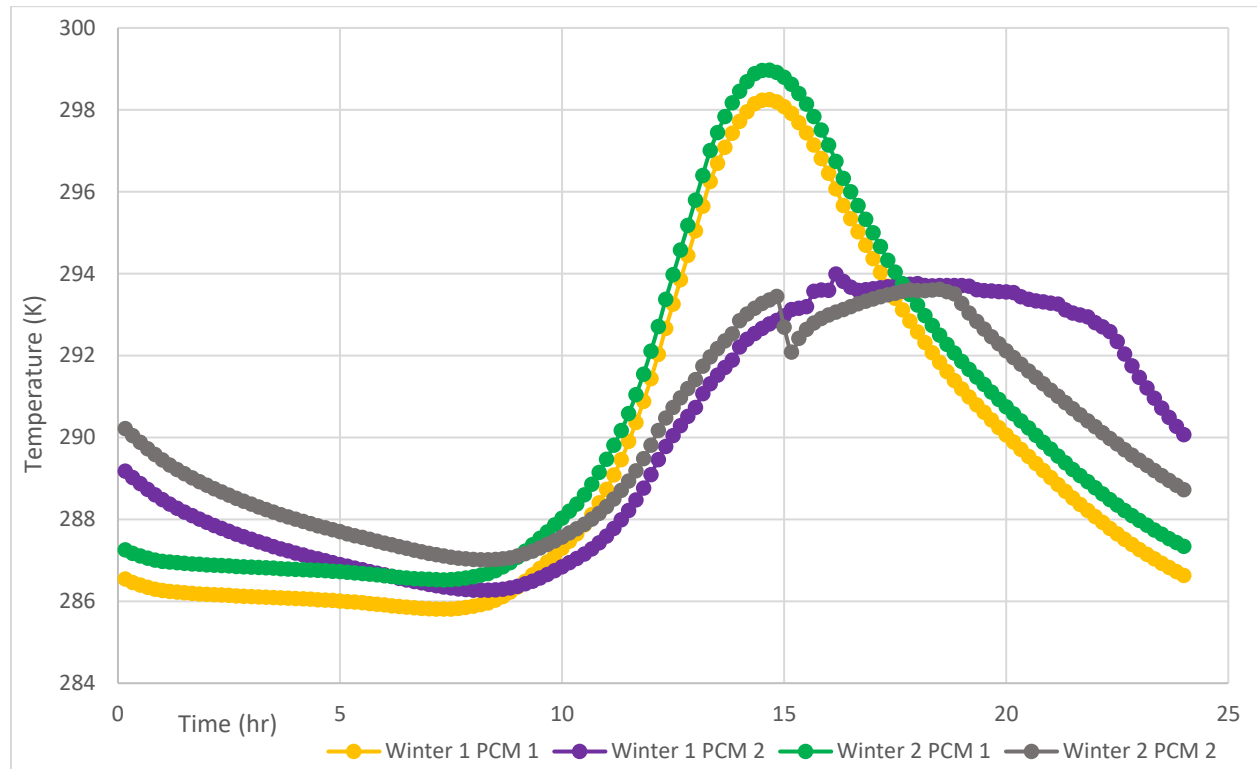


Figure 61. Comparison of PCM mass-averaged temperature profiles between Winter 1 PCM 1, Winter 1 PCM 2, Winter 2 PCM 1, and Winter 2 PCM 2 with PCM inside Insulation + Stud layer wall model

The inner wall heat flux profiles for all the cases have been shown in Figure 62 and Figure 63. These are the profiles give an insight into whether this wall model will be beneficial from an energy savings point of view. Between 0-10 hours the inner wall surface heat flux increases by approximately 1.4 W/m² in both No PCM cases and beyond that starts dropping quickly. The direction of inner wall surface heat flux changes at around 15 hours and the heat starts flowing from the inner wall surface to inside the house. It continues flowing in this direction till approximately 20 hours. Beyond 20 hours the heat flux changes direction again. Between 0-10.5 hours the inner wall surface heat flux values of Winter 1 No PCM and Winter 1 PCM 1 have no significant difference and between 11.5-15.5 hours there is a difference in

magnitude but not in direction. Between 16.5-19.5 hours the inner wall heat flux leaving the inner wall surface and entering the house drops from its peak value and during this time Winter 1 PCM 1 has smaller magnitude than Winter 1 No PCM. The relative behavior of Winter 2 No PCM and Winter 2 PCM 1 is like the relation behavior of Winter 1 No PCM and Winter 1 PCM 1. The inner wall surface heat flux for PCM 2 shows significantly different behavior than the No PCM and PCM 1 cases. For both Winter 1 and Winter 2 the inner wall surface heat flux is between 0-1 W/m² at 0.5 hours and increases continuously till 10.5 hours. At 10.5 hours the inner wall surface heat flux for Winter 1 PCM 2 is 4.6 W/m² and for Winter 2 PCM 2 is 5.5 W/m². These are the peak values and are followed by a period of decrease in heat flux. For Winter 1 PCM 2 the inner wall surface heat flux drops to 0 W/m² between 17.5-18.5 hours and changes direction beyond this point. Between 18.5-24 hours the inner wall surface heat flux for the Winter 1 PCM 2 flows from the inner wall surface to inside the house and this is desirable to reduce the energy consumption. But the total heat flowing in this direction is much smaller than the PCM 1 and No PCM cases. For Winter 2 PCM 2 the inner wall surface heat flux drops to 1 W/m² at 20.5 hours and then increases in magnitude. Thus, for the Winter 2 PCM 2 the inner wall surface heat flux is always traveling from inside the house to the inner wall surface and never in the opposite direction. The cumulative heat entering the inner wall surface from inside the house is 178292 J/m² for Winter 1 No PCM, 192521 J/m² for Winter 1 PCM 1, and 178530 J/m² for Winter 1 PCM 2. Comparing Winter 1 No PCM with Winter 1 PCM 1 the heat leaving the house and entering the inner wall surface increases by 7.9% and comparing Winter 1 No PCM with Winter 1 PCM 2 the heat leaving the house and entering the inner wall surface increases by 0.13%. The cumulative heat entering the inner wall surface from inside the house is 245071 J/m² for Winter 2 No PCM, 263721 J/m² for Winter 2 PCM 1, and 279965 J/m² for Winter 2 PCM 2. Comparing Winter 2 No PCM with Winter 2 PCM 1 the heat leaving the house and entering the inner wall surface increases by 7.6% and comparing Winter 2 No PCM with Winter 2 PCM 2 the heat leaving the house and entering the inner wall surface increases by 14%. Thus,

in all the cases after adding PCM there is an increase in the heat leaving the house and this is not desirable to reduce the energy consumption of heating the house. Increased heat leaving the house in the PCM cases indicates that more heating energy will be required to maintain the freestream temperature with the PCM added to the walls. For PCM 1, the percentage increase in the heat leaving the house is 7.9% for Winter 1 and 7.6% for Winter 2. This indicates that there is no significant change in heating energy required for PCM 1 with change in freestream temperature. For PCM 2, the percentage increase in the heat leaving the house 0.13% for Winter 1 and 14% for Winter 2. This shows that in the PCM 2 cases the heating energy consumption is much more sensitive to the freestream temperature.

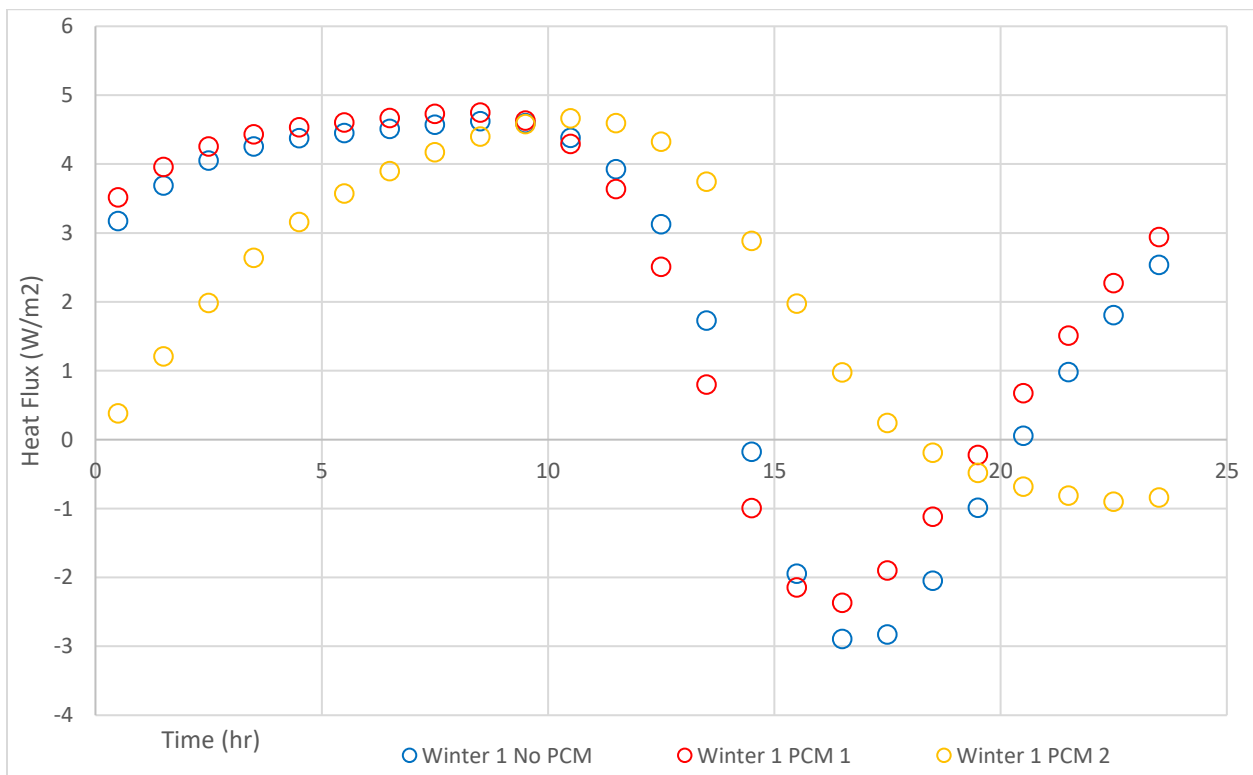


Figure 62. Comparison of inner wall surface heat flux profiles between Winter 1 No PCM, Winter 1 PCM 1, and Winter 1 PCM 2 with PCM inside Insulation +Stud layer wall model

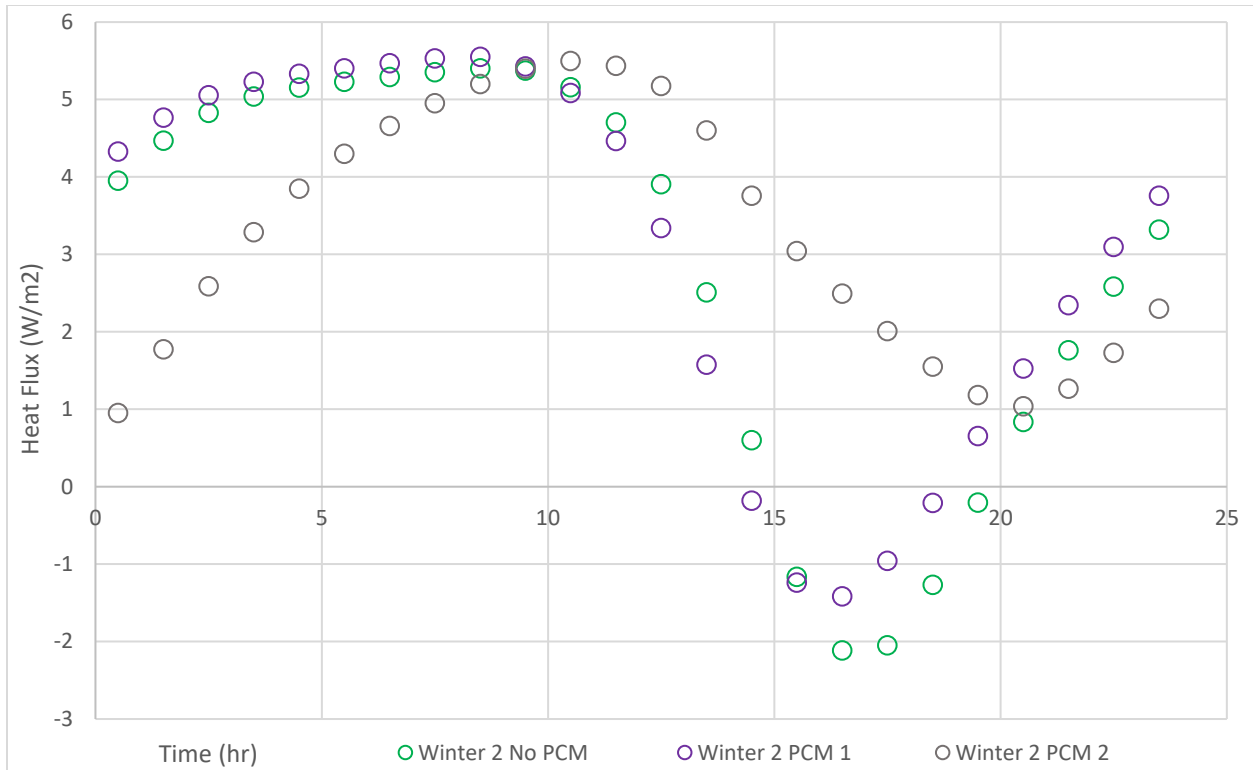


Figure 63. Comparison of inner wall surface heat flux profiles between Winter 2 No PCM, Winter 2 PCM 1, and Winter 2 PCM 2 with PCM inside Insulation + Stud layer wall model

Figure 64 shows the outer wall heat flux profile for all the PCM inside Insulation + Stud layer cases. The heat flux values at the outer wall surface between all the different cases are all very close to each other except for the values of Winter 1 PCM 2 and Winter 2 PCM 2 between 15.5-24 hours.

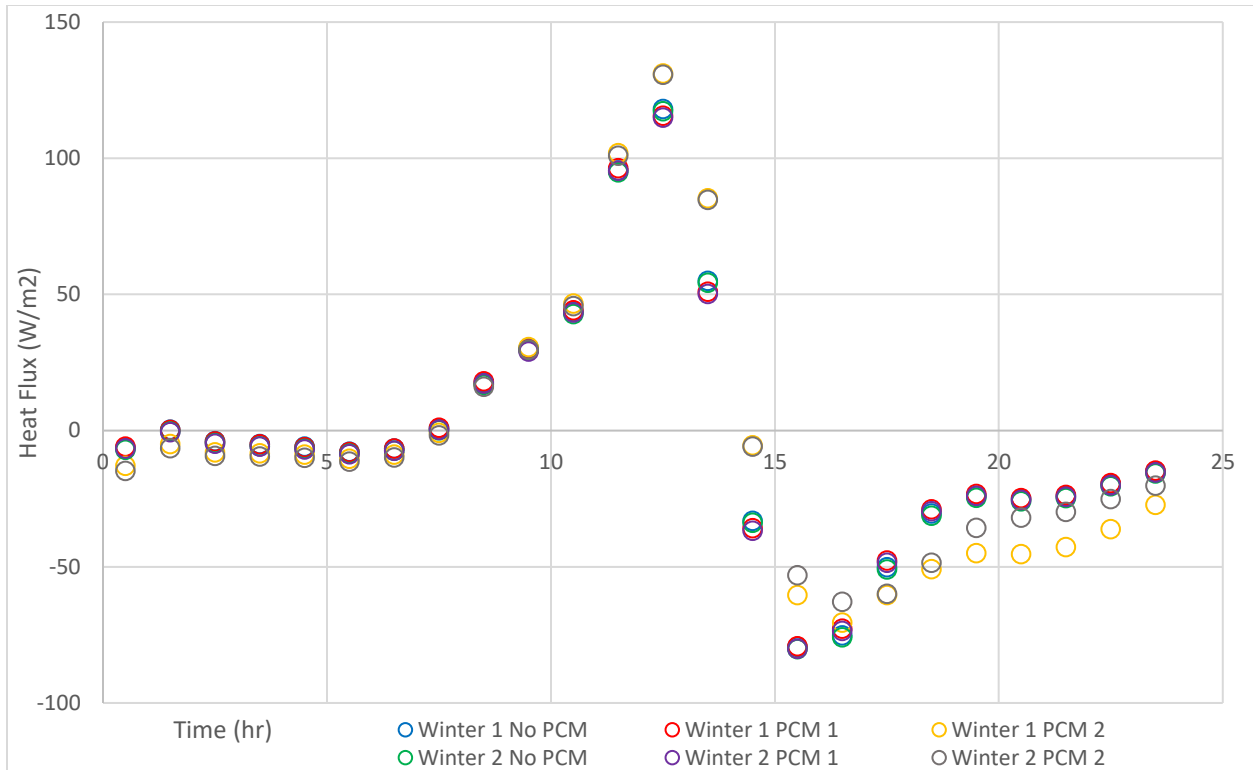


Figure 64. Comparison of outer wall surface heat flux profiles between Winter 1 No PCM, Winter 1 PCM 1, Winter 1 PCM 2, Winter 2 No PCM, Winter 2 PCM 1, and Winter 2 PCM 2 with PCM inside Insulation + Stud layer wall model

PCM Next to the Studs

When the PCM is placed inside the insulation + stud layer in the block wall the low conductivity of this layer reduces effective heat transfer to the PCM. The advantage of this location is that its behavior is not completely dictated by the indoor conditions and is more receptive to changes in the outdoor conditions than when the PCM is located at the inner wall surface. To be able to leverage this advantage of being located closer to outdoor conditions but to undo the impact of the thermal conductivity of the insulation + stud layer the idea of placing the PCM right next to studs was investigated.

Modeling Domain

As these cases require the PCM to be placed next to the studs the Blended Wall model was not used instead the Full Wall model with slight changes to include the PCM next to studs was generated. The top

view of the Full Wall model with No PCM and the top view of the Full Wall model with PCM Next to the Stud is shown in Figure 65. The only difference between the two models was the addition of the PCM next to the stud and the reduced insulation volume caused by this change.

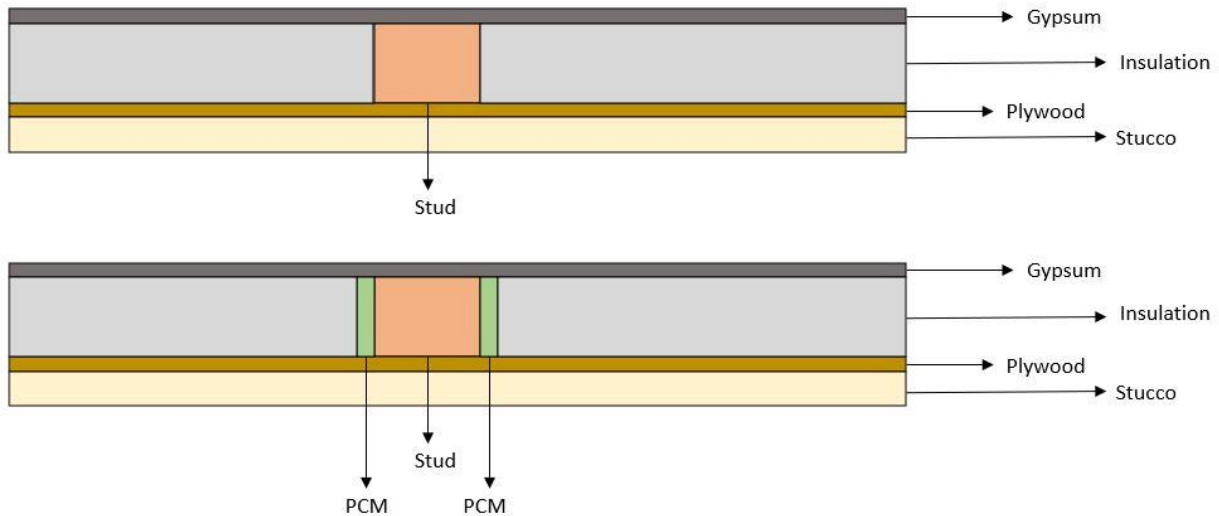


Figure 65. Full wall model with PCM Next to the Stud

Wall Material Properties

The thermophysical properties of gypsum, fir wood, insulation, plywood, and stucco are given in Table 2. The density and thermal conductivity of PCM 1 are provided in Table 4 and the specific heat capacity variation with temperature was captured using the UDF and the details of it are provided in Table 5. The density of PCM 2 is provided in Table 6 and the specific heat capacity variation with temperature of PCM 2 was modelled using piecewise linear profiles as shown in Figure 44. The thermal conductivity of solid PCM 2 (273.15K-294.15K) and of liquid PCM 2 (294.95K-400K) is given in Table 6. The variation of thermal conductivity with temperature in the mushy zone (294.15K-294.95K) was modelled using the equation given in Table 8. Depending on the case the appropriate PCM material properties were used.

Boundary Conditions

The boundary conditions applied on the PCM Next to the Stud cases were exactly like the boundary conditions imposed on PCM 2 and No PCM cases with Inner Wall Convective Boundary Condition cases. As shown in Figure 2, the insulated boundary condition was imposed on Surfaces 1 and 2, the symmetry boundary condition was imposed on Surfaces 3 and 4, the convective boundary condition was imposed on Surface 5, and Outer Wall surface temperature profile obtained from EnergyPlus on Surface 6. For PCM Next to the Stud cases only Winter representative days were tested. The outer wall temperature profile imposed on all the cases was exactly same and only the inner wall convective boundary condition was changed. Table 11 summarizes the different boundary conditions imposed on the inner wall in the different cases.

Table 11. Different cases run for PCM Next to the Stud and their inner wall surface boundary conditions

| Case | Convective Heat Transfer Coefficient (W/m ² K) | Free Stream Temperature (K) |
|-----------------|---|-----------------------------|
| Winter 1 No PCM | 1.744 | 292.65 |
| Winter 1 PCM 1 | 1.744 | 292.65 |
| Winter 1 PCM 2 | 1.744 | 292.65 |
| Winter 2 No PCM | 1.744 | 294.5 |
| Winter 2 PCM 1 | 1.744 | 294.5 |
| Winter 2 PCM 2 | 1.744 | 294.5 |

Initial Conditions and Simulation Time

The initial conditions and simulation time for the PCM Next to the Stud cases was exactly like the No PCM cases. The 24- hour temperature profiles were run consecutively for 3 days. The identical heat flux profiles of day 2 and day 3 that were obtained as an output were used to ensure that the simulation results were independent of the initial condition.

Solver Settings and Mesh Quality

The SIMPLE scheme was used for pressure-velocity coupling. A second-order implicit scheme was used for the transient formulation. The use of an implicit scheme ensures there was no possibility of the calculations becoming unstable and this also provides greater flexibility in selecting the time step size. The time step used in these simulations was 300 seconds and the solutions were recorded after every 2-time steps. The total number of elements in the mesh was 7697200, maximum skewness of the mesh was 0.214, and average skewness of the mesh was 0.015.

Results

Figure 66 show variation of the outer wall surface temperature variation over the 24-hour cycle and this is imposed as a boundary condition on all these cases. Between 0-7.5 hours the outer wall surface temperature remains almost constant around 281K and after 7.5 hours the temperature starts rising quickly and this is the impact of the solar radiation hitting the outside wall. The outer wall surface temperature peaks at 13.33 hours and has a value of 308.5K. Beyond this the temperature continuously drop until 24-hours but shows a more rapid decent up to 17 hours and then drops gradually to 281K. This is the outer wall surface temperature for all the PCM Next to the Stud Winter cases.

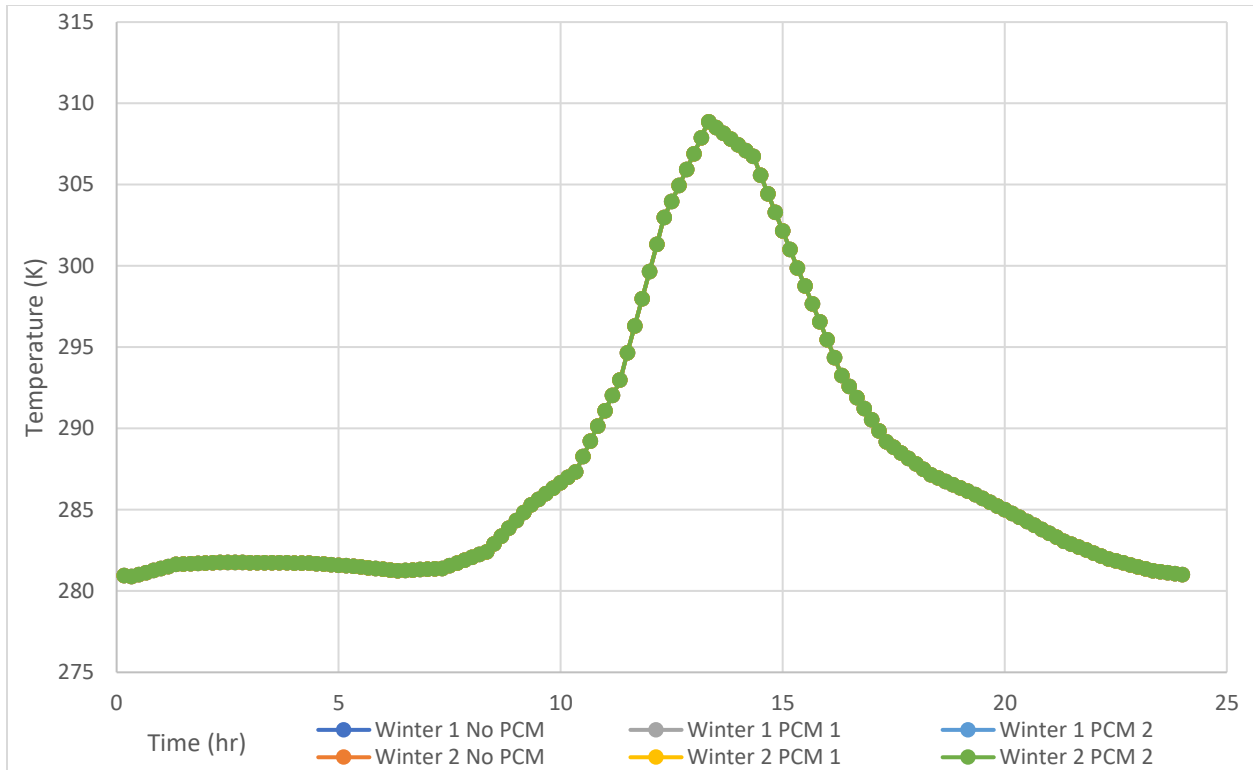


Figure 66. Comparison of outer wall surface temperature profiles between Winter 1 No PCM, Winter 1 PCM 1, Winter 1 PCM 2, Winter 2 No PCM, Winter 2 PCM 1, and Winter 2 PCM 2 with PCM Next to the Stud wall model

The inner wall surface temperatures have been shown in Figure 67 and Figure 68. The inner wall surface temperature was not imposed as a boundary condition and thus, the inner wall surface temperature used in the plots is an area weighted average temperature. It can be seen clearly that the trends Winter 1 and Winter 2 are very similar. The Winter 1 cases have a lower average temperature than Winter 2. In both Winter 1 and Winter 2, the behavior of the No PCM case and the PCM 1 case is very similar and no impact of the adding PCM 1 is reflected on the inner wall surface temperature. Between 0-8.5 hours the inner wall surface temperature drops and between 8.5-16.5 hours the inner wall surface temperature rises and then beyond 16.5 hours it drops again and this trend is seen in Winter 1 No PCM, Winter 1 PCM 1, Winter 2 No PCM, and Winter 2 PCM 1. The behavior of the PCM 2 cases is however significantly different. In these cases, between 0-9 hours the inner wall surface temperature decreases and between 9-16.5 hours the inner wall surface temperature increases. The increase in temperature between 9-16.5

hours for the PCM 2 cases is lower than the No PCM and PCM 1 cases and this can be attributed to the higher heat capacity of PCM 2. Between 16.5-20 hours the inner wall surface temperature of Winter 1 PCM 2 drops but at a much lower rate than the Winter 1 No PCM and Winter 1 PCM 1 cases. Similar trends can be seen between 16.5-21.5 hours in the Winter 2 cases.

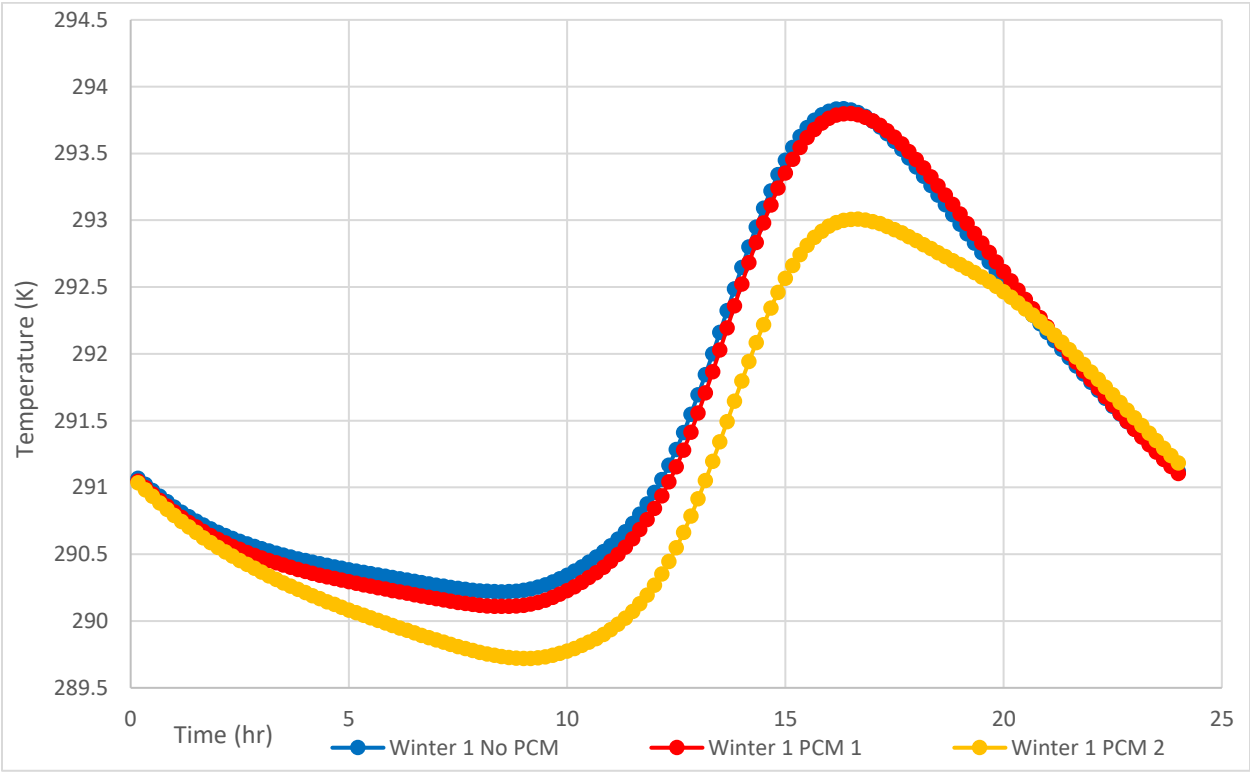


Figure 67. Comparison of inner wall surface temperature profiles between Winter 1 No PCM, Winter 1 PCM 1, and Winter 1 PCM 2 with PCM Next to the Stud wall model

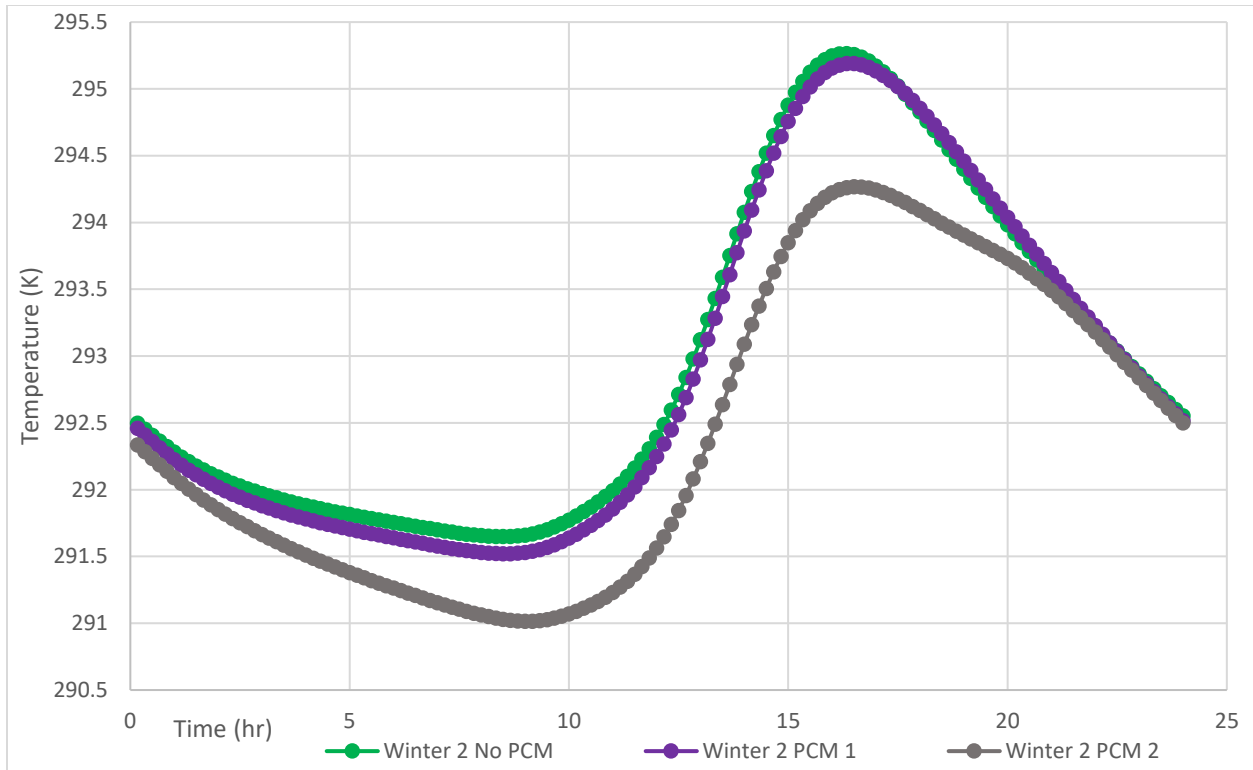


Figure 68. Comparison of inner wall surface temperature profiles between Winter 2 No PCM, Winter 2 PCM 1, and Winter 2 PCM 2 with PCM Next to the Stud wall model

In these cases, the PCM is not located at the inner wall surface and thus, to better understand the impact of the PCM the PCM mass averaged temperature variations through the 24-hour cycle are shown in Figure 69. The Winter 1 PCM 1 and the Winter 2 PCM 1 cases vary through a wide range of temperatures from approximately 286K to 297K. The Winter 2 PCM 1 variation is like Winter 1 PCM 1 but has a higher average temperature and this can be attributed to the higher freestream temperature in the Winter 2 case. Similarly, Winter 1 PCM 2 and Winter 2 PCM 2 show a similar trend with Winter 2 PCM 2 having a higher temperature throughout the 24-hour cycle. The temperature inside the PCM 2 varies from 286K to 294K. The temperature fluctuations inside PCM 1 and PCM 2 are significantly higher than the corresponding inner wall surface temperatures and this shows that at this location the PCM is more strongly affected by the outdoor conditions. PCM 2 has a melting range from 294.15-294.95K and thus, when the mass averaged temperature of PCM 2 reaches close to 294K some portion of PCM 2

starts melting. This partial melting of PCM leads to a higher mass averaged heat capacity and this can be understood by looking at Figure 44. Thus, due to the increased mass averaged heat capacity the mass averaged temperature of PCM 2 never goes beyond 294K in these cases.

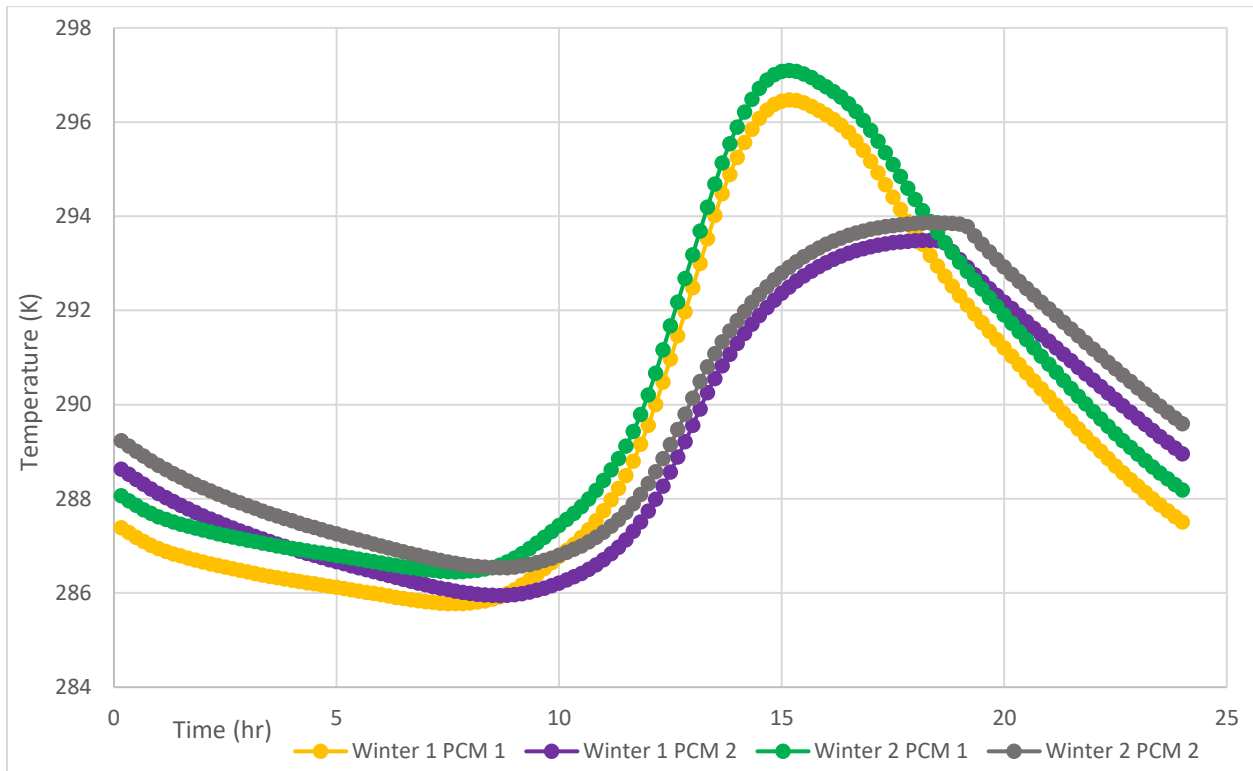


Figure 69. Comparison of PCM mass-averaged temperature profiles between Winter 1 PCM 1, Winter 1 PCM 2, Winter 2 PCM 1, and Winter 2 PCM 2 with PCM Next to the Stud wall model

Figure 70 and Figure 71 show the inner wall surface heat flux variation throughout the 24-hour cycle for all the different cases. Similar to the inner wall surface temperature the inner wall surface heat flux and the outer wall surface heat flux both are area weighted average values. Comparing the Winter 1 No PCM and Winter 2 No PCM between 0-13.5 hours and between 19.5-24 hours the heat flux entering the inner wall surface from inside the house is greater in the Winter 2 case. Additionally, the heat flux leaving the inner wall surface and entering the house between 14.5-19.5 hours is higher in the Winter 1 case. Comparing the PCM 1 cases with the corresponding No PCM cases it can be clearly seen that the inner

wall surface heat flux trends are very similar between the two cases. The PCM 1 cases show a slightly higher heat flux entering the inner wall surface from inside the house between 0-14.5 hours. Winter 1 PCM 2 shows significantly different behavior than Winter 1 No PCM and Winter 1 PCM 1. The heat flux entering the inner wall surface from inside the house between 0-14.5 hours in the Winter 1 PCM 2 case is higher than the other Winter 1 cases. The heat flux leaving the inside surface and entering the house lasts for shorter duration and the total heat traveling in this direction in the Winter 1 PCM 2 case is smaller than the Winter 1 No PCM and Winter 1 PCM 1 cases. Similarly, Winter 2 PCM 2 shows a much different behavior than Winter 2 No PCM and Winter 2 PCM 1. In the Winter 2 PCM 2 case the heat flux is always travelling to the inner wall surface from inside the house and this is not desirable. As previously discussed, the goal of adding PCM in Winter is to increase the heat flux leaving the inner wall surface and entering the house. While analyzing the graphs this translates into having a higher negative flux and ensuring it lasts for a longer period. Throughout the 24-hour cycle the heat flux is positive for longer periods of time than it is negative and thus, in a cumulative sense this means a wall configuration with lower value of heat flux integrated over the 24-hour cycle is a more energy efficient option. The total heat entering the inner wall surface from inside the house is 168045 J/m² for Winter 1 No PCM, 175990 J/m² for Winter 1 PCM 1, and 227028 J/m² for Winter 1 PCM 2. Comparing these values it can be easily understood that adding the PCM Next to the Studs is not a good option especially for if the PCM is PCM 2. In Winter 1 PCM 2 case, the total heat entering the inner wall surface from inside the house is 35% higher than Winter 1 No PCM and thus, more energy will be spent in maintaining a freestream temperature of 292.65K if PCM 2 is added next to the studs. The total heat entering the inner wall surface from inside the house is 230937 J/m² for Winter 2 No PCM, 241888 J/m² for Winter 2 PCM 1, and 310989 J/m² for Winter 2 PCM 2. In the Winter 2 PCM 2 case, the total heat entering the inner wall surface from inside the house is 34% higher than Winter 2 No PCM if the PCM 2 is added next to the

studs. Thus, adding PCM Next to the Stud is not at all an energy efficient solution instead it will increase the energy consumption spent on heating the house during Winter.

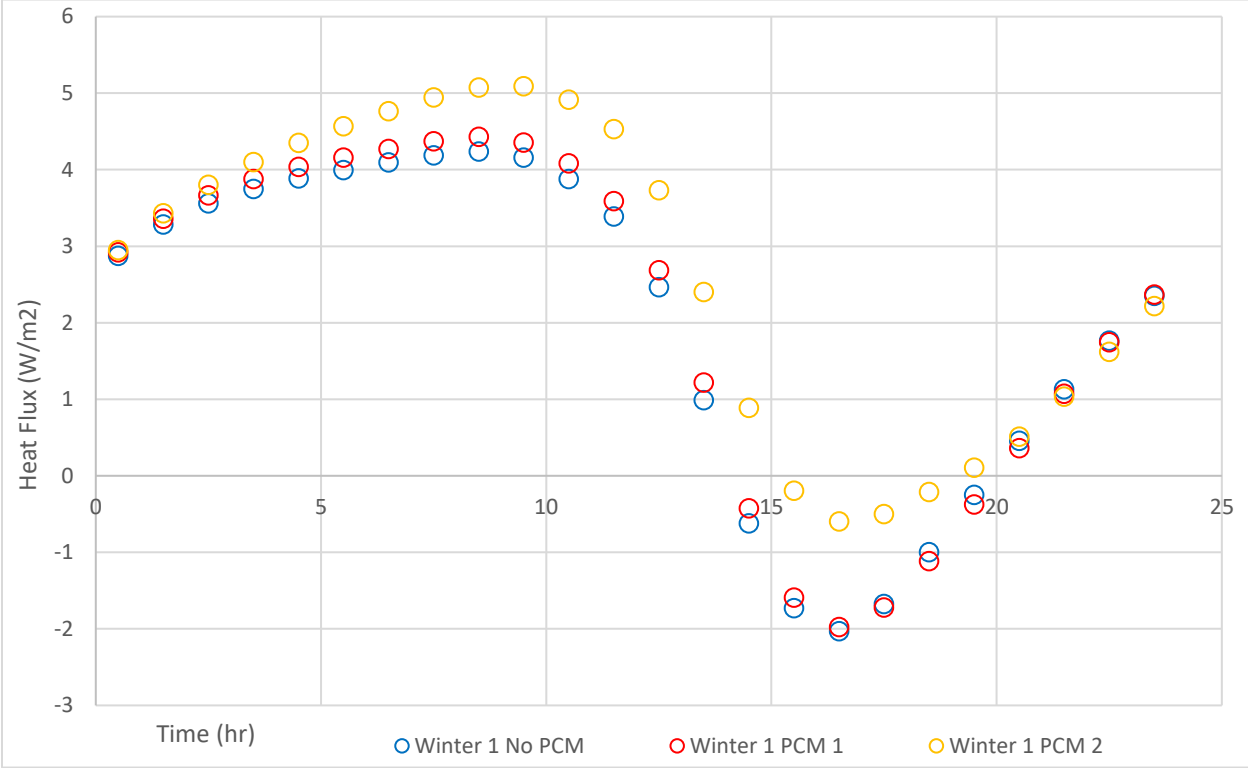


Figure 70. Comparison of inner wall surface heat flux profiles between Winter 1 No PCM, Winter 1 PCM 1, and Winter 1 PCM 2 with PCM Next to the Stud wall model

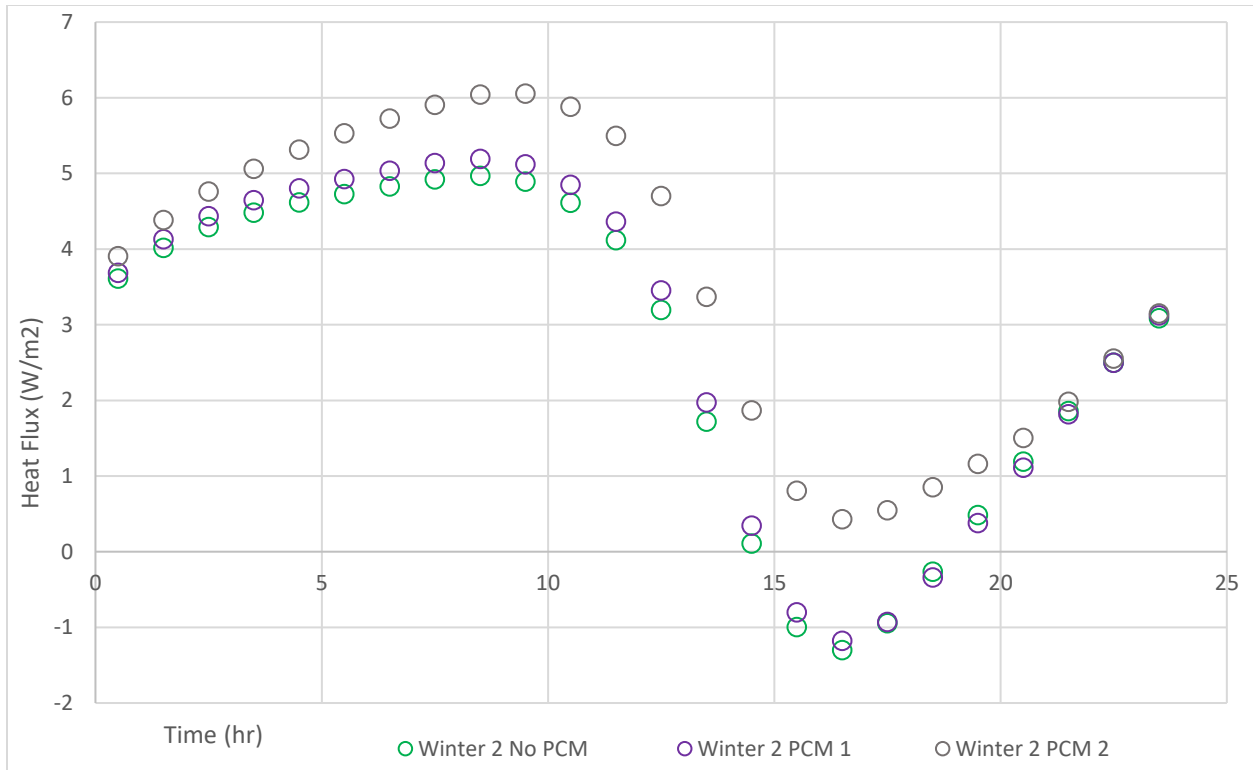


Figure 71. Comparison of inner wall surface heat flux profiles between Winter 2 No PCM, Winter 2 PCM 1, and Winter 2 PCM 2 with PCM Next to the Stud wall model

Figure 72 shows the outer wall surface heat flux variation over the 24-hour cycle. The outer wall surface heat variation of all the cases is very similar and this trend has been consistently observed in all the different wall configurations.

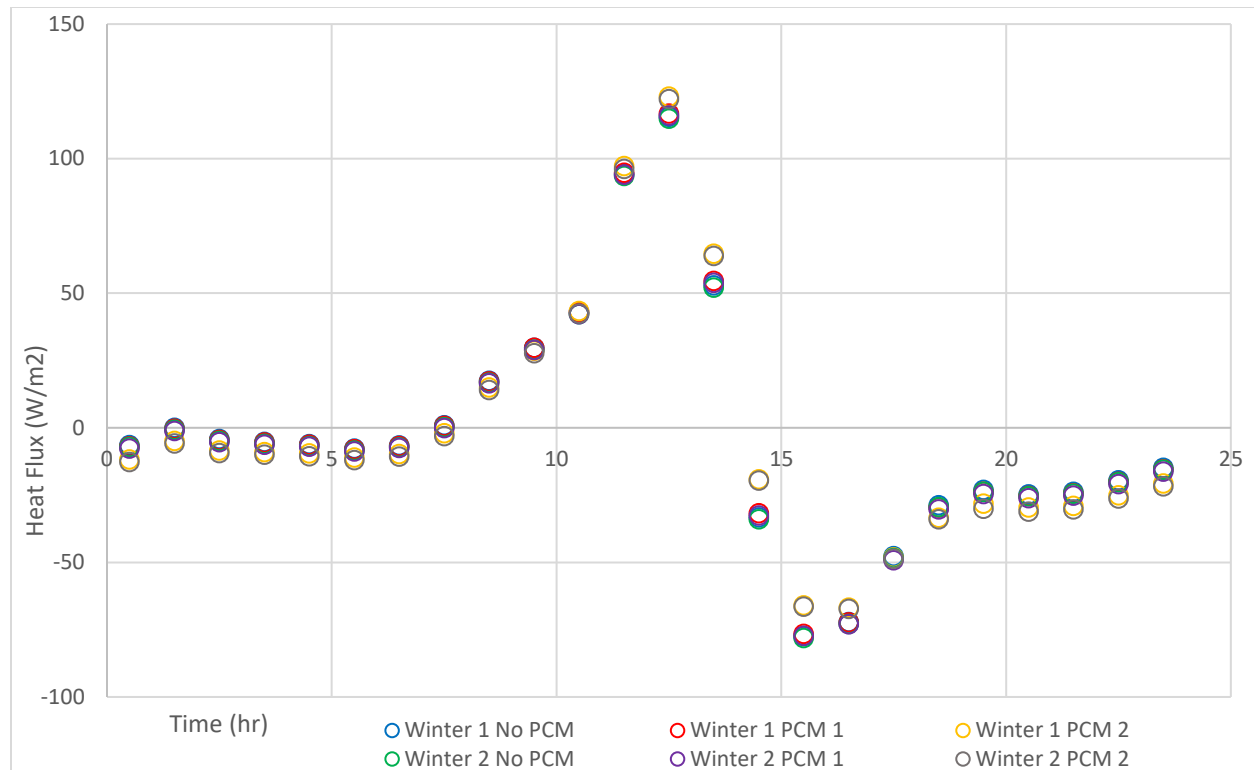


Figure 72. Comparison of outer wall surface heat flux profiles between Winter 1 No PCM, Winter 1 PCM 1, Winter 1 PCM 2, Winter 2 No PCM, Winter 2 PCM 1, and Winter 2 PCM 2 with PCM Next to the Stud wall model

PCM 1 and PCM 2 show significantly different behavior at the two locations investigated in this chapter. From all the different cases investigated in this chapter the cumulative heat entering the inner wall surface from inside the house always increases and thus, more energy is consumed in each case. The cumulative heat entering the inner wall surface from inside the house for PCM 1 increases by 7.9% in Winter 1 and 7.6% in Winter 2 for the PCM inside Insulation + Stud layer. The cumulative heat entering the inner wall surface from inside the house for PCM 2 increases by 0.13% in Winter 1 and 14% in Winter 2 for the PCM inside Insulation + Stud layer. Indicating that for this location PCM 2 behavior is highly sensitive to freestream temperature. The cumulative heat entering the inner wall surface from inside the house for PCM 1 increases by 4.7% in Winter 1 and 4.7% in Winter 2 for the PCM Next to Studs. The cumulative heat entering the inner wall surface from inside the house for PCM 2 increases by 35% in Winter 1 and 34% in Winter 2 for the PCM Next to Studs. Thus, for PCM Next to Stud location the

performance of PCM 2 is much worse than PCM 1. But even in the case of PCM 1 the cumulative heat entering the inner wall surface from inside the house increases and thus, does not reduce energy consumption.

Conclusions

In this research work, a typical California residential wall in Climate Zone 9 was simulated under three representative days of Winter, Summer, and Shoulder using temperature boundary conditions on both walls and under two representative days of Winter and Summer using inner wall convection and outer wall temperature boundary conditions. Based on the comparisons of the results it was found that the Blended Wall model results agreed better with the EnergyPlus results than the Full Wall model. This can be attributed to the Blended Wall model being an exact replica of the wall model used in EnergyPlus. Based on these findings and for reducing the computational effort all PCM integrated wall models were simulated using the Blended Wall model.

PCM 1 was modeled using the solid Cp curve approach and the specific heat versus temperature curve was broken into 17 second order polynomials to accurately capture the PCM 1 melting behavior.

Increasing the quantity of PCM 1 integrated in the wall model showed impacts on the temperature and heat flux values but no significant impact was observed. The heat flux at the inner wall surface showed that adding PCM 1 did not reduce the energy consumption of heating for the Winter day and Shoulder day but a reduction of cooling energy was observed in the Summer day. Based on the comparison of EnergyPlus and ANSYS Fluent results it was found that the default mesh resolution used in the EnergyPlus simulations led to the temperature gradient within PCM 1 to be not accurately captured. This was confirmed when two EnergyPlus models with different mesh resolutions and all other parameters being the same showed different results.

A validation study was carried out and it was able to successfully predict the solid-liquid interface location as a function of time. The enthalpy porosity approach was used in these simulations but due a lack of viscosity data for PCM 2 the solid Cp curve approach was used for PCM 2 as well. The specific heat versus temperature curve was constructed in the form of a trapezium and this form was used in all

the PCM 2 wall model simulations. Adding PCM 2 to the inner wall surface for Winter slightly increased the heating energy consumption. For Summer adding PCM 2 slightly reduced the cooling energy consumption.

Both PCM 1 and PCM 2 were tested for two more locations for Winter. The first location tested was PCM cubes equally distributed inside Insulation + Stud layer and the second located testes was PCM Next to Studs. Based on the results, it was observed that for PCM inside Insulation + Stud layer adding PCM 1 had no impact but PCM 2 increased the heating energy consumption. The freestream temperature was an important parameter that drastically affected heating energy consumption when PCM 2 was placed inside Insulation + Stud layer. For PCM Next to Studs the heating energy consumption increased in both PCM 1 and PCM 2 cases but a higher increase was seen in PCM 2 case.

This study shows that adding PCM to wall envelope is not always beneficial and needs a thorough study accounting for PCM properties, climatic conditions, and occupant behavior to make sure energy efficient solutions are developed.

References

- [1] EIA U. How much energy is consumed in residential and commercial buildings in the United States. US Energy Information Administration (EIA) Washington, DC. 2014.
- [2] Energy Information Administration. 2011 March. Emissions of greenhouse gases in the United States 2009. Washington, DC: Pub. No.: DOE/EIA-0573 (2009).
- [3] Burch D et al. A field study of the effect of wall mass on the Heating and cooling loads of residential buildings. In: Proceedings of the building thermal mass seminar, Knoxville, TN; 1982
- [4] Dexter ME. Energy conservation design guidelines: including mass and insulation in building walls. ASHRAE J 1980;22(3):35–8.
- [5] A. de Gracia, L.F. Cabeza, Phase change materials and thermal energy storage for buildings, Energy Build. 103 (2015) 414–419.
- [6] Soares N, Costa JJ, Gaspar AR, Santos P. Review of passive PCM latent heat thermal energy storage systems towards buildings' energy efficiency. Energy and buildings. 2013 Apr 1;59:82-103.
- [7] Saffari M, De Gracia A, Fernández C, Cabeza LF. Simulation-based optimization of PCM melting temperature to improve the energy performance in buildings. Applied Energy. 2017 Sep 15;202:420-34.
- [8] Tabares-Velasco PC, Christensen C, Bianchi M, Booten C. Verification and validation of EnergyPlus conduction finite difference and phase change material models for opaque wall assemblies. National Renewable Energy Lab.(NREL), Golden, CO (United States); 2012 Jul 1.
- [9] J. Kosny, D. Yarbrough, W. Miller, S. Shrestha, E. Kossecka, E. Lee, Numerical and experimental analysis of building envelopes containing blown fiberglass insulation thermally enhanced with phase change material (PCM), in: Proceedings of the 1st Central European Symposium on Building Physics, Cracow, Poland, 2010.
- [10] J. Kosny, S. Shrestha, T. Stovall, D. Yarbrough, Theoretical and experimental thermal performance analysis of complex thermal storage membrane containing bio-based phase-change material (PCM), in: Thermal Performance of the Exterior Envelopes of Whole Buildings XI, 2010.
- [11] G. Evola, N. Papa, F. Sicurella, E. Wurtz, Simulation of the behaviour of phase change materials for the improvement of thermal comfort in lightweight buildings, in: Proceedings of Building Simulation 2011, Sydney, Australia, 2011
- [12] A. Tardieu, S. Behzadi, J.J.J. Chen, M.M. Farid, Computer simulation and experimental measurements for an experimental PCM-impregnated office building, in: Proceedings of Building Simulation 2011, Sydney, Australia, 2011.
- [13] D. Tetlow, Y. Su, S.B. Riffat, EnergyPlus simulation analysis of incorporating microencapsulated PCMs (Phase Change Materials) with internal wall insulation (IWI) for hard-to-treat (HTT) houses in the UK, in: 10th International Conference on Sustainable Energy Technologies, Istanbul, Turkey, 2011.
- [14] P. Schossig, H.-M. Henning, S. Gschwander, T. Haussmann, Microencapsulated phase-change materials integrated into construction materials, Solar Energy Materials and Solar Cells 89 (2–3) (2005) 297–306.

- [15] F. Kuznik, J. Virgone, K. Johannes, Development and validation of a new TRNSYS type for the simulation of external building walls containing PCM, *Energy and Buildings* 42 (7) (2010) 1004–1009.
- [16] Saffari M, de Gracia A, Ushak S, Cabeza LF. Passive cooling of buildings with phase change materials using whole-building energy simulation tools: A review. *Renewable and Sustainable Energy Reviews*. 2017 Dec 1;80:1239-55.
- [17] Wijesuriya S, Brandt M, Tabares-Velasco PC. Parametric analysis of a residential building with phase change material (PCM)-enhanced drywall, precooling, and variable electric rates in a hot and dry climate. *Applied energy*. 2018 Jul 15;222:497-514.
- [18] Jamil H, Alam M, Sanjayan J, Wilson J. Investigation of PCM as retrofitting option to enhance occupant thermal comfort in a modern residential building. *Energy and Buildings*. 2016 Dec 1;133:217-29.
- [19] Lee KO, Medina MA, Raith E, Sun X. Assessing the integration of a thin phase change material (PCM) layer in a residential building wall for heat transfer reduction and management. *Applied Energy*. 2015 Jan 1;137:699-706.
- [20] Dutil Y, Rousse DR, Salah NB, Lassue S, Zalewski L. A review on phase-change materials: Mathematical modeling and simulations. *Renewable and sustainable Energy reviews*. 2011 Jan 1;15(1):112-30.
- [21] Slattery JC. *Advanced transport phenomena*. Cambridge University Press; 1999 Jul 13.
- [22] Carslaw HS, Jaeger JC. *Conduction of heat in solids*. Oxford: Clarendon Press; 1959.
- [23] Lunardini VJ. *Heat transfer in cold climates*. New York: Van Nostrand Reinhold; 1981
- [24] V.R. Voller, C. Prakash, A fixed grid numerical modelling methodology for convection-diffusion mushy region phase-change problems, *Int. J. Heat Mass Transf.* 30 (8) (1987) 17091719.
- [25] Zeneli M, Nikolopoulos A, Karellas S, Nikolopoulos N. Numerical methods for solid-liquid phase-change problems. In *Ultra-High Temperature Thermal Energy Storage, Transfer and Conversion 2021* Jan 1 (pp. 165-199). Woodhead Publishing.
- [26] E. Assis, L. Katsman, G. Ziskind, R. Letan, Numerical and experimental study of melting in a spherical shell, *Int. J. Heat Mass Transf.* 50 (9) (2007) 17901804.
- [27] E. Assis, G. Ziskind, R. Letan, Numerical and experimental study of solidification in a spherical shell, *J. Heat Transf.* 131 (2) (2009) 024502.
- [28] Kamkari B, Amlashi HJ. Numerical simulation and experimental verification of constrained melting of phase change material in inclined rectangular enclosures. *International Communications in Heat and Mass Transfer*. 2017 Nov 1;88:211-9.
- [29] Enermodal Engineering Limited, "Characterization of Framing Factors For New Low-Rise Residential Building Envelopes (904-RP)," August 2001.

- [30] US Department of Energy, "PNNL Residential Prototype Building Models," 2018. [Online]. Available: https://www.energycodes.gov/development/residential/iecc_models.
- [31] Oak Ridge National Laboratory, "Thermal Properties of Wood and Wood Panel Products for Use in Buildings," U.S. Deptment of Energy, 1988.
- [32] CertainTeed PCM 1, "OPTIMA Fiber Glass Loose-Fill Insulation for Sidewall Reinsulation," [Online]. Available: <https://www.certainteed.com/resources/30-24-225.pdf>. [Accessed 2020].
- [33] Fisher DE, Pedersen CO. Convective heat transfer in building energy and thermal load calculations. American Society of Heating, Refrigerating and Air-Conditioning Engineers, Inc., Atlanta, GA (United States); 1997 Dec 31.
- [34] Ziskind G. Modeling of heat transfer in phase change materials for thermal energy storage systems. In *Advances in Thermal Energy Storage Systems* 2021 Jan 1 (pp. 359-379). Woodhead Publishing.
- [35] Kishore RA, Bianchi MV, Booten C, Vidal J, Jackson R. Optimizing PCM-integrated walls for potential energy savings in US Buildings. *Energy and Buildings*. 2020 Nov 1;226:110355.
- [36] X. Jin, M.A. Medina, X. Zhang, On the importance of the location of PCMs in building walls for enhanced thermal performance, *Appl. Energy* 106 (2013) 72–78.
- [37] X. Jin, S. Zhang, X. Xu, X. Zhang, Effects of PCM state on its phase change performance and the thermal performance of building walls, *Build. Environ.* 81 (2014) 334–339.
- [38] A. Fateh, F. Klinker, M. Brütting, H. Weinsläder, F. Devia, Numerical and experimental investigation of an insulation layer with phase change materials (PCMs), *Energy Build.* 153 (2017) 231–240.
- [39] A. Fateh, D. Borelli, F. Devia, H. Weinsläder, Summer thermal performances of PCM-integrated insulation layers for light-weight building walls: Effect of orientation and melting point temperature, *Therm. Sci. Eng. Progr.* 6 (2018) 361–369